Dynamical Systems Analysis of HIV Immunopathogenesis and the Effects of Antiretroviral Treatment Interruption

by

©Jessica Rose

A Thesis Submitted to the School of Graduate Studies in partial fulfillment of the requirement for the degree of Master of Science

Faculty of Medicine
Memorial University of Newfoundland

September, 2006

St. John's, Newfoundland, Canada

Abstract

In the absence of a successful vaccine against HIV-1, alternative means to cope with the HIV pandemic have been explored. Antiretroviral (ARV) treatment is commonly prescribed to HIV-infected individuals in an attempt to control the infection. However, ARV treatment is very rigorous and generally comprises a highly toxic and costly multi-drug regimen designed for strict, life-long adherence. ARV treatment interruption is an alternative treatment strategy designed to maximize clinical benefits and alleviate some of the complications associated with continuous treatment. It is theorized that treatment interruption can reset the virological setpoint by inducing controlled resurgences of virus to boost HIV-specific $CD8^+$ T cell activity to control viral replication.

Dynamical systems analysis is a mathematical tool used to describe the behavior of complex systems. This allows an unobtrusive, safe way to test treatment interruption regimens. I have developed a novel mathematical model that describes the dynamical interactions between HIV-specific T cell and virus populations for two clinically-defined subgroups of HIV-1-infected individuals called fast and slow progressors. The model is based on antiviral activity imposed by HIV-specific $CD8^+$ T cells that specifically target the virus by removing virally-infected cells and the model accurately mimics clinical dis-

ease progression patterns in these subgroups. Model results accurately predict that treatment interruption induces resurgence of virus to boost HIV-specific $CD8^+$ T cell activity in both subgroups, but does not reset the virological setpoint in either. These results are experimentally corroborated through an assessment of quantitative and qualitative changes in HIV-specific $CD8^+$ T cell activities when virus loads are high (off-treatment) and low/undetectable (on-treatment).

In this thesis, I provide an introduction to HIV and dynamical systems, a complete analysis of the model derived to describe HIV immunopathogenesis, a report on clinical and experimental observation of a small cohort of HIV-1-infected individuals and a description of the integration of the mathematical, clinical and experimental results.

Acknowledgements

I would like to extend my warm thanks to my supervisor Michael Grant. He has been a limitless source of information and help throughout the development of this thesis. I would also like to thank my co-supervisor Andy Foster for his patience and time, and Sheila Drover for her encouragement and thoughtful input. I wish to thank all of the immunology Faculty and students for their support and encouragement throughout the degree process. Thanks to Maureen Gallant for getting me started and making benchwork fun. Special thanks to Sharon Oldford and Lisa Barrett. I will always look to both of you for inspiration.

I would also like to extend my thanks to Greg Simmons and family. Thanks for all of the smiles, laughter, meals and wine.

Huge thanks to my mom and dad for listening to my long presentations and always encouraging me to continue.

And of course, thanks to Encuentro Flamenco. You guys have been such a light for me in the past year. Thanks and keep on dancing!

Contents

List of Tables

List of Figures

List of Abbreviations

HIV - human immunodeficiency virus

ARV - antiretroviral

AIDS - acquired immune deficiency syndrome

RNA - ribonucleic acid

DNA - deoxyribonucleic acid

DC - dendritic cell

APC - antigen-presenting cell

MHC - major histocompatability complex

TCR - T cell receptor

CTL - cytotoxic T lymphocyte

IL-2 - interleukin-2

IFN- γ - interferon gamma

TNF - tumor necrosis factor

NRTI - nucleside reverse transcriptase inhibitor

NNRTI - nonnucleoside reverse transcriptase inhibitor

PI - protease inhibitor

FI - fusion inhibitor

HAART - highly active antiretroviral therapy

ODE - ordinary differential equation

VL - virus load

SFC - spot-forming cell

vnef - vaccinia virus vector expressing HIV nef

vvk1 - vaccinia virus vector expressing HIV gag/pol

vpe16 - vaccinia virus vector expressing HIV env

Chapter 1

Introduction

Human immunodeficiency virus type 1 (HIV-1), the causative agent of acquired immune deficiency syndrome (AIDS), was isolated and identified in 1983 [Gallo *et al.*, 1984]. HIV is a retrovirus: it stores its genetic information as single-stranded ribonucleic acid (RNA) molecules instead of double-stranded deoxyribonucleic acid (DNA) and reverses the normal genetic writing process by converting viral RNA to viral DNA as part of its life cycle. HIV is a member of a subgroup of the retrovirus family known as the lentiviruses because it causes disease slowly. In the absence of treatment, infection generally spans a period of approximately 10 years. HIV and AIDS remain at pandemic levels with an estimated 40 million people living with HIV infection and 5 million newly infected individuals in 2005. More than 25 million people have died of AIDS since 1981 and there is no known cure [UNAIDS/WHO 2005 report].

1.1 Host Infection

HIV is transmitted via blood or other body fluids, and infection with HIV always results in chronic infection. Following infection with HIV, the amount of virus detectable in the blood of the host, called the virus load, rises dramatically. This increase in virus load is associated with flu-like symptoms, tending to last for a few weeks to months, which disappear as the virus load recedes to a lower stable level called the virological setpoint. The infected individual generally remains asymptomatic for years until eventually succumbing to AIDS.

The definition of AIDS is ambiguous. In the United States, an HIV-infected individual is said to have AIDS if their helper T cell count falls below 200 per microlitre (ul) of peripheral blood [Centers for Disease Control, 2005]. In Canada, an individual is considered to have AIDS if they develop an AIDS-defining illness. There are cases of HIV-infected individuals who develop AIDS, but following salvage or late treatment treatment regimens[1], no longer have AIDS according to these definitions.

1.2 HIV Immunopathogenesis

HIV immunopathogenesis is characterized by three phases: the acute phase, the chronic phase and AIDS. Figure 1.1 is a schematic graph showing how T cell and virus populations change throughout pathogenesis.

[1]Salvage Treatment: A drug combination that is used after other combinations have failed. Often, salvage treatment is used to refer to regimens designed to combat highly resistant HIV. Also called rescue therapy.

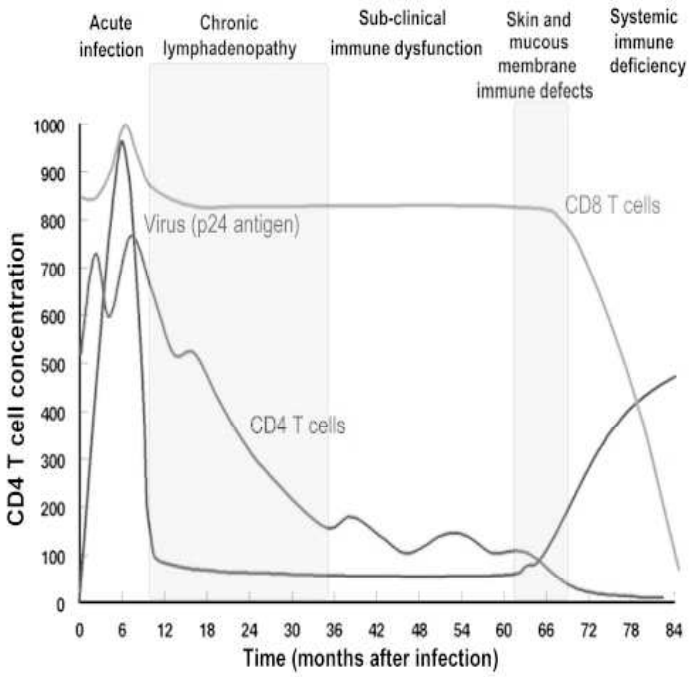

Figure 1.1: HIV immunopathogenesis - Adapted from Microbiology and Immunology online - University of South Carolina - School of Medicine

In the early phase of acute HIV infection, the virus load increases reaching concentrations of up to 100 million copies HIV RNA per millilitre of plasma [Piatak *et al.*, 1993; Mellors *et al.*, 1995]. The presence of the virus at high levels in the host induces potent cellular immune responses throughout the following weeks. These immune responses act to lower the viral load by efficiently removing infected cells from the system until the imposed pressure from the cellular immune response induces a state where the T cell and virus populations are roughly in equilibrium. This equilibrium or balance implies

that each population is in a stable state whereby they stay at relatively constant levels. The virus load at the equilibrium state (the virological or viral setpoint) is a strong predictor of the rate of disease progression [Altfeld *et al.*, 2005; Mellors *et al.*, 1995; Notermans *et al.*, 1998]. Establishment of a virological setpoint generally marks the resolution of the acute phase and the beginning of the chronic phase of infection. During the chronic phase, the virus persists at setpoint levels and continuously stimulates the host immune system via ongoing replication. It is during the chronic phase of infection that the helper T cell ($CD4^+$ T cell) population is slowly and steadily depleted. This is the hallmark of HIV infection. The exact reason for this apparent slow steady depletion of these cells remains elusive.

1.3 Cellular Infection

HIV preferentially infects helper T cells; the cells that coordinate cellular immune reponses [Dalgleish *et al.*, 1984; Klatzmann *et al.*, 1984; McCune, 2001]. This leads to their eventual depletion and results in the collapse of the immune system. The virus attaches to helper T cells via a high affinity interaction between the cell-surface molecule CD4 (T4 antigen) and the external gp120 portion of the viral envelope protein complex. This binding is associated with coreceptor binding to cellular chemokine receptors CCR5 or CXCR4 on the $CD4^+$ cell. Whether the virus binds coreceptor CCR5 or CXCR4 determines the tropism of the virus. Individuals who lack a CCR5 coreceptor on their T cells are virtually 100% resistant to HIV infection indicating the necessity of this co-receptor for cell infection to occur. The union of gp120 and CD4 causes

a conformational change to occur in the gp120 glycoprotein which allows another part of gp120 to bind either CCR5 or CXCR4. After this secondary interaction, the transmembrane portion of the envelope protein gp41 undergoes a conformational change and embeds a fusogenic part of itself into the host cell membrane [Levy; 1996]. The host cell and the viral envelope fuse and the viral contents are released into the cytoplasm of the host cell. The viral capsid is lost and viral RNA begins to be transcribed via reverse transcriptase into viral double-stranded DNA (dsDNA) called the *provirus*. This dsDNA gets integrated into the host cell DNA via another viral constituent enzyme called integrase, rendering the cell infected for life. The integrated DNA is called the *integrated provirus*. The integrated provirus serves as a template for the synthesis of viral RNA. Cellular activation is necessary for integration of the proviral HIV DNA into the host cell genome after transportation of the pre-integration complex into the nucleus. When the infected cell is activated, viral RNA is synthesized and moves into the cytoplasm. Viral messenger RNA (mRNA) is subsequently translated into structural proteins and enzymes necessary for synthesis of viral proteins and assembly of new virions. The mRNA carries information that codes for viral proteins and enzymes necessary for synthesis of viral proteins and assembly of new virions. Viral RNA and associated proteins are packaged into new virus particles that mature into new infectious virions. This assembly begins at the cell membrane where the virion forms and buds from the cell surface membrane. These new virions undergo further maturation whereby the structural components undergo further processing following budding.

Viral DNA integration into the host-cell genome is irreversible. Some cells

become virus producers. Other cells remain latently infected. Latent infection means that the cell is infected; the provirus is present, but the cell has not yet become activated to begin the viral replication cycle. Some cells may never become activated, or they may become activated at a later time point in disease progression. Even if the virus is cleared from the bloodstream, it can lie dormant in latently infected cells, later activated to produce teams of new viral progeny.

All $CD4^+$ T cells are all susceptible to infection by HIV [Janeway *et al.*, 2001; Douek *et al.*, 2003; Ribeiro *et al.*, 2002]. However, studies show that HIV preferentially infects HIV-specific $CD4^+$ T cells [Douek *et al.*, 2002]. The preferential infection of HIV-specific $CD4^+$ T cells means that these cells are preferentially depleted as well. More on this follows in Chapter 2.

1.4 Immune Response

The immune response to HIV is very much the same as the immune response to any viral infection. This response includes the activation of both cellular and humoral immunity. Once the virus breaches the mucosal barriers, resident phagocytic cells such as macrophages and dendritic cells (DC), "take-up" viral antigens and home to the local draining lymph node. En route to the lymph node, these cells change functionally and phenotypically to become extremely proficient antigen-presenting cells (APC). DC are the most potent inducers of specific immune responses and are considered essential for the initiation of primary antigen-specific immune responses. Antibodies are produced as part of these primary antigen-specific responses to clear the virus from the

body. These antibodies can be detected in the blood during infection and are used to diagnose infection. When antibodies are detectable in the plasma or blood, an individual is said to have seroconverted and is deemed HIV positive. This usually occurs within six months of exposure to HIV and is the clearest evidence of an adaptive immune response to infection with HIV.

A vital part of the adaptive immune reponse is the cellular or cell-mediated response. It involves coordinated interactions between activated antigen-specific $CD4^+$ and $CD8^+$ T cells that leads to the destruction of virally-infected cells by antigen-specific $CD8^+$ T cells. This creates a paradoxical situation. The fact that the HIV-specific $CD4^+$ T cells, which are necessary for an efficient immune response against the virus, become targets for HIV-specific $CD8^+$ T cells causes further decay in the $CD4^+$ T cell population. The HIV-specific $CD4^+$ T cell population, on average, comprises approximately 1/100 total $CD4^+$ cells in the chronic phase of infection [Douek *et al.*, 2002].

HIV viral peptides can only be recognized via HIV-specific T cell receptor (TCR) major histocompatability complex (MHC) interactions. When an HIV peptide is presented via a TCR:MHC II interaction by an APC to an HIV-specific $CD4^+$ T cell, the cell becomes activated. The activation of the cell causes it to proliferate and differentiate into an effector cell. As effector cells, HIV-specific $CD4^+$ T cells act to coordinate other cells of the immune system to try to eradicate the virus from the host. During acute infection *in vivo*, rapidly proliferating HIV-specific $CD4^+$ T cells, in transition from naïve to full effector phenotype, are highly susceptible to HIV infection [Douek *et al.*, 2002; Mehandru *et al.*, 2004; Qingsheng *et al.*, 2005].

HIV-specific $CD4^+$ T cells help other cells, such as HIV-specific $CD8^+$ T

cells, proliferate and differentiate into effector cells by secreting cytokines such as interleukin-2 (IL-2). IL-2 is a T cell growth factor and is essential for the maintenance of an effective cellular immune response. $CD8^+$ T cells produce a cytokine called interferon-gamma (IFN-γ), that has antiviral properties.

HIV-specific $CD8^+$ T cells recognize HIV antigens in the context of an MHC class I-peptide complex on an APC and acquire a range of antiviral activities including the ability to kill virally-infected cells. $CD8^+$ T cells that kill infected cells are called cytotoxic T lymphocytes (CTL). CTL can kill virally-infected cells using a perforin-granzyme-based pathway. Perforin functions to "perforate" the membranes of virally-infected cells to allow entry of the enzyme granzyme, to trigger apoptosis of the infected target cell. CTL can kill their targets rapidly because they store these preformed cytotoxic proteins in inactive forms in a lytic granule and can kill many targets in succession [Janeway *et al.*, 2001; Isaaz *et al.*, 1995]. *In vitro* and *in vivo* studies have shown that CTL aptly kill virally-infected cells [Macatonia *et al.*, 1991; Musey *et al.*, 1997]. The best evidence for the clinical importance of the control of HIV-infected cells by HIV-specific CTL comes from studies relating the numbers and activity of $CD8^+$ T cells to viral load. The number of HIV-specific $CD8^+$ T cells is inversely correlated to plasma RNA viral load: when HIV-specific $CD8^+$ T cell numbers are high, the virus load is low. Similarly, patients with high levels of HIV-specific $CD8^+$ T cells show slower progression of disease than those with low levels [Landay *et al.*, 1993; Borrow *et al.*, 1994; Betts *et al.*, 2005; Hess *et al.*, 2004]. HIV-specific $CD8^+$ T cells can also carry out effector functions as non-cytolytic $CD8^+$ T cells by producing antiviral cytokines such as IFN-γ and tumor necrosis factors (TNF)-α and β. IFN-γ directly inhibits viral repli-

cation, and also induces the increased expression of MHC class I and other molecules involved in peptide loading of the newly synthesized MHC class I peptides in infected cells. This increases the chance that infected cells will be recognized as target cells for cytotoxic attack [Janeway *et al.*, 2001; McMichael & Rowland-Jones, 2001]. TNF-α and β can act synergistically with IFN-γ to enhance the antiviral attack. Ultimately, the immune response against HIV controls but does not eradicate HIV from the host.

As part of the cellular immune response against HIV, some HIV-specific T cells become long-lived memory cells. These memory cells, upon secondary, tertiary, etc. encounters with HIV, are primed to impose subsequent immune responses when re-challenged by the virus. The development of immunological memory is the hallmark of the adaptive immune response and is why we can become immune to some viruses, such as Varicella-Zoster Virus (VZV): the virus that causes chicken pox and shingles [Janeway *et al.*, 2001]. Secondary immune responses are typically fast and efficient: the host does not know that the immune system has been re-challenged. Once the infectious agent has been cleared from the body, the immune response effectively ends. However, because HIV is a chronic infection, the processes of T cell activation, proliferation and differentiation are ongoing. In some HIV-infected individuals, the continued presence of HIV can somehow impair these processes. For example, many studies have shown that HIV can eventually prevent the terminal differentiation of effector memory T cells into fully-functional mature effector cells (CD45RA+ CCR7-) [Champagne *et al.*, 2001; Van Baarle, 2002; Shankar *et al.*, 2000; Hess *et al.*, 2004; Yue *et al.*, 2004]. Cytokines necessary for maintenance of effective proliferative responses and proper maturation are

also reduced in some HIV-infected individuals [McNeil *et al.*, 2001; Kawamura *et al.*, 2003]. Naturally, impairment of any stage of the immune response provides the virus an advantage.

As previously indicated, several factors contribute to the slow steady depletion of $CD4^+$ T cells. One of these is the direct cytopathocity of HIV. Each infected cell that becomes activated as part of an immune response, not necessarily against HIV, becomes a virus factory. Eventually, these cells may succumb to death by continuous viral budding or via apoptotic mechanisms mediated by CTL.

1.5 Treatment

In the absence of a successful vaccine, alternative means are needed to cope with HIV. Presently, the only somewhat practical solution to the problem is antiretroviral drug treatment. Antiretroviral treatment effectively reduces the virus load in most HIV-1-infected individuals. There are currently four major classes of antiretroviral drugs: nucleoside analogue reverse transcriptase inhibitors (NRTIs), nonnucleoside reverse transcriptase inhibitors (NNRTIs), protease inhibitors (PIs) and fusion inhibitors (FIs). These drugs act at different points during the infection/replication process but all suppress viral replication. FIs prevent the host cell from becoming infected. NRTIs and NNRTIs prevent the provirus from being produced. PIs on the other hand act subsequent to infection of the host cell to prevent the formation of new virions. Ultimately, these drugs should be taken in combination to reap the full benefits of combination therapy. Highly active antiretroviral treatment (HAART)

generally comprises a combination of three NRTIs, NNRTIs and PIs and has proven quite effective in suppressing viral replication and reducing virus loads to undetectable levels, thereby prolonging the lives of HIV-infected individuals. However, due to toxicity of the drugs to the individual, adherence problems are prevalent among HAART users [Office of AIDS Research Advisory Council, 2004].

The toxicity of HAART can lead to secondary health problems and the necessity for additional prescription drugs to control clinical complications. In addition, antiretroviral drugs are quite costly to manufacture and distribute. Strict adherence is important in the context of HAART since the virus replicates very quickly. Non-adherence is associated with viral rebound and can induce the emergence of drug resistant virus that repopulates the host. In short, it is potentially dangerous to randomly interrupt drug treatment once it has been initiated because it is not known what the short-term or long-term effects will be.

Antiretroviral treatment has also been associated with changes in HIV-specific $CD8^+$ T cell activity while suppressing viral replication and thus reducing antigenic stimulation [Casazza *et al.*, 2005; Lacabaratz-Porret *et al.*, 2003; Appay *et al.*, 2002]. Without treatment, a high number of HIV-specific $CD8^+$ T cells often persists into late infection and can still be detectable when AIDS develops in some HIV-1-infected individuals [Appay *et al.*, 2002]. However, it is the quality, not just the quantity of these cells that is important in determining how an individual progresses through disease. This will be discussed further in Chapter 6. Since treatment can be initiated at any point during infection, it is important to investigate the clinical and immunological

effects of introducing and withdrawing treatment, such as changes in HIV-specific $CD8^+$ T cell activity, during the acute and chronic phases of infection to maximize potential benefits of treatment regimens during these phases. For example, studies show that initiation of antiretroviral treatment during the acute phase of infection preserves HIV-specific T cell populations to promote better prognoses and to reduce virological setpoints [Borrow *et al.*, 1994; Altfeld *et al.*, 2001; Rosenberg *et al.*, 2000; Oxenius *et al.*, 2000].

The chronic phase of infection is associated with an equilibrium state of the host. Antiretroviral treatment perturbs this equilibrium state by reducing the virus load dramatically. Therefore, it is vital to understand how the immune system players, such as the HIV-specific T cell populations, respond to this perturbation before attempting to assign treatment interruption regimens [Nikolova *et al.*, 2005; Benito *et al.*, 2003].

1.5.1 Treatment interruption

The goal of any interruption scheme is to maintain clinical benefits of treatment, such as low or undetectable virus load, while concurrently reducing drug toxicity to the individual. Monitored or structured treatment interruption studies allow an investigation into the clinical and immunological effects of missing or interrupting treatment. Studies show that HIV-specific immune responses can increase during a treatment interruption [Garcia *et al.*, 2000; Montaner, 2001]. This "boost" in the HIV-specific immune response (due to an increase in virus antigen load) does not necessarily represent constructive immune enhancement [Ortiz *et al.*, 2002]. There is variability in results from clinical trials. Some provide evidence to support constructive immune

enhancement and others provide evidence to refute this.

One of the reasons for variablity in experimental and clinical studies is the variability in test subjects. No two HIV-infected individuals progress through disease in exactly the same manner. Therefore, unless we know ahead of time how an individual is progessing through disease, only generalizations can be made as to how antiretroviral treatment will affect them, both clinically and immunologically, or when it is advisable to interrupt treatment. If we can pre-classify HIV-infected individuals in terms of disease progression, we may more confidently determine whether or not they will benefit from treatment interruption.

1.6 Fast and slow progressors

Studies have shown that HIV-infected individuals can be subgrouped with respect to disease progression rates [Jansen *et al.*, 2004]. Each HIV-infected individual in this study fits into one of two categories; those who reasonably control viral replication in the absence of treatment and those who do not. Reasonable control implies a balance between the HIV-specific $CD8^+$ T cells and the virus whereby the virus load is maintained at levels associated with slow or inapparent disease progression (low virological setpoint). More specifically, if an HIV-infected individual experiences rapidly falling CD4 counts and rapid viral rebound following treatment interruption, they are classified as a fast progressor. If an HIV-infected individual maintains a stable CD4 count and a virus load at a low level following treatment interruption, they are classified as a slow progressor. For the purposes of this thesis, a controllable or

low level comprises an average off-treatment virus load less than or equal to 4.5 (logarithmic scale) RNA copies per millilitre (ml) of blood. Conversely, an uncontrollable level comprises an average off-treatment virus load greater than 4.5 RNA copies per ml of blood.

The balance between the HIV-specific $CD8^+$ T cells and the virus in the HIV-infected study subjects can be examined by measuring the HIV-specific $CD8^+$ T cell activity on and off-treatment when the virus load is both low (undetectable) and high, respectively. The study participants in the cohort were not engaged in a structured treatment interruption trial, but periodically interrupted treatment either of their own volition, or under the advice of their clinician.

1.7 Why use modeling?

Since the outcome of a clinical trial may not be desirable and the immunological effects of interrupting treatment are not yet clearly defined, it is prudent to explore alternative means to investigate the effects of interrupting treatment. Mathematical modeling allows for an unobtrusive, safe means by which to test various treatment interruption strategies. Mathematical models are the tools we use to gain theoretical access to the real world. I have developed a novel mathematical model to examine the effects of treatment interruption and to investigate whether or not treatment interruption can be used to boost immune HIV-specific $CD8^+$ T cell responses to lower the virological setpoint.

In the following chapter, I provide an introduction to mathematical modeling of dynamical systems and describe how the model will be analysed and

how this analysis will be used to answer some of the questions raised here.

Chapter 2

Modeling of dynamical systems

> No human investigation can be called real science if it cannot be demonstrated mathematically. - Leonardo da Vinci (1452-1519)

This chapter is devoted to defining mathematical concepts using theorems and mathematical definitions. See introductory differential equations texts, such as Boyce and DiPrima [2004] for details.

2.1 Mathematical Models

Mathematical modeling of dynamical systems is a very useful tool for analyzing how a system evolves in time and how it reacts to perturbations. Mathematical models, in general, are sets of equations that describe the behaviour of a system via dependent and independent variables. The HIV-infected immune system can be modeled as a dynamical system of many variables including immune cell and virus populations. HIV pathogenesis is associated with changes in the size of each variable population as the immune system attempts to elim-

inate the virus from the host. The state of the HIV-infected immune system at any time t is specified by the values of the variables at t. Mathematical models that describe this system involve *nonlinear* differential equations because the variables in the model usually do not change in direct proportion to other variables. In general, exact solutions cannot be found for nonlinear systems. Therefore, analysis of such nonlinear dynamical systems is commonly approached in a qualitative manner, especially when the system involves many variables. This is because the components of the equations that make up the system are not known precisely. Dynamical systems analysis allows us to find the eventual behaviour of a system without having to know parameter values accurately or even having to know the terms of the system precisely. By analyzing the system in a qualitative manner, we do not have to rely on numerical techniques which, in turn, rely on the validity or precision of the equations from which they originate.

In this study, I analyze the system by determining the stability of the system in the neighborhood of equilibrium points, or fixed points, according to the following protocol:

- finding the fixed points of the system of equations
- linearizing the system in the neighborhoods of the fixed points
- determining the eigenvalues of the resulting linearized equations to assess stabilities of fixed points

This protocol allows the determination of the stability properties of any fixed points that may exist. *Maple* software was used to determine all fixed points and eigenvalues.

2.2 Finding the Fixed Points

Fixed points are locations in phase space. Phase space is the set of all possible states of a dynamical system. The dimension of the phase space is the number of variables in the system. The path in phase space traced out by a solution of a dynamical system is called an orbit. A fixed point is a special type of orbit that is just a single point in phase space as the system changes with time.

Phase plane analysis is a way to determine the locations and stabilites of fixed points in phase space. It characterizes a system and its solutions in a single picture called a phase portrait or a phase diagram. Figure 2.1 is a phase diagram illustrating the location of a single fixed point in three-dimensional phase space. This particular fixed point is an asymptotically stable spiral node and is located at the point $(x, y, z) = (2, 2, 4)$. All orbits in $(x - y - z)$-phase space spiral inward to this stable fixed point. Directional arrows are not shown in the diagram.

A fixed point, also known as an equilibrium or steady state, corresponds to a motionless state of a system. The fixed point can be stable or unstable, depending on nature of the eigenvalues of the fixed point. The fixed point in Figure 2.1 is (asymptotically) stable in that it attracts nearby orbits in phase space. A fixed point that is unstable repels nearby orbits in phase space.

Theorem 2.2.1. *Consider the nonlinear system of ordinary differential equations*

$$\frac{dx_i}{dt} = f_i(\mathbf{x}), \ \ for \ i = 1, \ldots, n \tag{2.2.1}$$

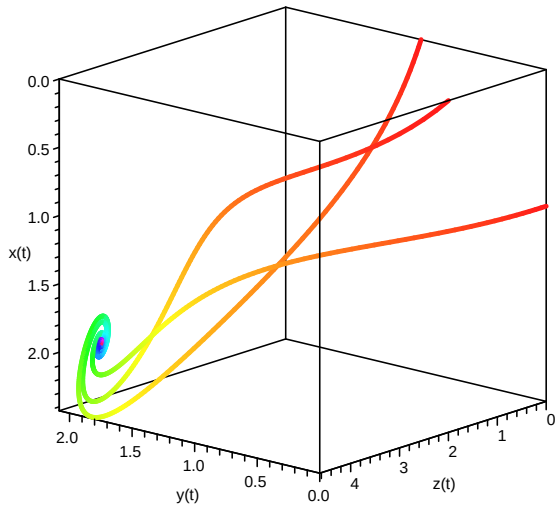

Figure 2.1: A phase diagram for a three-dimensional system showing a single stable fixed point at $(x, y, z) = (2, 2, 4)$.

where f_i are nonlinear functions of $\mathbf{x}$*, and*

$$\mathbf{x} = (x_1, \ldots, x_n).$$

We can write (2.2.1) in vector notation as $\dot{\mathbf{x}} = \mathbf{f}(\mathbf{x})$.

Definition 2.2.1. *A fixed point $\overline{\mathbf{x}} \in \mathbb{R}^n$ is a point for which*

$$f_i(\overline{\mathbf{x}}) = 0$$

for all $i = 1, \ldots, n$.

This means that the point $\overline{x}$ corresponds to a constant solution of the differential equation system (2.2.1). The fixed point corresponds to an equilibrium

solution of the equation: $\mathbf{x}(t) = \overline{\mathbf{x}}$ that satisfies the system of equations for all time.

Every fixed point inherently has a stability property. To determine the stability property of a fixed point, we must solve the eigenvalue problem. To do this, we must first understand ideas and techniques of linear algebra.

2.3 Solution of a system of linear ODEs

Solving a system of linear (or nonlinear) differential equations can be facilitated using linear algebra. Linear algebra is the part of algebra that deals with the theory of linear equations and linear transformation. We use these theories to solve the eigenvalue problem.

A set of n simultaneous linear algebraic equations in n variables,

$$\begin{array}{cccccc} a_{11}x_1+ & a_{12}x_2+ & \cdots+ & a_{1n}x_n & = b_1 \\ \vdots & & & & \vdots \\ a_{n1}x_1+ & a_{n2}x_n+ & \cdots+ & a_{nn}x_n & = b_n \end{array}$$

can be written as

$$\mathbf{Ax} = \mathbf{b},$$

where the $n \times n$ matrix $\mathbf{A}$ and the vector $\mathbf{b}$ are given and the components of $\mathbf{x}$ are to be determined.

The equation

$$\mathbf{Ax} = \mathbf{b}$$

can be viewed as a linear transformation that transforms a given vector $\mathbf{x}$ into

a new vector $\mathbf{b}$. To find such vectors, we set

$$\mathbf{b} = \lambda \mathbf{x}$$

where λ is a scalar proportionality factor, and seek solutions of the equations

$$\mathbf{A}\mathbf{x} = \lambda \mathbf{x}$$

or

$$(\mathbf{A} - \lambda \mathbf{I})\mathbf{x} = \mathbf{0},$$

where $\mathbf{I}$ is the identity matrix. The latter equation has nonzero solutions if and only if λ is chosen so that

$$det(\mathbf{A} - \lambda \mathbf{I}) = 0.$$

This equation is called the characteristic equation. Values of λ that satisfy the characteristic equation are called eigenvalues of the matrix $\mathbf{A}$. Thus, the eigenvalues of $\mathbf{A}$ are the roots or solutions of the characteristic equation.

It turns out that the eigenvalue problem for systems of linear algebraic equations is connected to the solution of systems of linear differential equations. The solution of a system of linear differential equations reduces to the eigenvalue problem for algebraic equations in the following way.

An non-autonomous system of n linear differential equations

$$\begin{aligned} \dot{x}_1 &= a_{11}(t)x_1 + \quad a_{12}(t)x_2 + \quad \cdots + \quad a_{1n}(t)x_n \\ &\vdots \\ \dot{x}_n &= a_{n1}(t)x_1 + \quad a_{n2}(t)x_2 + \quad \cdots + \quad a_{nn}(t)x_n \end{aligned}$$

can be written as

$$\dot{\mathbf{x}} = \mathbf{A}(t)\mathbf{x},$$

where $x_1, x_2, \ldots, x_n$ are the components of a vector $\mathbf{x}$, and $a_{11}(t), \ldots, a_{nn}(t)$ are the elements of an $n \times n$ matrix $\mathbf{A}(t)$.

The eigenvalues of a matrix $\mathbf{A}$ can be used to find solutions for differential equations in the following way:

Theorem 2.3.1. *The system of differential equations* $\dot{\mathbf{x}} = \mathbf{A}\mathbf{x}$ *has solution* $\mathbf{x}(t) = c\mathbf{v}e^{\lambda t}$ *if and only if for the matrix* $\mathbf{A}$*,* λ *is an eigenvalue and* $\mathbf{v}$ *its corresponding eigenvector.*

2.4 Nonlinear systems of ODEs

To linearize a nonlinear system of differential equations $\dot{\mathbf{x}} = \mathbf{f}(\mathbf{x})$ near any point $\mathbf{x}$, we calculate and solve the Jacobian matrix of the system.

Definition 2.4.1. *The Jacobian matrix is the matrix of all first-order partial derivatives of a vector-valued function. It represents the best linear approximation to a differentiable function near a given point.*

Given the system $\dot{\mathbf{x}} = \mathbf{f}(\mathbf{x})$, we linearize around a fixed point using the Jacobian to obtain $\dot{\mathbf{x}} = \mathbf{J}\mathbf{x}$, where $\mathbf{J}$ is evaluated at the fixed point.

Consider the vector-valued function that contains the real-valued component functions $f_1(x_1, x_2)$ and $f_2(x_1, x_2)$. The partial derivatives of these functions can be organized in a 2×2 matrix as follows:

$$\mathbf{J} = \begin{pmatrix} \frac{\partial f_1}{\partial x_1} & \frac{\partial f_1}{\partial x_2} \\ \frac{\partial f_2}{\partial x_1} & \frac{\partial f_2}{\partial x_2} \end{pmatrix} \tag{2.4.1}$$

The characteristic equation and eigenvalues are found by applying the rules described for linear systems. However, instead of solving the eigenvalue problem using the matrix **A** (see section 2.3), we solve

$$\mathbf{Jx} = \lambda\mathbf{x}$$

or

$$(\mathbf{J} - \lambda\mathbf{I})\mathbf{x} = \mathbf{0},$$

where the Jacobian matrix **J** takes the place of the matrix **A**. Thus the eigenvalues can be found by solving the characteristic equation

$$det(\mathbf{J} - \lambda\mathbf{I}) = 0.$$

The solutions of the characteristic equation are precisely the eigenvalues of the matrix **J**.

2.5 Stability of a fixed point

The stability properties of fixed points for nonlinear systems are generally the same as for linear systems in the neighborhood of the fixed point. From the solutions of linear systems we gain information about the stabilites of fixed points from direct inspection of the eigenvalues. Eigenvalues can be real-valued or complex. Complex eigenvalues always exist in pairs and cause oscillatory effects in system solutions. If the real parts of all eigenvalues are negative, then the fixed point is stable.

For stable fixed points, all solutions with initial conditions in the neighborhood of the fixed point will approach it as $t \to \infty$. If one or more eigenvalues

of a fixed point have positive real parts, the fixed point is unstable. Some or all of the solutions with initial conditions starting in the neighborhood of the fixed point will diverge from it as $t \to \infty$. Thus, upon inspection of the real parts of the eigenvalues for a given n^{th}-order nonlinear system of ordinary differential equations, the stability of the given fixed point can be determined.

Fixed points can be locally or globally stable. A fixed point is locally stable with orbits from nearby initial conditions tending to the stable fixed point if the eigenvalues of a linearized system have negative real parts. A fixed point is globally stable if *all* initial conditions have orbits tending to the stable fixed point.

So far, I have described how to obtain qualitative information about nonlinear systems of equations without having to solve them. The determination of fixed points and their stabilities based on the nature of the eigenvalues provides a geometric picture of the system solutions. In order to further assess the qualitative nature of a dynamical system, bifurcation theory can be employed.

2.6 Bifurcation Analysis

Bifurcation analysis is a powerful tool in dynamical systems. It allows a visualization of qualitative changes that may occur in a dynamical system as a single parameter is varied, and tells us about the sensitivity of the system to parameter changes. Its power lies in the fact that the system behaviour and how it reacts to perturbations (changes in parameter values) can be known, without having to know exact parameter values. Approximations or estimates of parameter values provide a starting point from which these behaviours can

be examined, and are usually obtained experimentally.

Qualitative changes in a system can be visualized by generating bifurcation diagrams. A bifurcation diagram is a plot which gives fixed point solutions as a function of a (control) parameter. This plot represents all possible long-term behaviours of the system as the parameter is varied. The diagram is made up of branches that are either solid or dotted lines representing the locations of stable or unstable fixed points of the system, respectively.

Treatment is represented by a parameter in the model developed for this thesis. Since this parameter represents an external stimulus on the system (the system functions *normally* in the absence of this stimulus), its value can be varied in a controlled way to see how the system reacts according to changes in fixed points and their stabilites. Therefore, bifurcation analysis will allow a visualization of the effects of treatment on the system.

A bifurcation in mathematics involves the divergence of the eventual state of a dynamical system. At a bifurcation value of a parameter, the qualitative nature of the solution of the system changes in that the number of fixed points and/or the stability of fixed points changes.

Solutions are different on either side of a bifurcation point. For example, if a critical parameter changes, a fixed point that once was stable, may become unstable, as is the case in a transcritical bifurcation. A solution that may represent a undesirable state for an HIV-infected individual may involve stable low levels of T cells and detectable virus load in the absence of treatment. A more favorable state may be induced using treatment. Treatment lowers the virus load to undetectable levels and generally raises T cell counts. Since some system behaviours may be harder to change than others that may be

highly sensitive to small pertubation or change, it is necessary to study the mechanisms by which various system behaviours arise before attempting to manipulate the system.

Bifurcation analysis is also useful when examining potential qualitative changes that may occur when other parameters in the system are varied. In this study, bifurcation theory will be used to test the effects of modulating treatment efficacy on the system and to examine the effects of varying a parameter that represents the removal rate of infected cells from the system. (Refer to Chapter 4.)

2.6.1 Types of bifurcations

There are several common types of bifurcations. A saddle-node bifurcation is a local bifurcation in which two fixed points of a dynamical system annihilate one another. Figure 2.2 is a bifurcation diagram showing a saddle-node bifurcation. The phase space variable is $\overline{x}$ and the control parameter is c. The bifurcation point is at c=0 and $\overline{x} = 0$ ($(c, \overline{x}) = (0, 0)$). Stable and unstable fixed points are drawn as solid and dotted lines, respectively. The diagram shows all possible long-term behaviours of $\overline{x}$ for a range of values for c. For example, when c=1, there are two fixed points: one is stable (solid branch) and one is unstable (dotted branch).

A saddle-node bifurcation is the most common (generic) type of bifurcation in biological systems. However, saddle-node bifurcations do not arise for the model developed for this thesis. Rather, transcritical bifurcations are seen. Transcritical bifurcations are saddle-node bifurcations but with a special kind of symmetry in the equations, albeit not obvious. The equations in the model

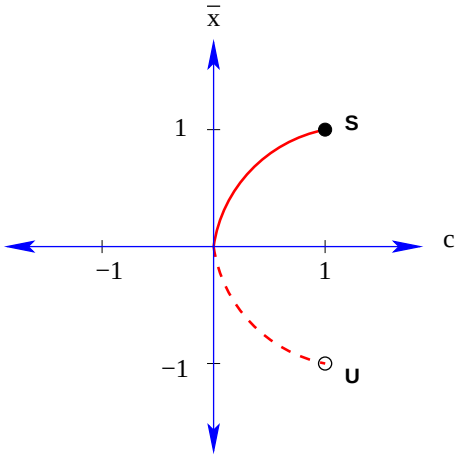

Figure 2.2: A bifurcation diagram showing a saddle-node bifurcation

developed for this thesis have this special symmetry, thus we see transcritical bifurcations and not saddle-node bifurcations.

A transcritical bifurcation involves an exchange of stability between two fixed points. At a particular parameter value, the fixed point transfers its stability to another fixed point. Figure 2.3 is a bifurcation diagram showing a transcritical bifurcation. The phase space variable is $\overline{x}$ and the control parameter is c.

Figure 2.3 shows that there is an exchange in stability at the bifurcation point $c = 1$ and $\overline{x} = 1$ $((c, \overline{x}) = (1, 1))$ where two branches of fixed points intersect and transfer their stability types.

In this study, only **stable** fixed points are analyzed because the system will move from an initial state toward stable fixed points and away from unstable fixed points.

Armed with the above mathematical theories and definitions, I first intro-

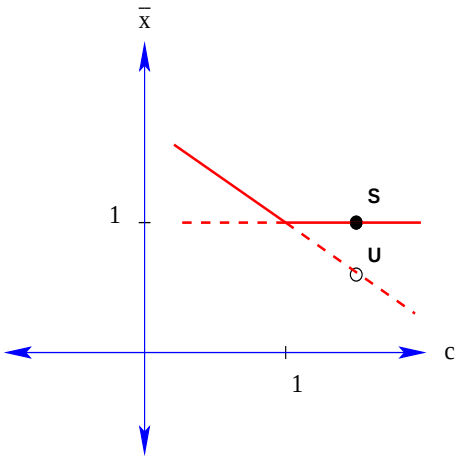

Figure 2.3: A bifurcation diagram showing a transcritical bifurcation

duce a basic model of HIV infection and describe its strengths and weaknesses. The novel model developed for the thesis is then introduced and I proceed with an analysis of the model system. The analysis adheres to the following methodology.

1. solve the system for fixed points
2. determine the stability of these fixed points via eigenvalues
3. generate phase diagrams in three-space to show how variable trajectories from various initial conditions move through four-space
4. plot numerical solutions of the system variables with respect to time
5. generate bifurcation diagrams to illustrate how fixed point solutions change as a control parameter is varied

Plotting the numerical solutions of a system gives us trajectories or time series of each variable in the system. This is a another graphical method that allows us to obtain information about a system and its solutions. Bifurcation diagrams give us a much broader view of the system behaviour because we can visualize many trajectories at one time.

2.7 The Basic Model - A Dynamical System

Perhaps the most well known dynamical system describing HIV pathogenesis is that of Perelson *et al.* [1995]. This basic model describes the rate of change of three variables: uninfected target cells, T, infected target cells, T^*, and virus particles, V, at any time t. The equations for this basic model are as follows:

$$\frac{dT}{dt} = s + pT\left(1 - \frac{T}{T_{max}}\right) - d_T T - kVT \tag{2.7.1a}$$

$$\frac{dT^*}{dt} = kVT - \delta T^* \tag{2.7.1b}$$

$$\frac{dV}{dt} = N\delta T^* - cV \tag{2.7.1c}$$

The parameters are s, p, T_{max}, d_T, k, δ, N and c and represent rate constants. Uninfected target cells enter the system from the thymus at a constant rate s. The growth of this population is assumed to be logistic in that it can only grow until it reaches a carrying capacity T_{max}. This carrying capacity is regulated by homeostatic mechanisms that regulate overall T cell numbers: there is a finite number of cells that can occupy the body at any given time. p is the intrinsic growth rate. T cells will ultimately die at some constant rate

d_T, also as part of normal homeostatic mechanisms.

When the virus enters the system, the susceptible uninfected target cell population becomes infected at rate k (proportional to T and V). This creates the population of infected target cells, T^*, whose members die at a constant rate δ. As each infected cell dies a certain number of virions (N) are released into the body. The virus also dies by natural processes at a constant rate c.

The model predicts a single stable fixed point $(\overline{T}, \overline{T}^*, \overline{V})$ with positive fixed point coordinates. These coordinates vary according to the parameter values selected.

This basic model has allowed crucial insights into the 'fast' dynamics of the virus and how it reacts to antiretroviral treatment. Antiretroviral treatment is introduced to the equations as a parameter that modifies the infection rate k or the production rate of virus $N\delta$. The viral turnover rate is extremely high; higher than previously estimated or assumed [Perelson *et al.*, 1995; Ho *et al.*, 1995]. Numerous other models utilize the fundamental concepts of this basic model as it quite elegantly and simplistically describes the general behaviours of the variables T, T^* and V and how they change together in time both in the presence and absence of treatment.

Perelson has had many collaborations to develop an array of mathematical models that describe various aspects of HIV infection. Essunger and Perelson [1994] analyze models that describe the interactions between virgin, activated and memory $CD4^+$ T cells and HIV. These models use a previously developed model as a template [McClean & Nowak, 1992] but are novel in their explicit treatment of a latent stage in HIV infection. All terms in the models are expressed in predator-prey, logistic or density dependent forms.

Callaway and Perelson [2002] describe a set of models that are derived from the standard model to explain sustained low on-treatment viral loads. These models include quiescent, chronically-infected and latently-infected cells, account for the role of follicular dendritic cells, cell-mediated immunity and also differential effects of antiretroviral drugs.

Denise Kirschner has also assumed a prevalent role in the development of mathematical models of HIV infection. In 1993, Kirschner collaborated with Perelson and DeBoer [Perelson *et al.*, 1993] to describe the dynamics of HIV infection of $CD4^+$ T cells. This model describes the interactions between uninfected, latently and actively-infected T cell and virus populations. The model shows that HIV cytopathicity of peripheral $CD4^+$ T cells and their precursors account for T cell depletion and explains low levels of infected cells and ongoing viral replication. In 1996, she developed a three-dimensional mathematical model that includes uninfected $CD4^+$ T cells, infected $CD4^+$ T cells and the virus [Kirschner, 1996]. A novel aspect of this model was the incorporation of a term that describes the T cell-mediated immune response against HIV mediated by $CD4^+$ and $CD8^+$ T cell populations. The term is a saturation term and represents the growth of both $CD4^+$ and $CD8^+$ T cell populations due to antigenic stimulation due to the presence of the virus.

Antigen specificity is a key element to consider when incorporating the T cell-mediated immune response against HIV into a mathematical model [Altes *et al.*, 2003]. With respect to cellular immune responses, only HIV-specific cells can respond to and mount effective anti-HIV attacks. Leon Cooper published the first mathematical model [Cooper, 1986] to include the antigen-specific immune response to HIV. The model considers the effect of the immune response

by including antigen-specific T and B cells and how they respond to HIV. The model accounts for interactions between antigen and antigen presenting cells, but assumes that they occur only between B cells and the virus.[1] All terms in the model are of constant, density-dependent or predator-prey forms.

There are many other ordinary differential equation models of HIV infection that describe the interactions between immune cell populations and HIV. The development and use of these models was often for the same basic purposes: to describe HIV infection as realistically as possible in an attempt to elucidate parameter values, explain the slow steady depletion of $CD4^+$ T cells, or show the effects of treatment and treatment interruption [Notermans *et al.*, 1998; Komarova *et al.*, 2003; Frost *et al.*, 2002; Nowak & Bangham, 1996; Ding & Wu, 1999; Coffin, 1995; Borghans *et al.*, 1999; Agrawal & Linderman, 1996; Altes *et al.*, 2003; Bajaria *et al.*, 2002; Blower, 2001; Hraba & Dolezal, 1996, Wodarz & Nowak, 2002; Nowak *et al.*, 1997; Stafford *et al.*, 1999; Witten & Perelson, 2004; Kirschner *et al.*, 2000; Brandt *et al.*, 2001; Perelson & Nelson, 1999; Perelson, 2002].

The use of mathematical models to predict the effects of interrupting treatment have become increasingly prevalent throughout the years [Adams *et al.*, 2004; Lori & Lisziewicz, 2001; De Jong *et al.*, 1997]. Significantly, Bonhoeffer *et al.* [2000] developed a set of population dynamical models to study the effect of structured treatment interruptions on immune effector cells, latently-infected cells and drug resistance. They use three versions of the same model to test the effects of treatment interruption on the model system. The terms in the model are of constant, density-dependent and predator-prey form. The

[1] B cells are one of three types of professional antigen presenting cell.

models show that if the effector cell population grows during the treatment phase of a treatment interruption regimen, then transient or sustained virus control can be achieved whereby the virological setpoint is reduced to lower levels.

One of the purposes of this thesis is to examine the role of HIV-specific $CD8^+$ T cells in determining disease progression patterns with the aim of testing treatment interruption regimens. To do this, I explicitly include these cells as a variable population in a model of HIV immunopathogenesis. Studies show that the virus is controlled by the development of potent HIV-specific $CD8^+$ T cell responses [Musey *et al.*, 1997; Kalams *et al.*, 1999; Dalod *et al.*, 1999]. Studies have also shown a direct correlation between that activities of HIV-specific $CD8^+$ T cells in the acute and chronic phases of infection, the virological setpoint level and subsequent disease progression patterns. HIV-specific $CD8^+$ T cells kill virally-infected $CD4^+$ T cells, thereby constituting a source of depletion of both antigen-specific and non-specific $CD4^+$ T cells. Therefore, the explicit inclusion of a variable in a model that represents the HIV-specific $CD8^+$ T cell population can allow us to more precisely describe and examine the dynamical interactions between these and other HIV-specific T cell and virus populations. In turn, this will allow us to make accurate predictions about disease progression patterns and the effects of treatment and treatment interruptions with respect to the roles of HIV-specific T cells.

In assigning meaning to model variables, I consider the fact that cellular immune responses against HIV are mediated by HIV-specific T cells: they are the only subset of T cells that have the ability to recognize the virus and mount effective anti-HIV responses. It is assumed that the immune response

is directly proportional to the number of HIV-specific ($CD4^+$) T cells [Altes *et al.*, 2003; Callaway *et al.*, 1999; Kalams *et al.*, 1999].

The novelty of the model arises from its description of the dynamical interactions between HIV-specific T cell and virus populations. I explicitly include a variable that represents the $CD8^+$ T cell population and make the T cell populations antigen specific. The model borrows from previously discussed conceptual ideas in deriving some of the terms. In the following chapter, I provide a description of the model variables and parameters. To assess the impact of including a variable that represents the HIV-specific $CD8^+$ T cells on disease progression and attainment of the virological setpoint, I perform an analysis of the system when this population of cells is included both implicitly and explicitly in the system.

Chapter 3

Model of HIV Immunopathogenesis

The model is four-dimensional and describes the dynamical interactions between three HIV-specific immune cell populations and HIV. The variables in the model are given in Table 3.1 and represent populations expressed as a concentration per microlitre (ul) of blood.

Table 3.1: Description of model variables

variable	description	units
U	uninfected HIV-specific $CD4^+$ T cells	cells/ul
I	infected HIV-specific $CD4^+$ T cells	cells/ul
C	HIV-specific $CD8^+$ T cells	cells/ul
V	plasma virus	virions/ul

As previously described, I am interested in the activities of HIV-specific $CD8^+$ T cells. Therefore, I express the variable populations as HIV-specific T cell populations.

The parameters in the model are described in Table 3.2. The parameters are rates reported in the literature with exception of ρ.

Table 3.2: Description of model parameters

$a_1 =$	influx rate of uninfected HIV-specific $CD4^+$ T cells
$a_2 =$	proliferation rate of uninfected HIV-specific $CD4^+$ T cells due to antigenic stimulation
$\alpha =$	saturation rate constant for uninfected HIV-specific $CD4^+$ T cells
$a_3 =$	rate of encounters $\times$ the probability that uninfected HIV-specific $CD4^+$ T cells are converted to infected cells when an encounter occurs, $U \rightarrow V$
$a_4 =$	death rate of uninfected HIV-specific $CD4^+$ T cells
$b_1 =$	rate at which infected HIV-specific $CD4^+$ T cells are killed by effector $CD8^+$ T cells (CTL)
$b_2 =$	death rate of infected HIV-specific $CD4^+$ T cells
$c_1 =$	influx rate of HIV-specific $CD8^+$ T cells
$c_2 =$	proliferation rate of HIV-specific $CD8^+$ T cells due to antigenic stimulation
$\delta =$	saturation rate constant for HIV-specific $CD8^+$ T cells
$c_3 =$	death rate of HIV-specific $CD8^+$ T cells
$g_1 =$	clearance rate of plasma virus
$h =$	the number of virions released per infected $CD4^+$ T cell
$\rho =$	conversion constant = the fraction of the total $CD4^+$ T cell population that is HIV-specific
$r =$	antiretroviral treatment

ρ is a dimensionless parameter which converts the number of virions re-

leased per infected HIV-specific CD4$^+$ T cell to the number released per infected CD4$^+$ T cell. For simplicity, I assume that the ratio of HIV-specific CD4$^+$ T cells to total CD4$^+$ T cells is constant throughout infection. This accounts for the fact that virions can be produced by all infected CD4$^+$ T cells and not just infected HIV-specific CD4$^+$ T cells.

The model is as follows:

$$\frac{dU}{dt} = a_1 + \frac{a_2 UV}{\alpha + V} - a_3 UV - a_4 U \tag{3.0.1a}$$

$$\frac{dI}{dt} = a_3 UV - b_1 IC - b_2 I \tag{3.0.1b}$$

$$\frac{dC}{dt} = c_1 + \frac{c_2 CV}{\delta + V} - c_3 C \tag{3.0.1c}$$

$$\frac{dV}{dt} = \frac{1}{r+1} b_2 \rho h I - g_1 V \tag{3.0.1d}$$

3.1 Description of Terms

The terms in the model are of constant, saturation, density-dependent or predator-prey form and are described in the following subsections.

3.1.1 Equation 1

(3.0.1a) is composed of four terms: two terms to account for growth and two terms to account for loss of the uninfected HIV-specific CD4$^+$ T cells. The term a_1 is a rate constant and represents the influx of these cells, assumedly of thymic origin. The second term represents the production of HIV-specific CD4$^+$ T cells due to antigenic stimulation by the virus where a_2 is the proliferation rate constant. Proliferation is the dominant growth factor for this subset

of cells. α represents the saturation constant whereby there is some maximum rate of proliferation (a_2U) when all the antigenically stimulated cells are saturated: an increase in antigenic stimulation will not further increase the growth rate of the infected cell population. The third term in the equation represents the switch in status from uninfected to infected which is dependent on V. a_3 is the infection rate constant, and infection is assumed to occur at a rate proportional to the density of virions and uninfected target cells. a_4 is the death rate constant. Death is assumed to be proportional to the density of uninfected HIV-specific $CD4^+$ T cells.

3.1.2 Equation 2

In accordance with (3.0.1a), the first term in (3.0.1b) represents the growth of infected HIV-specific $CD4^+$ T cells where a_3 is the infection rate constant. Infection is assumed to occur at a rate proportional to the product of the density of virions and uninfected target cells. The second term represents the loss or removal of infected HIV-specific $CD4^+$ T cells due to antiviral effects of HIV-specific $CD8^+$ T cells. The constant b_1 is the removal rate. Removal is assumed to occur at a rate proportional to the product of the density of infected HIV-specific $CD4^+$ T cells and HIV-specific $CD8^+$ T cells. These cells are assumed to impose various antiviral effects on infected cells; the end product being their removal from the system. The third term represents natural death of infected cells where b_2 is the death rate. This death rate is assumed to be proportional to the density of infected HIV-specific $CD4^+$ T cells, and is larger than that of the uninfected cells.

3.1.3 Equation 3

(3.0.1c) is much like (3.0.1a) but comprises only three terms: two to account for growth and one to account for loss of HIV-specific $CD8^+$ T cells. The first term in (3.0.1c) represents the influx rate of HIV-specific $CD8^+$ T cells, also of thymic origin. The second term represents the production of HIV-specific $CD8^+$ T cells due to antigenic stimulation, where c_2 is the proliferation rate constant. δ represents the saturation rate constant whereby the rate becomes saturated at high virus concentrations. Proliferation is assumed to occur at a rate proportional to the product of the density of $CD8^+$ T cells and the virus at time t, and will only result in a rise in the HIV-specific $CD8^+$ T cell population up to a certain point. The third term in (3.0.1c) represents the natural loss of HIV-specific $CD8^+$ T cells where the constant c_3 represents the death rate. Death is proportional to the population of HIV-specific $CD8^+$ T cells itself.

3.1.4 Equation 4

(3.0.1d) comprises two terms to account for growth and loss of the virus population. The growth term assumes that the production of new virions is dependent on the infected cell population. The rate at which new virions are produced (enter the system) is proportional to the HIV-specific $CD4^+$ T cell population in that when an infected HIV-specific cell dies, it releases a number of new infectious virions into the surrounding environment. However, the overall production of new virions will be dependent on the total infected cell population, which is assumed to be proportional to the infected HIV-specific

$CD4^+$ T cell population at any time t. We can simply multiply the rate at which plasma virions are produced in the HIV-specific population (b_2h) by ρ to obtain the rate of virions released by the total infected $CD4^+$ T cell population. The loss term represents the natural clearance of plasma virions where g_1 is the clearance rate.

Antiretroviral treatment is incorporated into the model in the form of a single parameter (r) that modifies the production rate of the new virions. Protease inhibitors greatly decrease the production of new infectious virus by interfering with the infection process. The more potent or efficient the protease inhibitor is, which is dependent on dosage and timing, the greater the value of the parameter r. I assume that the protease inhibitor does not decrease the rate of viral production by 100% but by approximately 99% (approximately a 2-log drop in virus load). In chapter 4, I examine the effects of varying the value of r using bifurcation analysis.

3.2 Assigning values to the parameters

Typically, in a lower order system of equations, the system would be solved prior to inputting numerical parameter values to obtain general expressions for the fixed point solutions of the system. These general expressions allow the stipulation of conditions whereby if a parameter lies in a certain range, then certain behaviours are elicited by the system. However, in higher order systems, such as the model system in this thesis, these general expressions can become quite cumbersome making it virtually impossible to stipulate parameter conditions. This problem is circumvented by inputting numerical parameter

values reported from the literature into the model equations prior to solving for fixed points. In doing so, instead of general expressions for fixed points, numerical values are obtained. Table 3.3 summarizes the selected numerical parameter values with literature sources.

Table 3.3: Parameter values, units and sources

parameter	value	units	source
a_1	10	$\frac{cells}{ul \times day}$	Kirschner & Perelson, 1995
a_2	0.05	$\frac{1}{day}$	Perelson *et al.*, 1999
α	1000	$\frac{virions}{ul}$	Kirschner, 1996
a_3	0.001	$\frac{ul}{virions \times day}$	Kirschner *et al.*, 2000
a_4	0.02	$\frac{1}{day}$	Kirschner & Perelson, 1995
b_1	0.05	$\frac{ul}{cells \times day}$	Bonhoeffer *et al.*, 2000
b_2	0.5	$\frac{1}{day}$	Essunger & Perelson, 1994
c_1	1	$\frac{cells}{ul \times day}$	Adams *et al.*, 2004
c_2	0.05	$\frac{1}{day}$	Bonhoeffer *et al.*, 2000
c_3	0.1	$\frac{1}{day}$	Bonhoeffer *et al.*, 2000
δ	1000	$\frac{virions}{ul}$	Kirschner, 1996
g_1	13	$\frac{1}{day}$	Callaway & Perelson, 2002
h	600	$\frac{virions}{CD4\ T\ cell}$	Essunger & Perelson, 1994
ρ	100	$\frac{CD4}{HIV-specific\ CD4}$	Douek *et al.*, 2000

These numerical parameter values are first input into the equations and then the protocol outlined in Chapter 2 is used to analyze the model system.

3.3 Omission of the C equation

The best way to determine the effects of explicitly including the C equation (3.0.1c) in the model is to omit it from the original system and perform an analysis of the remaining three-dimensional system where the activities of the $CD8^+$ T cells are implicitly characterized. In doing so, I can test whether the three-dimensional system, which excludes this equation, yields different predicted behaviour from the four-dimensional system.

The three-dimensional system is identical to the four-dimensional system with the exception of the I equation (3.0.1b): it no longer contains a term that accounts for the loss of infected cells from an extraneous source.

The three-dimensional model is as follows:

$$\frac{dU}{dt} = a_1 + \frac{a_2 UV}{\alpha + V} - a_3 UV - a_4 U \tag{3.3.1a}$$

$$\frac{dI}{dt} = a_3 UV - b_2 I \tag{3.3.1b}$$

$$\frac{dV}{dt} = \frac{1}{r+1} b_2 h \rho I - g_1 V, \tag{3.3.1c}$$

where the parameters are as described in Tables 3.2 and 3.3.

3.3.1 Fixed points and stabilities

The fixed points $(\overline{U}, \overline{I}, \overline{V})$ are found by setting the right-hand-sides of equations (3.3.1) equal to zero and solving the algebraic equations. The numerical parameter values (Table 3.3) are substituted into the model to obtain the following three nontrivial fixed points,

$$
\begin{aligned}
(\overline{U}, \overline{I}, \overline{V}) &= (500, 0, 0), && \text{(3.3.2a)} \\
&= (0.22, -0.43, -998.94), && \text{(3.3.2b)} \\
&= (0.22, 20.01, 46182.79). && \text{(3.3.2c)}
\end{aligned}
$$

In the absence of treatment, the model predicts the existence of two equilibrium states (3.3.2a) and (3.3.2b) associated with viral clearance from the host. (3.3.2a) shows that the uninfected cell population is healthy but susceptible to infection. However, the infected cell and virus populations have died out. Similarly in (3.3.2b), the uninfected cell population is healthy and small, but the infected cell and virus populations have died out. HIV is never completely eradicated from the host. Therefore, biologically, these equilibrium points are unrealistic in that negative values cannot be present. However, fixed point (3.3.2c) comprises three positive values for $\overline{U}$, $\overline{I}$ and $\overline{V}$. This means that the host is living with the virus. More specifically, the fixed point that corresponds to this state implies that the host is living with the virus but is not controlling the virus. This is based on the fact that the viral setpoint is 46182.79. (Refer to Chapter 1.)

The eigenvalues for fixed points (3.3.2a) and (3.3.2b) are

$$\lambda_{1,2,3} = -0.02, 115.88, -129.38,$$

and

$$\lambda_{1,2,3} = -89.09, 14.72 + 55.03i, 14.72 - 55.03i,$$

indicating that (3.3.2a) is an unstable saddle point and (3.3.2b) is an unstable spiral saddle point. This is due to the positive real-valued components of each

set of eigenvalues. The third fixed point (3.3.2c) is stable by its eigenvalues

$$\lambda_{1,2,3} = -46.35, -0.51, -12.80.$$

This is due to the negative real-valued eigenvalues.

Thus, for the chosen parameter set, the three-dimensional model system predicts the existence of three fixed points: two of which are unstable and one of which is stable and biologically relevant. Based on numerical simulations, no other stable phenomena were observed. The remainder of this section focuses solely on the stable fixed point (3.3.2c) since the system moves from an initial state (U_0, I_0, V_0) toward the stable fixed point and away from the other fixed points based on these simulations.

3.3.2 Location and nature of fixed point

The location and stability of the stable fixed point in three-dimensional space can be illustrated by generating a three-dimensional phase diagram as shown in Figure 3.1. To reiterate, the fixed point is

$$(\overline{U}, \overline{I}, \overline{V}) = (0.22, 20.01, 46182.79)$$

and has eigenvalues

$$\lambda_{1,2,3} = -46.35, -0.51, -12.80.$$

The eigenvalues tell us not only about the stability of the fixed point, but the nature. Since the eigenvalues comprise three real-valued components, the fixed point is a node. In Figure 3.1, three orbits are shown originating from three different, randomly selected initial conditions $(U_0, I_0, V_0) = (1, 5, 50)$,

$(5, 1, 50)$ and $(1, 1, 50)$. All three orbits head toward the stable fixed point $(\overline{U}, \overline{I}, \overline{V}) = (0.22, 20.01, 46182.79)$ in phase space.

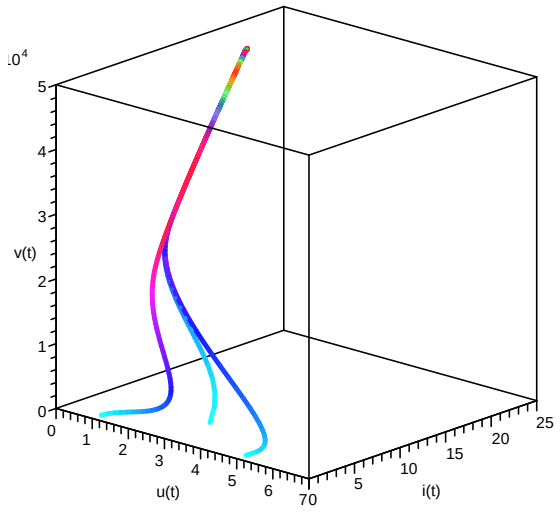

(a) $U - I - V$-plane

Figure 3.1: Phase diagram in the $U - I - V$-plane with initial conditions $(U_0, I_0, V_0) = (1, 5, 50), (5, 1, 50), (1, 1, 50)$

3.4 Solving the system

The fixed point can be visualized in another way. The system can be solved and the variable solutions plotted against time in a time series plot. This is a useful graphical method in that it can be used to predict how each variable trajectory approaches the fixed point or equilibrium state and how much time this takes.

The equilibrium state corresponds to the fixed point with coordinates $(\overline{U}, \overline{I}, \overline{V})$.

The acute phase of infection is generally marked by transient rapid changes in immune cell and virus populations as the variable populations approach the equilibrium state. The chronic phase of infection is marked by the arrival at the equilibrium state. Once the equilibrium state is reached, the variable populations (as a system) stay there unless an external influence, such as treatment, displaces them or the individual moves out of the chronic phase and into AIDS. The model does not attempt to predict the transition to an AIDS state. Since I am interested in the dynamical interactions during the chronic phase of infection and am investigating the changes in the variables during treatment interruption, it is not noteworthy that the model does not predict an AIDS state. This is discussed further in Chapter 6. As described in the previous section, perturbation of the equilibrium state with treatment does not cause the system to switch to another equilibrium state: it returns to the original one. This is because there is only one stable equilibrium state predicted by the model for the chosen parameter set. For each two-dimensional time-series plot, the x-axis is the time (days), and the y-axis is the number of T cells in each respective T cell population and the virus load at time t. The paths traced out by the variable trajectories are analogous to HIV disease progression. When the trajectories plateau, they have reached the equilibrium state.

To plot the solutions, the parameter set (Table 3.3) and a set of initial conditions are required as input into the system of equations. I chose the initial condition $(U_0, I_0, V_0) = (1, 1, 50)$ as it was used previously as an initial condition for the phase diagram (Figure 3.1).

Figure 3.2 is the time series plot of the numerical solutions with $r = 0$. All variables are plotted on a logarithmic scale due to the fact that the virus exists at high numbers. The uninfected cell population is seen in red, the infected cell population in blue and the virus population in green.

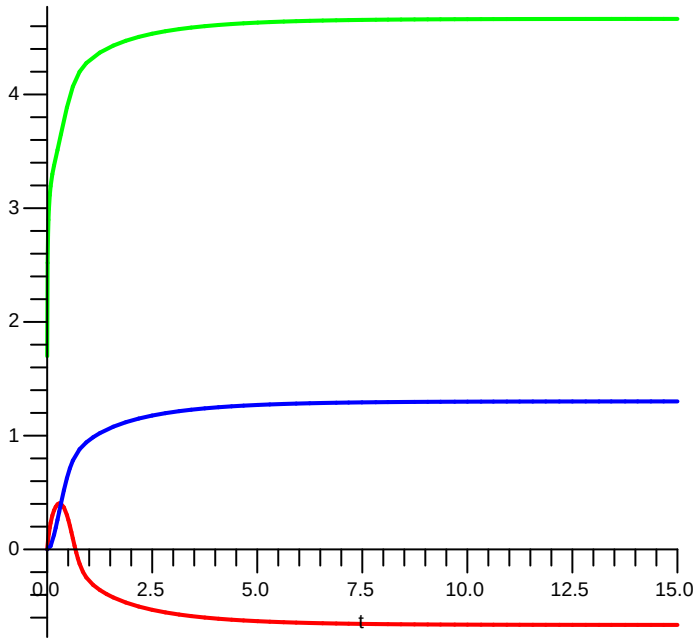

(a) $(0.22, 20.02, 46182.79) \rightarrow (-0.66, 1.30, 4.66)$

Figure 3.2: Time (days) series plot of U, I and V when $r = 0$ showing fixed point (linear and log scales)

Figure 3.2 shows that the dynamics are very fast. The equilibrium state is attained very early in disease progression. According to the system solu-

tions, the virus population (V) immediately begins to grow directly to reach a high off-treatment equilibrium level (setpoint) ($\overline{V} = 4.66$). Subsequently, the uninfected HIV-specific $CD4^+$ T cell population grows due to antigenic stimulation and subsequently decays due to infection by the virus. The infected HIV-specific $CD4^+$ T cell population grows slowly as the uninfected cell population decays until both populations reach the equilibrium state. After approximately 8 days, all three populations have reached the equilibrium state. No oscillations are predicted.

Clinical trends in changing T cell counts and virus loads in early infection are in agreement with this result. However, in a clinical setting the equilibrium state never occurs as early as 8 days post-infection. It usually takes up to one year for an individual to reach this state and enter the chronic phase of infection. I address this in Chapter 4.

3.4.1 Fixed points and stability with treatment

Now that it is known how the system behaves off-treatment, I want to know how it behaves on-treatment. This is done by direct inspection of fixed points and eigenvalues generated for progressively higher parameter values and also using bifurcation analysis. Changing the value of r is analogous to examining the effects of changing the dosage or potency of treatment. How well treatment lowers the viral setpoint ($\overline{V}$) will depend on how much it reduces the viral production rate.

For each value of r, there is one corresponding stable fixed point. Ultimately, I set a value for the treatment parameter r based on the how effectively it reduces the viral production rate to lower the viral setpoint to an

undetectable level. I am aiming to use a value of r that reduces the viral setpoint to one percent of its non-treatment value ("a 2-log drop"), as this is how treatment efficacy is measured. By clinical standards, a viral load of less than 50 HIV RNA copies per cubic ml plasma or a viral load of less than 398 HIV RNA copies per cubic ml plasma are considered undetectable, depending on the sensitivity of the RNA detection assay used. This will be reflected in the value obtained for $\overline{V}$ in the fixed point.

Table 3.4 shows the respective changes in each of $\overline{U}$, $\overline{I}$ and $\overline{V}$ as the treatment parameter r is assigned progressively higher values. Also shown are the changes in eigenvalues and stabilities of each fixed point.

Table 3.4: The effects of assigning sequentially higher values to r

r	$\overline{U}$	$\overline{I}$	$\overline{V}$	eigenvalues	stability
0	0.22	20.02	46182.79	-46.35,-0.51,-12.80	S
100	21.88	19.81	452.55	-0.22+0.04i,-0.22-0.04i,-13.52	S
500	108.55	16.42	75.64	-0.04+0.18i,-0.04-0.18i,-13.50	S
1000	216.88	11.90	27.44	-0.02+0.11i,-0.02-0.11i,-13.50	S
1500	325.22	7.35	11.31	-0.02+0.07i,-0.02-0.07i,-13.50	S
2000	433.55	2.80	3.23	-0.01+0.04i,-0.01-0.04i,-13.50	S
2200	476.88	0.94	1.02	-0.01+0.02i,-0.01-0.02i,-13.50	S
2307	500	0	0	-0.02,-0.000064,-13.50	S

For progressively higher values of r, there are more uninfected cells at equilibrium as indicated by the changes in the value of $\overline{U}$. For progressively higher values of r, there are fewer infected cells and lower viral setpoints at equilibrium as indicated by changes in the values of $\overline{I}$ and $\overline{V}$.

The eigenvalues associated with each fixed point change accordingly as the value of r is varied. When $r = 0$, they indicate that the fixed point is a stable node, as previously established. For values of $r = 100$ to $r = 2000$, the eigenvalues comprise both (negative) real-valued and complex parts indicating that the corresponding fixed points are asymptotically stable spiral node points. Eigenvalues with complex parts cause oscillatory effects in the system as illustrated in Figure 3.3. When the value of r is increased to $r = 2307$, the eigenvalues contain a near zero value indicating a switch in stability at this point. I discuss the switch of stability in the system when the bifurcation analysis is done in subsection 3.4.3. The changes in eigenvalues and the induction of oscillations can be visualized by plotting the system solutions for various values of r in time series plots.

3.4.2 Solving the system with treatment

Figure 3.3 illustrates the effects on the solutions when the value of r is assigned progressively higher values. Since treatment regimens can be initiated at any time point post-infection (usually following acute phase resolution), treatment is initiated on day 30.

Figure 3.3 shows that for progressively higher r values, the viral production rate progressively decreases to reflect progressively 'preferable' fixed point values which are analogous to disease equilibrium states. Treatment induces damped oscillations in all cases indicating transient instability in the system. In general, as the value of r is increased, the uninfected cell population grows to successively higher peak values, and the infected cell and virus populations decay to successively lower trough values. In addition, the oscillations increase

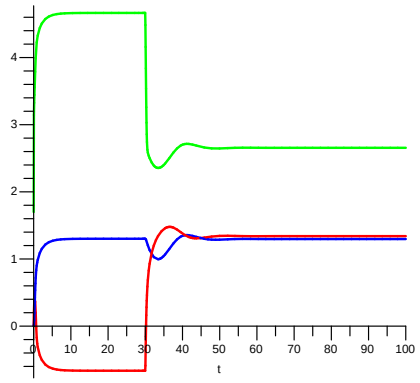

(a) $(21.88, 19.81, 452.55) \rightarrow (1.34, 1.30, 2.66)$, $r = 100$

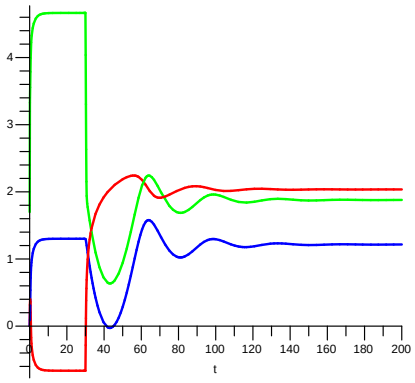

(b) $(108.55, 16.42, 75.64) \rightarrow (2.04, 1.22, 1.88)$, $r = 500$

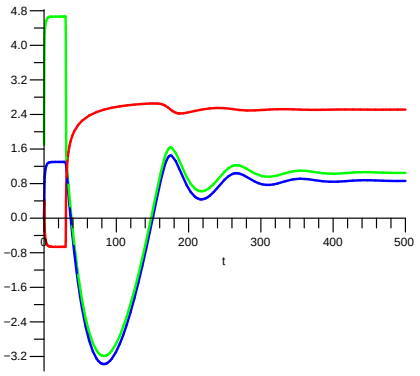

(c) $(325.22, 7.35, 11.31) \rightarrow (2.51, 0.87, 1.05)$, $r = 1500$

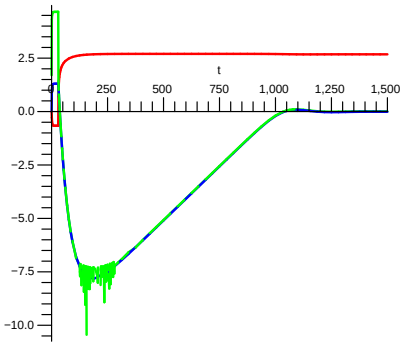

(d) $(476.88, 0.97, 1.02) \rightarrow (2.68, -0.01, 0.0086)$, $r = 2200$

Figure 3.3: Time (days) series plots for U, I, V (linear and log scales) for progressively higher values of r

in period and amplitude as the value of r is increased, and are not sustained. Thus, the higher the value of r, the longer it takes for the system to reach the equilibrium state. According to Table 3.4 and Figure 3.3, a value of $r = 100$ reduces the virus load by 2-logarithms. This is equivalent to a 99% reduction in the viral production rate.

Figure 3.3(d) demonstrates that as the value of r increases, $\overline{I}$ and $\overline{V}$ decay to reach such low levels that they almost become extinct. This is indicated by the roughness in the variable trajectories that trough around day 250. This roughness is attributable to the fact that the values for $\overline{I}$ and $\overline{V}$ during this period are minute. Importantly, this activity also indicates that there exists a critical value of r whereby if its value surpasses some critical value, the I and V populations will become extinct. This can be confirmed using bifurcation theory.

As far as visualizing system changes as the parameter r is varied, time series plots are useful in determing time-associated changes in the system. However, a more complete way to visualize the changes in the behaviour of the system as the parameter r is varied is to use bifurcation diagrams.

3.4.3 Bifurcation analysis

Figures 3.4(a), (b) and (c) show how $\overline{U}$, $\overline{I}$ and $\overline{V}$ change as the parameter r is varied, respectively. Each diagram shows the respective fixed point value at a particular value of r.

Figure 3.4 confirms that the fixed points are stable for a large range of r values. At values of $r < 2307$, the fixed points are stable with positive coordinates. The value of r is directly related to $\overline{U}$ and indirectly related to $\overline{I}$ and

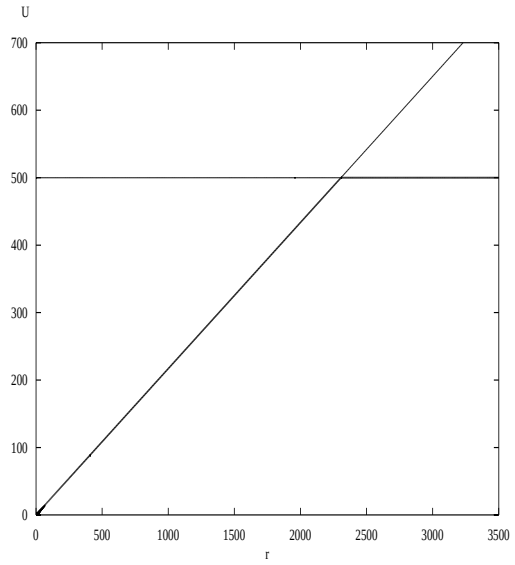

(a) Variation of r with respect to $\overline{U}$

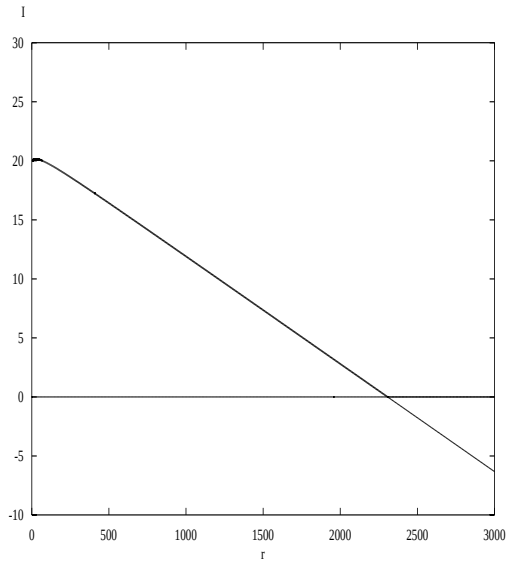

(b) Variation of r with respect to $\overline{I}$

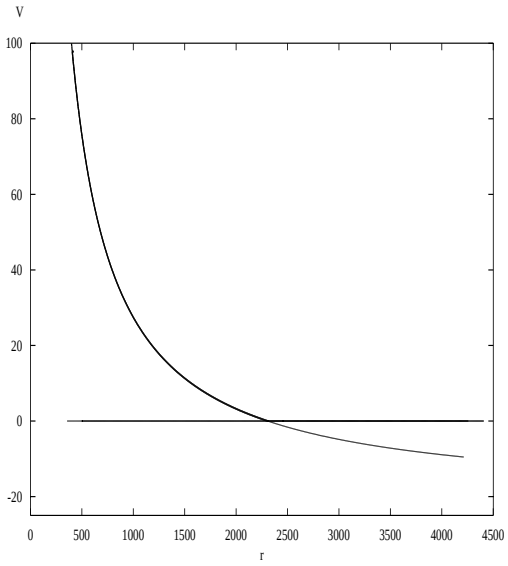

(c) Variation of r with respect to $\overline{V}$

Figure 3.4: Bifurcation diagrams showing changes in $\overline{U}$, $\overline{I}$ and $\overline{V}$ as r is varied.

$\overline{V}$: large r corresponds to large $\overline{U}$ and small $\overline{I}$ and $\overline{V}$. A transcritical bifurcation occurs at $r = 2307$. At the bifurcation point, the fixed points exchange stability where the original stable fixed point solution with positive fixed point coordinates becomes unstable, and the unstable fixed point (3.3.2a) becomes stable. This fixed point $(\overline{U}, \overline{I}, \overline{V}) = (500, 0, 0)$ remains stable for all values $r \geq 2307$. When $r = 2307$, the viral production rate is reduced by 99.96%. This means that treatment drives the infected cell and virus populations to extinction when it reduces the viral production rate by at least 99.96%.

At these high treatment efficacies where the virus production rate is reduced by at least 99.96%, the turnover rate of the virus is modified such that the loss rates of virus from the system exceed the production rate. Since treatment reduces the production rate of the virus in the model, it makes sense that increasing the effectiveness of treatment to a point below 100% will reduce the viral production rate below the virus removal rates to result in the virus-free equilibrium: a 0% production rate is not required to bring the bring the virus population to 0 as long as the overall loss of virus from the system is greater than the gain.

The fact that this can theoretically happen does not mean that it does in reality. In fact, in reality, protease inhibitors do not act to reduce the viral production rate by virtually 100% (99.96%) but by approximately 99%. The model simply predicts that if drugs were in fact efficient enough to reduce the viral production rate by virtually 100% (99.96%), then the virus would be eradicated from the system because the loss rates of the virus would exceed the production rate.

Studies show that this prediction can be clinically confirmed. $CD4^+$ T cell

depletion has been suggested as a way to eliminate the virus from the system [Tepic, 2004]. By suddenly removing (surgically depleting) a fraction of $CD4^+$ T cells, the system is perturbed such that the removal rate or death rate of the $CD4^+$ T cells changes to increase past some critical value [DeBoer & Boucher, 1996]. Thus, the rate at which $CD4^+$ T cells die is altered (increased) to reduce the susceptible pool of cells to allow the system to clear the virus.

Therefore, even though the model allows for the theoretical existence of a virus-free equilibrium state induced by treatment, this state is never attained in reality because treatment is never this efficient.

Bifurcation analysis confirms the existence of a disease equilibrium state whereby the equilibrium virus load successively decreases as the efficacy of treatment is increased. It also confirms the existence of a virus-free equilibrium at near 100% treatment efficacy. Since the disease equilibrium state can be perturbed using any given treatment efficacy (r), a value of $r = 100$ is selected to test treatment interruption regimens because it mimics the effects of efficient protease inhibitors when input into the model. That is, it reduces the viral setpoint by 2-logs.

3.4.4 Treatment interruption

According to Table 3.4, when the treatment parameter has a value of $r = 100$, the viral setpoint is reduced by 2-logs to a low detectable level ($\overline{V} = 452.55$) by clinical standards by reducing the viral production rate by 99%. The fixed point associated with the treatment parameter with value $r = 100$ is

$$(\overline{U}, \overline{I}, \overline{V}) = (21.88, 19.81, 452.55),$$

and it is stable. See Table 3.4.

To demonstrate the effects of treatment interruption, the system is solved while intermittantly assigning treatment parameter values $r = 0$ (off-treatment) and $r = 100$ (on-treatment) using a piecewise linear function. The solutions are then plotted in a time series plot as before.

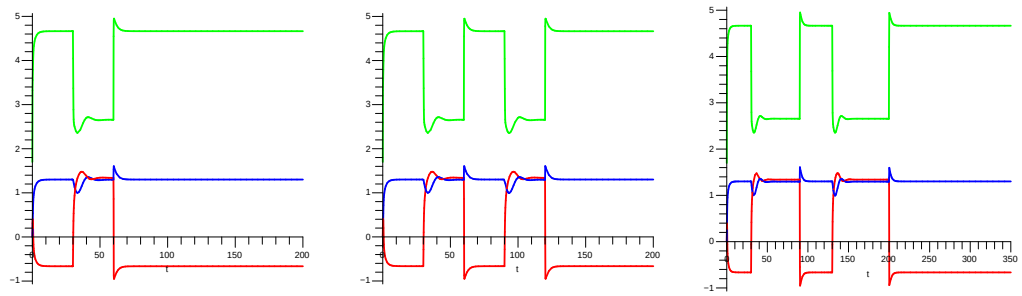

(a) 30/30/off (b) 30/30/30/30/off (c) 30/60/40/70/off

Figure 3.5: Time (days) series plots for U, I and V showing three treatment interruption regimens with $(\overline{U}, \overline{I}, \overline{V}) = (0.22, 20.01, 46182.79)$

Figure 3.5 shows the time series plots for three different treatment interruption regimens. In all cases, treatment is initiated 30 days post-infection. The first regimen is a 30 day-off, 30 day-on, off regimen. The second is a 30 day-off, 30 day-on, 30 day-off, 30 day-on, off regimen and the third is a 30 day-off, 60 day-on, 40 day-off, 70 day-on, off regimen. The aim in selecting these three regimens is to demonstrate the effects of a single interruption, multiple interruptions and interruptions of different durations. Figure 3.5(a) shows a

30 day off-treatment period followed directly by a 30-day on-treatment period which is subsequently interrupted indefinitely. Following the perturbation of the system with a single treatment phase (30 days), the system returns to its original pre-treatment equilibrium state. Figure 3.5(b) shows that following two perturbations with treatment the system again returns to its original pre-treatment equilibrium state. The behaviours of the variable trajectories are identical for both treatment interruption regimens in 3.5(a) and (b). The uninfected cell population grows and the infected cell and virus populations decay when treatment is on. But, the number of interruptions does not appear to affect the end result which is the arrival at the pre-treatment equilibrium state. To determine whether durations of treatment or interruption phases would cause the same result, we modified both as seen in Figure 3.5(c). Even when the durations of the on-treatment and off-treatment phases are modified, the outcome is the same as for the other regimens: the system returns to its original pre-treatment state. The only time the system does not return to this state is when treatment is kept on as seen in Figure 3.6. In this case, the system returns to the original on-treatment equilibrium state. The conclusion is the same: whether treatment is kept on or taken off, what happens in the interim in a treatment interruption regimen does not affect the re-arrival at either the off or on-treatment equilibrium states. This was a predictable result in that there is only single stable fixed point: only one place to go.

In summary, the three-dimensional model predicts that following a very short acute phase, the system solutions reach an equilibrium state. The fixed

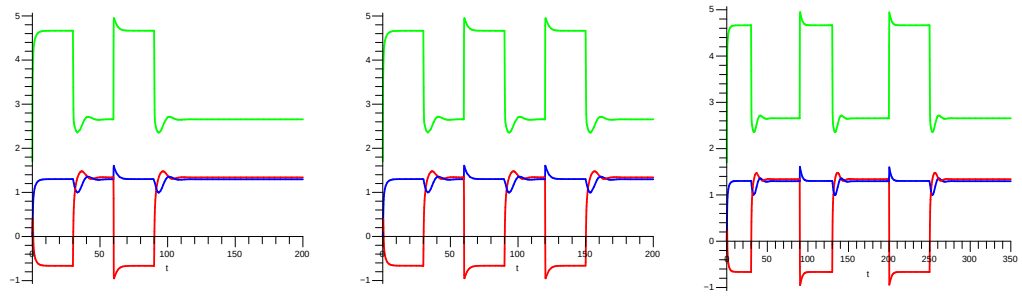

(a) 30/30/30/on (b) 30/30/30/30/30/on (c) 30/60/40/70/50/on

Figure 3.6: Time (days) series plots for U, I and V showing three treatment interruption regimens with $(\overline{U}, \overline{I}, \overline{V}) = (21.88, 19.81, 452.55)$

point values that correspond to the equilibrium state reflect a lack of control of virus in that the viral setpoint is 4.66. The fixed point coordinates $\overline{U}$ and $\overline{I}$ indicate that there are almost no uninfected HIV-specific CD4$^+$ T cells and many times more infected cells than uninfected cells. Treatment acts to lower the viral setpoint when the treatment parameter has value in the range $0 < r < 2307$ and eliminates the virus when it is equal to or exceeds a value of $r = 2307$. When we fix the value of r at $r = 100$, it decreases the viral production rate by 99%, subsequently lowering the viral setpoint by 99%. Treatment transiently delays disease progression and increases the uninfected cell population while decreasing the infected cell and virus populations. If treatment is kept on, the model predicts that an individual can indefinitely maintain an undetectable viral setpoint and a hearty HIV-specific CD4$^+$ T cell count. One of the most important findings is that treatment interruptions do not work to lower the viral setpoint. Unless treatment is re-initiated and

kept on following a treatment interruption, the off-treatment equilibrium state reappears, according to three-dimensional model predictions.

Now that the system behaviour without the C equation is known, the behaviour of the complete four-dimensional system can be examined following the same protocol. With the inclusion of C as a variable, which again represents the HIV-specific $CD8^+$ T cell population, I will be able to investigate how the HIV-specific $CD8^+$ T cell population changes in the context of treatment interruptions. I will therefore be able to confirm whether treatment interruptions can be used to boost these responses during the off-treatment phases.

Chapter 4

The model

The four-dimensional model is as follows:

$$\frac{dU}{dt} = a_1 + \frac{a_2 UV}{\alpha + V} - a_3 UV - a_4 U \tag{4.0.1a}$$

$$\frac{dI}{dt} = a_3 UV - b_1 IC - b_2 I \tag{4.0.1b}$$

$$\frac{dC}{dt} = c_1 + \frac{c_2 CV}{\delta + V} - c_3 C \tag{4.0.1c}$$

$$\frac{dV}{dt} = \frac{1}{r+1} b_2 h \rho I - g_1 V. \tag{4.0.1d}$$

4.1 Fixed points and stabilities

The fixed points $(\overline{U}, \overline{I}, \overline{C}, \overline{V})$ are found by setting the right-hand-sides of the equations (4.0.1) equal to zero and solving the resultant algebraic equations. The numerical parameter values from Table 3.3 were substituted into the equations to obtain the following four fixed points,

$$
\begin{aligned}
(\overline{U}, \overline{I}, \overline{C}, \overline{V}) &= (500, 0, 10, 0), && \text{(4.1.1a)} \\
&= (0.22, -0.43, 0.02, -998.94), && \text{(4.1.1b)} \\
&= (-4.98, -0.83, -239.94, -1923.06), && \text{(4.1.1c)} \\
&= (0.63, 6.93, 18.89, 16003.28). && \text{(4.1.1d)}
\end{aligned}
$$

The four-dimensional model predicts the existence of two equilibrium states (4.1.1a) and (4.1.1b) associated with viral clearance from the host and an equilibrium state (4.4.1c) associated with the death of the host. The model also predicts an equilibrium state (4.1.1d) where the host is living with the virus. The fixed point that corresponds to this state comprises four positive coordinates ($\overline{U}$, $\overline{I}$, $\overline{C}$, $\overline{V}$) whereby the host is controlling the virus reasonably well. This is based on the fact that the viral setpoint is 16003.28. (Refer to Chapter 1.)

The eigenvalues for fixed points (4.1.1a), (4.1.1b) and (4.1.1c) are

$$\lambda_{1,2,3,4} = -0.02, -0.10, 115.62, -129.62,$$

$$\lambda_{1,2,3,4} = 14.70 + 54.96i, 14.70 - 54.96i, -88.95, -47.14,$$

and

$$\lambda_{1,2,3,4} = 3.51 + 5.58i, 3.51 - 5.58i, -6.63, 0.13$$

indicating that each of these fixed points is unstable where (4.1.1a) is an unstable saddle point and (4.1.1b) and (4.4.1c) are unstable spiral saddle points. However, the fourth fixed point (4.1.1d) is stable by its eigenvalues

$$\lambda_{1,2,3,4} = -19.24, -9.55, -1.63, -0.05,$$

which indicate that it is a stable node.

Thus, the four-dimensional model predicts the existence of four equilibrium states; three of which are unstable and one of which is stable and biologically relevant. The fact that there are negative values in fixed points (4.1.1a) and (4.1.1b) implies a non-realisitic state in that HIV is never entirely cleared from the host. This is not a problem since these fixed points are unstable.

The remainder of this section focuses on the stable fixed point (4.0.1d) since the system moves from an initial state (U_0, I_0, C_0, V_0) toward the stable fixed point and away from the unstable fixed points. Although global stability of the stable fixed point has not been demonstrated, numerical simulations have not demonstrated the existence of more complicated behaviour.

4.1.1 Quantitative comparison of fixed points with and without C equation

Recall that the stable fixed point coordinates for U, I, (C) and V in the three and four-dimensional systems are

$$(\overline{U}, \overline{I}, \overline{V}) = (0.22, 20.01, 46182.79)$$

and

$$(\overline{U}, \overline{I}, \overline{C}, \overline{V}) = (0.63, 6.93, 18.89, 16003.28),$$

respectively. It appears upon direct inspection of the fixed point values that it is "preferable" to explicitly include the C equation in the system as it appears to subject "positive pressure" on the system: it decreases the viral setpoint $(\overline{V})$ and the infected cell population at equilibrium $(\overline{I})$ and increases the uninfected cell population at equilibrium $(\overline{U})$. (An HIV-infected individual with

a virus load of 4.2 would be considered to be controlling the virus better than an individual with a virus load of 4.66.) Specifically, when the C equation is explicitly included in the model there is a larger predicted population of uninfected cells (three times as large), a smaller predicted population of infected cells (three times as small) and a smaller predicted virus population (three times as small) at off-treatment equilibrium. Therefore, the explicit inclusion of the C equation as a variable in the system renders the fixed point solution more desirable and also realistic because HIV-specific $CD8^+$ T cells in fact do impose antiviral pressure on the virus to reduce the virus load. I make further comparisons between the three and four-dimensional systems upon further analysis of the four-dimensional system.

As previously discussed, phase diagrams are useful for visualizing the locations and stabilities of stable fixed points. Figure 4.1 shows the location and stability of the stable fixed point

$$(\overline{U}, \overline{I}, \overline{C}, \overline{V}) = (0.63, 6.93, 18.89, 16003.28)$$

in three-dimensional phase space. To reiterate, its eigenvalues are

$$\lambda_{1,2,3,4} = -19.24, -9.55, -1.63, -0.05$$

and tell us that this fixed point is a stable node, as depicted in the phase diagram.

Each of the three orbits originate from an initial condition (U_0, I_0, C_0, V_0) and traces out a distinct path in phase space to eventually arrive at the stable fixed point. The initial conditions were randomly selected to represent the number of T cells and amount of virus that an HIV-infected individual starts off with. The fact that we can randomly assign initial conditions means that

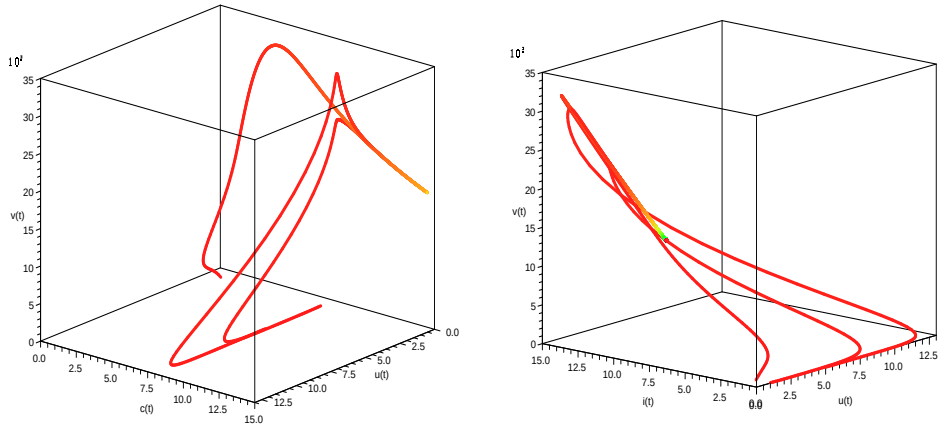

(a) $U - C - V$ space (b) $U - I - V$ space

Figure 4.1: Phase diagram from two perspectives with initial conditions $(U_0, I_0, C_0, V_0) = (1, 1, 1, 50), (5, 0, 8, 1), (1, 0, 8, 50)$

an infected individual can start off with any number of HIV-specific T cells ($CD4^+$ or $CD8^+$) and virus and will end up at this equilibrium state. This result will further be discussed in Chapter 7.

4.2 Solving the system

Now that we know the location of the fixed point in phase space, we want to know when the fixed point solution (equilibrium state) is reached with respect to time. We solve the system and plot a time series graph of the variable solutions using the parameter set from Table 3.3 and the initial condition $(U_0, I_0, C_0, V_0) = (1, 1, 1, 50)$. All variable populations are plotted on a loga-

rithmic scale. The uninfected cell population is seen in red, the infected cell population in blue, the HIV-specific $CD8^+$ T cell population is seen in cyan and the virus population is seen in green.

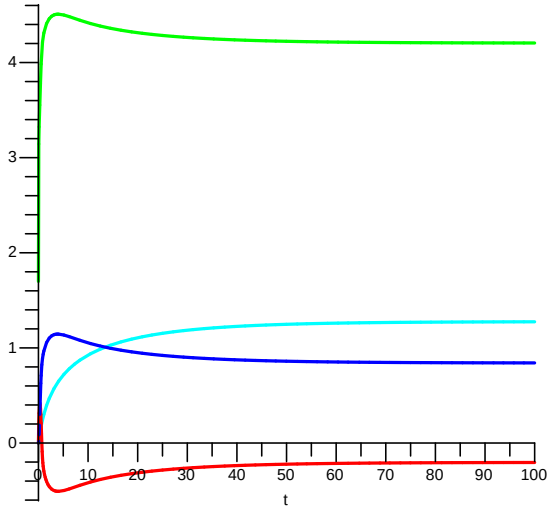

(a) $(\overline{U}, \overline{I}, \overline{C}, \overline{V}) = (0.63, 6.93, 18.89, 16003.28)$

Figure 4.2: Time (days) series plot of U, I, C and V (linear scale) $(r = 0)$

The variable trajectories follow similar patterns as for the three-dimensional system in that the populations reach the equilibrium state following a concomitant rise of virus, uninfected and infected T cell populations, and subsequent decay of the uninfected T cell population, as seen in Figure 4.2. In general, the populations change very quickly and immediately during the acute phase of infection. Just three hours post-infection, three of the four variable populations (U, I and V) have changed dramatically to reach peak or trough values.

See Figure 4.3 for details of blow-up of time axis.

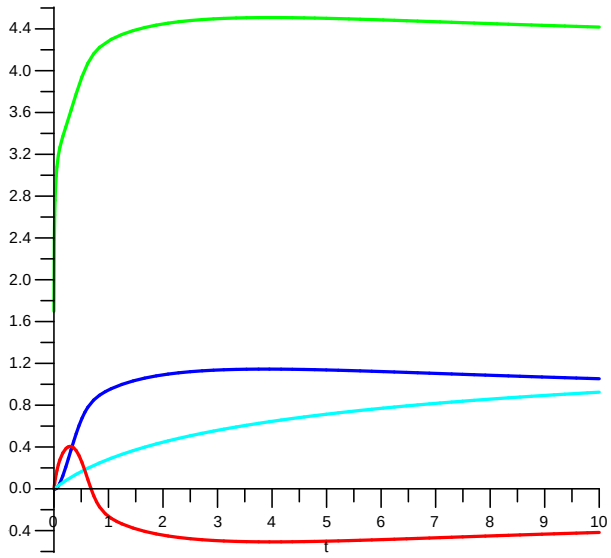

(a) $(\overline{U}, \overline{I}, \overline{C}, \overline{V}) = (0.63, 6.93, 18.89, 16003.28)$

Figure 4.3: Blow-up of time series plot of U, I, C and V (linear scale) $(r = 0)$

The virus population grows immediately following entry into the system. The uninfected HIV-specific $CD4^+$ T cell population grows for a brief period in response to the growing virus population. Because these cells are susceptible to infection, this population eventually decays quickly as they become infected. This decay is accompanied by growth of the infected HIV-specific $CD4^+$ T cell population. This is an expected result in that the cells that become infected originate from the uninfected cell pool. The HIV-specific $CD8^+$ T cell population grows more gradually as compared with the other three populations. It does not respond as quickly or dramatically to the presence of the

virus in the first few hours of infection. As the infection progresses past day 1, each variable population changes more slowly. (Refer to Figure 4.2.) As a result of the expanding HIV-specific $CD8^+$ T cell population and the lack of susceptible uninfected cells, the virus population continues to decay which in turn spurs the decay of the infected cell population and re-establishment of a small uninfected cell population. After approximately 80 days, all four populations have reached the equilibrium state as seen in Figure 4.2.

4.2.1 Comparison of time series plots for three and four-dimensional systems

If we compare the three and four-dimensional times series plots (Figure 4.4) we can see that it takes a longer period of time for all populations to reach the equilibrium state when C is explicitly included in the system as a variable (Figure 4.4b).

This result also lends to the realism of the four-dimensional system. It is a more realistic portrayal of the chronology of the progression through the acute and chronic phases of infection.

It is important to bear in mind that the model describes the activities of HIV-specific T cell populations, therefore it is possible that the rapid progression to the equilibrium state is characteristic of the specific interactions between HIV-specific populations and HIV. The infection rate of HIV-specific T cells is the highest found reported value ($a_3 = 0.001$) to account for the fact that these cells are preferentially infected and depleted. Also, the dynamics are

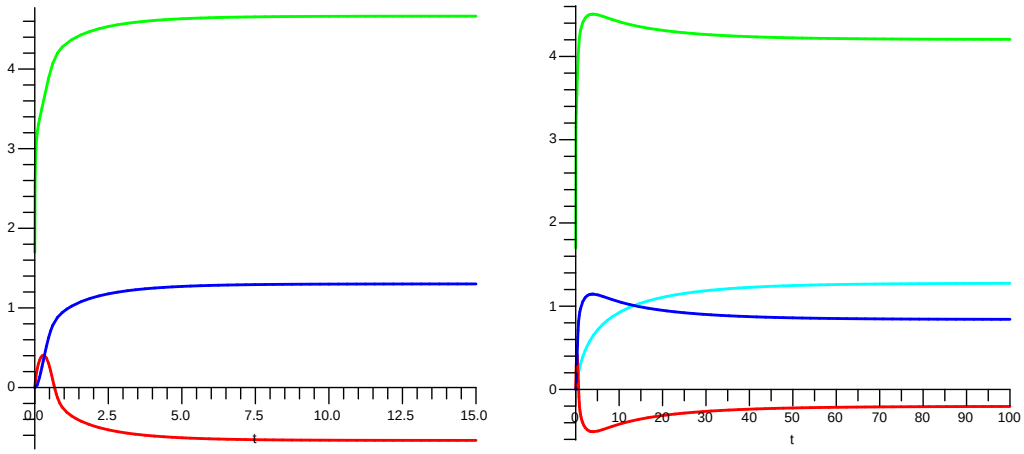

(a) $(0.22, 20.01, 46182.79)$, 3-D (b) $(0.63, 6.93, 18.89, 16003.28)$, 4-D

Figure 4.4: Time (days) series plots comparing the three and four-dimensional system solutions (linear scale) $(r = 0)$.

faster than they are for total T cell populations in that these antigen-specific populations respond immunologically to the virus.

4.3 Fixed points and stability with treatment

In order to assess and validate the effects of treatment on the four-dimensional system, we assign progressively higher values to the control parameter r and examine the changes in fixed points and eigenvalues. Table 4.1 shows the respective changes in each of $\overline{U}$, $\overline{I}$, $\overline{C}$ and $\overline{V}$ as the treatment parameter r is assigned progressively higher values. The eigenvalues for each set of fixed points change accordingly and reveal the stabilities of the fixed points.

Table 4.1: The effects of assigning sequentially higher values to r

r	$\overline{U}$	$\overline{I}$	$\overline{C}$	$\overline{V}$	eigenvalues	stability
0	0.63	6.93	18.89	16003.28	-19.24,-9.55,-1.63,-0.05	S
100	45.81	9.05	10.94	206.83	-14.06,-0.10+0.43i,-0.10-0.43i,-0.09	S
500	218.55	5.88	10.13	27.07	-14.01,-0.02+0.16i,-0.02-0.16i,-0.10	S
800	347.89	3.19	10.05	9.20	-14.00,-0.01+0.09i,-0.01-0.09i,-0.10	S
1000	434.11	1.39	10.02	3.19	-14.00,-0.01+0.05i,-0.01-0.05i,-0.10	S
1153	500.07	-0.0014	10.00	-0.0028	-14.00,-0.03,0.00012,-0.10	S

For progressively higher values of r, there are more uninfected cells at equilibrium, as indicated by changes in the value of $\overline{U}$ and progressively fewer infected cells and virus at equilibrium, as indicated by changes in the values of $\overline{I}$ and $\overline{V}$. The number of HIV-specific $CD8^+$ T cells at equilibrium changes as the value of r is increased from 0 to 100, as indicated by the change in the value of $\overline{C}$. But for values of r when $100 < r < 1000$, $\overline{C}$ does not change considerably. Even when the value r is increased from 1000 to 1153, causing the infected cell and virus populations to become extinct, $\overline{C}$ does not change much. This implies that $\overline{C}$ is less sensitive to changes not only in r, but to subsequent changes in the other variables. HIV-specific $CD8^+$ T cells typically respond quickly to changes in virus load, but these changes can vary among HIV-infected individuals depending on the quality of the HIV-specific $CD8^+$ T cells that respond. This result will further be discussed in section 4.4.1 and Chapters 6 and 7.

The eigenvalues associated with each fixed point change accordingly as the

value of r is varied. For $0 < r < 100$, the corresponding fixed points are stable nodes as indicated by the negative real-valued eigenvalues. For $100 < r < 1000$, the eigenvalues comprise both (negative) real-valued and complex parts indicating that the corresponding fixed points are asymptotically stable spiral node points. Eigenvalues with complex parts cause oscillatory effects in the system. When the value of r is increased to $r = 1153$, the eigenvalues contain a near zero value indicating a switch in stability of the system. I discuss the switch of stability in the system when the bifurcation analysis is done in the following subsection (4.3.1).

We can examine the behaviours of the variables as they change with respect to time at any stage of disease progression (not just at the equilibrium state) by generating time series plots. The plots confirm the induction of unsustained oscillations as the value of r is varied.

Figure 4.5 illustrates the effects on the system solutions as r is assigned progressively higher values. Treatment is initiated post-resolution of acute infection (day 100). As the value of r is increased, the corresponding fixed points reflect preferable disease equilibrium states as indicated by the fixed point values. Treatment ($r > 0$) induces unsustained oscillations in all cases. In general, as the value of r is increased, the uninfected cell population grows to successively higher peak values, and the infected cell and virus populations decay to successively lower trough values. In addition, the oscillations increase in period and amplitude as the value of r is increased. Thus the higher the value of r, the longer it takes for the system to reach the equilibrium states with corresponding successively lower viral setpoints. These results confirm that the actions of the treatment parameter on the system realistically mimics

the actions of protease inhibitors on the virus.

To better visualize long-term system changes as the parameter r is varied, we generate bifurcation diagrams. Again, this provides a complete picture of all possible states of the system for a large range of r values.

4.3.1 Bifurcation analysis - varying r

Figure 4.6 shows how $\overline{U}$, $\overline{I}$, $\overline{C}$ and $\overline{V}$ change as the parameter r is varied, and confirms that the fixed points are stable for a large range of r values. When $0 < r < 1153$, the fixed points are stable and positive.

There is a direct relationship between r and $\overline{U}$ and an indirect relationship between r and $\overline{I}$ and $\overline{V}$: large r corresponds to large $\overline{U}$ and small $\overline{I}$, $\overline{C}$ and $\overline{V}$. A transcritical bifurcation occurs at $r = 1153$ as seen more clearly in Figure 4.7.

At the bifurcation point, the system undergoes an exchange of stability. The original stable fixed point solution with positive coordinates becomes unstable and the unstable fixed point (4.4.1a) with $\overline{U} > 0$ and $\overline{C} > 0$ and $\overline{I} = 0$ and $\overline{V} = 0$ becomes stable at the bifurcation point. The fixed point $(\overline{U}, \overline{I}, \overline{C}, \overline{V}) = (500, 0, 10, 0)$ remains stable for all $r \geq 1153$. When $r = 1153$, the viral production rate is reduced by 99.91%. This means that treatment drives the infected cell and virus populations to extinction when it reduces the viral production rate by at least 99.91%. Thus, for very high treatment efficacies (virus production rate reduced by at least 99.91%), the model predicts the existence of a virus-free equilibrium state. As previously described in section 3.4.3, this prediction is theoretical. Treatment will never be this efficient in reality, and if it was, it would probably kill the patient due to high toxicity.

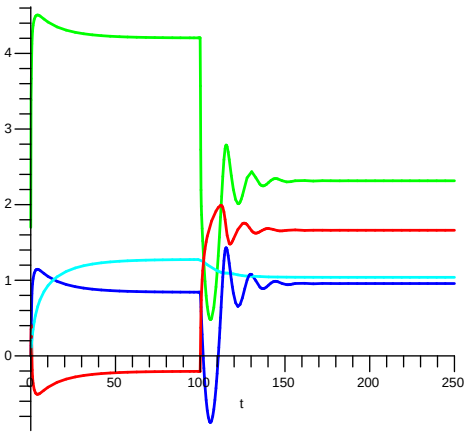

(a) $(45.81, 9.05, 10.94, 206.83)$, $r = 100$

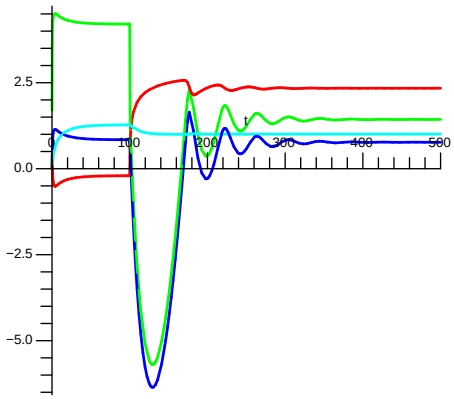

(b) $(218.55, 5.88, 10.13, 27.07)$, $r = 500$

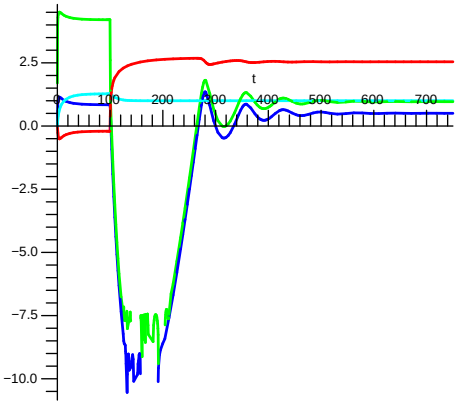

(c) $(347.89, 3.19, 10.05, 9.20)$, $r = 800$

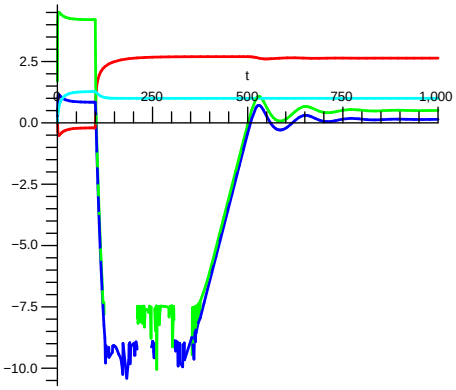

(d) $(434.11, 1.39, 10.02, 3.19)$, $r = 1000$

Figure 4.5: Time (days) series plots showing U, I, C and V for progressively higher values of r (log scale)

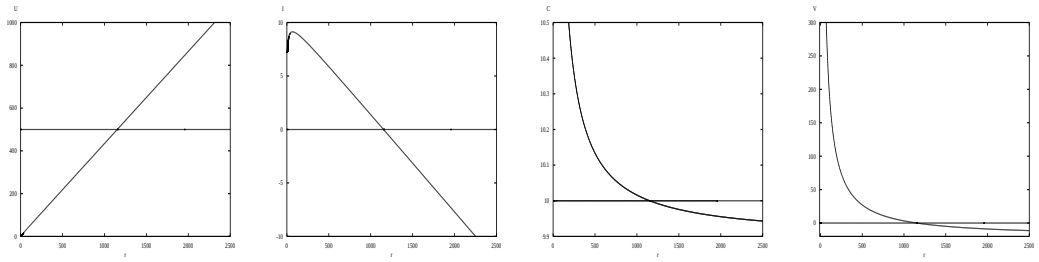

(a) Variation of r with respect to $\overline{U}$

(b) Variation of r with respect to $\overline{I}$

(c) Variation of r with respect to $\overline{C}$

(d) Variation of r with respect to $\overline{V}$

Figure 4.6: Bifurcation diagrams of $\overline{U}$, $\overline{I}$, $\overline{C}$ and $\overline{V}$ perspectives showing transcritical bifurcation at $r = 1153$.

The model simply predicts that if treatment does reduce the viral production rate below some threshold, the virus is eliminated from the system based on the fact that the death rates are higher than the production rates at these high treatment values.

Thus, bifurcation diagrams confirm analytical findings that demonstrate an inverse relationship between r and $\overline{V}$, and shows that there is an exchange of stability at the bifurcation value $r = 1153$. Treatment must reduce the viral production rate by more than 99.9% in order for this switch to occur, but we do not need 0% production to eradicate the virus as long as the loss rates exceed the production rate.

By comparing the bifurcation diagrams for the three and four-dimensional systems as the treatment parameter r is varied (Figure 4.8), we can see that the bifurcation value for the three-dimensional system occurs at a larger value for r. To reiterate, a transcritical bifurcation occurs at $r = 2307$ in the three-dimensional system and at $r = 1153$ in the four-dimensional system.

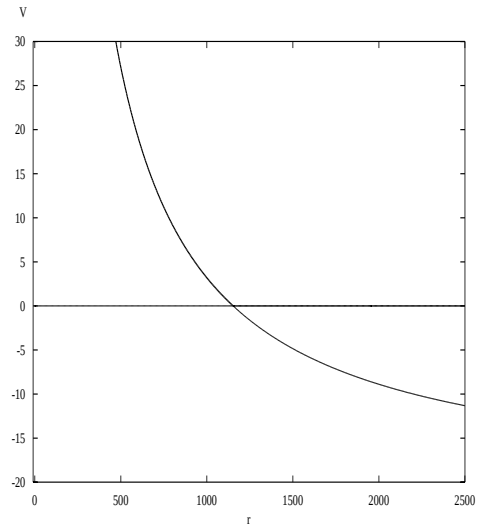

Figure 4.7: Bifurcation diagram - changes in $\overline{V}$ as r is varied. A transcritical bifurcation occurs at $r = 1153$.

This means that when C is explicitly included in the model as a variable, the treatment parameter does not need to be as large as it does when it is excluded to impose the same effects on the system. Therefore, bifurcation diagrams confirm that the explicit inclusion of C imposes pressure on the system whereby treatment need not be as potent to suppress the virus to undetectable levels (lower viral setpoint $\overline{V}$). This result is promising with respect to the predicted virus-free equilibrium state. The fact that treatment induces a virus-free equilibrium state by reducing the viral production rate less than it is reduced in the three-dimensional model when an additional variable that removes the virus from the system is explicitly included supports the fact that the model is portraying a valid picture of the effects of treatment. The number of ways for the virus to be removed from the system is larger and thus

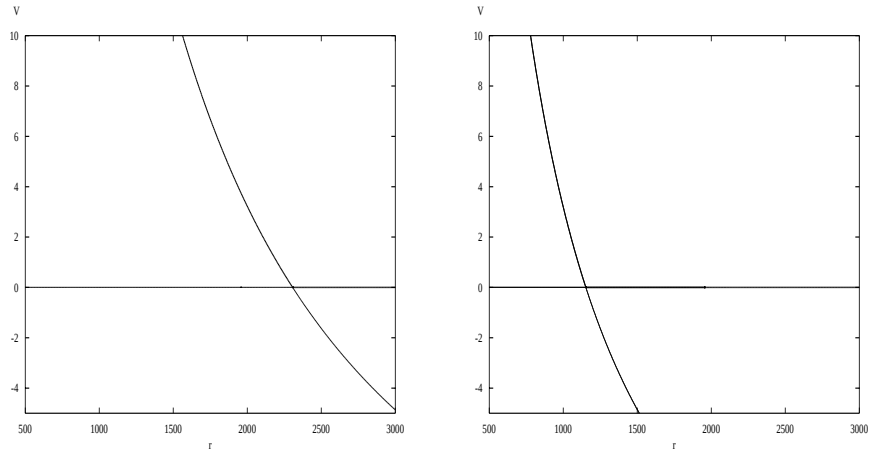

(a) 3-D, Bifurcation at $r = 2307$ (b) 4-D, Bifurcation at $r = 1153$

Figure 4.8: Comparison of bifurcation diagrams for three and four-dimensional systems - changes in $\overline{V}$ as r is varied.

the production rate of virus does not need to be reduced as much for this rate to be less than the death (virus removal) rates.

4.4 Treatment interruption

To examine the effects of treatment interruption on the system solutions we need to fix the value of r where $r > 0$. We select a value that is not too close to the bifurcation value and that reduces $\overline{V}$ to an undetectable level. According to Table 4.1 and Figure 4.5, when the treatment parameter has a value of $r = 100$, the viral setpoint is reduced to what is considered an undetectable level ($\overline{V}$=206.83) by clinical standards (based on the less sensitive RNA detection assay) by reducing the viral production rate by 98.7%. To

reiterate, the stable fixed point associated with the treatment parameter when $r = 100$ is

$$(\overline{U}, \overline{I}, \overline{C}, \overline{V}) = (45.81, 9.05, 10.94, 206.83)$$

with eigenvalues

$$\lambda_{1,2,3,4} = -14.06, -0.10 + 0.43i, -0.10 - 0.43i, -0.09.$$

Figure 4.9 is the phase diagram when $r = 100$ and confirms the location and stability of the stable fixed point. The fixed point is an asymptotically stable spiral node. Recall that the time series plot for $r = 100$ revealed the induction of oscillations. These oscillations are analogous to the spiralling effect in the phase diagram and are predictable by the natures of the eigenvalues.

To demonstrate the effects of treatment interruption using time series plots, we solve the system by intermittantly assigning treatment parameter values $r = 0$ (off-treatment) and $r = 100$ (on-treatment) using a piecewise linear function.

Figure 4.10 shows the time series plots for three different treatment interruption regimens. In all cases, treatment is initiated 100 days post-infection. The first regimen is a 100 day-off, 100 day-on, off regimen. The second is a 100 day-off, 100 day-on, 100 day-off, 100 day-on, off regimen, and the third is a 100 day-off, 100 day-on, 200 day-off, 90 day-on, off regimen. Figure 4.10(a) shows that when treatment is withdrawn after 100 days, the variable trajectories return to the pre-treatment equilibrium state. This means that following a perturbation of the system with a single treatment phase (100 days), the system returns to its original pre-treatment state. Figure 4.10(b) shows that following two perturbations with treatment, the system returns to its original

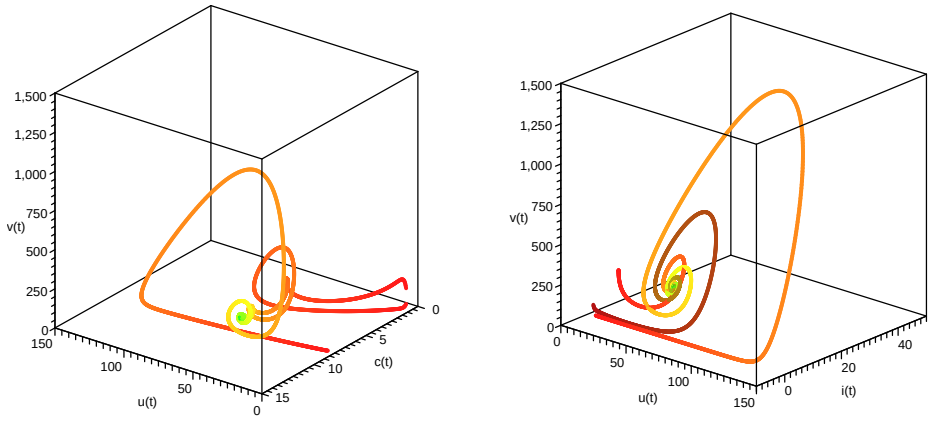

(a) $U - C - V$-plane (b) $U - I - V$-plane

Figure 4.9: Phase diagram from two perspectives with initial conditions $(U_0, I_0, C_0, V_0) = (1, 10, 1, 150), (5, 0, 8, 1), (1, 1, 1, 50)$

pre-treatment equilibrium state. The behaviours of the variable trajectories in the on phases are identical for both cases (a) and (b). Even when the durations of the on-treatment and off-treatment phases are modified, as seen in Figure 4.10(c), the outcome is the same as for the other regimens: the system returns to its original pre-treatment equilibrium state. The only time the system does not return to this state is when treatment is kept on as seen in Figure 4.11. In this case, the system returns to the original on-treatment (post-treatment) equilibrium state. The conclusion is the same: whether treatment is kept on or taken off, the timing and duration of a treatment regimen does not affect the re-arrival at either the post or pre-treatment equilibrium states, respectively.

Figures 4.10 and 4.11 demonstrate that treatment can be used to delay

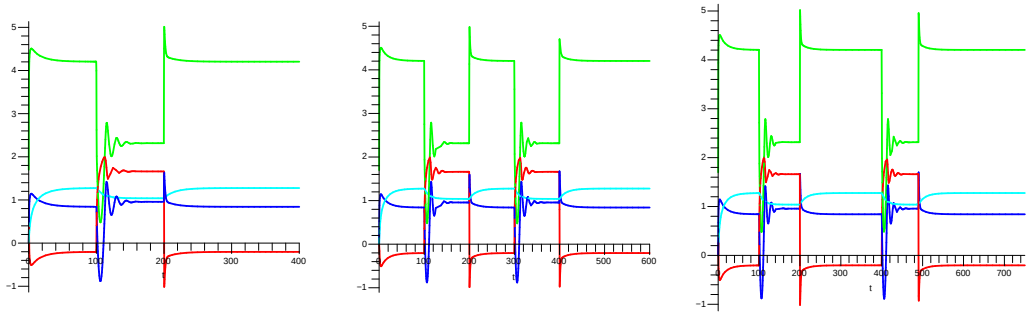

(a) 100/100/off (b) 100/100/100/100/off (c) 100/100/200/90/off

Figure 4.10: Time (days) series plots showing three different treatment interruption regimens: $(\overline{U}, \overline{I}, \overline{C}, \overline{V}) = (0.63, 6.93, 18.89, 16003.28)$

the onset of the pre-treatment (off-treatment) equilibrium. Theoretically, it appears possible to interrupt treatment at any time during infection and as often as desired. However, as innocuous as interrupting treatment may seem from these model predictions, in reality, it is most likely not due to a number of factors such as high rate of viral mutation, that are beyond the scope of the model.

If we examine the effects of interrupting treatment more closely, we see that immediately following the interruption, the HIV-specific $CD8^+$ T cell population grows as seen in Figure 4.12(a). Interrupting treatment does result in a transient boost in HIV-specific $CD8^+$ T cells, but this boost does not translate into a lower viral setpoint (Figure 4.12(b)).

This result is based on model predictions using a particular parameter set. This raises an important point: not everyone will have the same set.

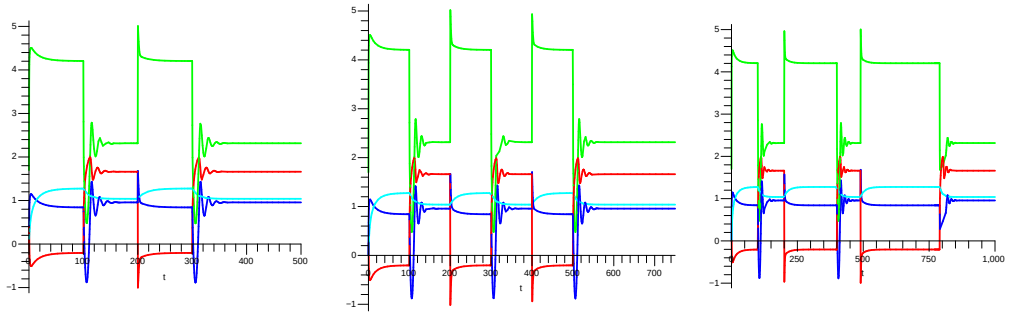

(a) 100/100/100/on

(b) 100/100/100/100/100/on

(c) 100/100/200/90/300/on

Figure 4.11: Time (days) series plots showing three different treatment interruption regimens: $(\overline{U}, \overline{I}, \overline{C}, \overline{V}) = (218.55, 5.88, 10.13, 27.07)$

4.4.1 Bifurcations - modifying b_1 on and off-treatment

The parameter b_1 represents the removal rate of infected HIV-specific $CD4^+$ T cells by the HIV-specific $CD8^+$ T cells. This rate is determined by the efficiency of the HIV-specific $CD8^+$ T cells to remove infected cells from the system. Immunologically, HIV-specific $CD8^+$ T cells that are functionally impaired may be less efficient at removing infected cells. Studies have shown that the reason for CTL exhaustion, resulting in faster disease progression as determined by the rates at which U and V change and the values of $\overline{U}$ and $\overline{V}$, is a defect in the maturation process of these cells into terminally-differentiated effector memory cells [Appay *et al.*, 2000; Champagne *et al.*, 2001; Hess *et al.*, 2004]. Thus, if the HIV-specific $CD8^+$ T cells are functionally impaired, the removal rate of HIV-infected cells will be slower implying faster disease

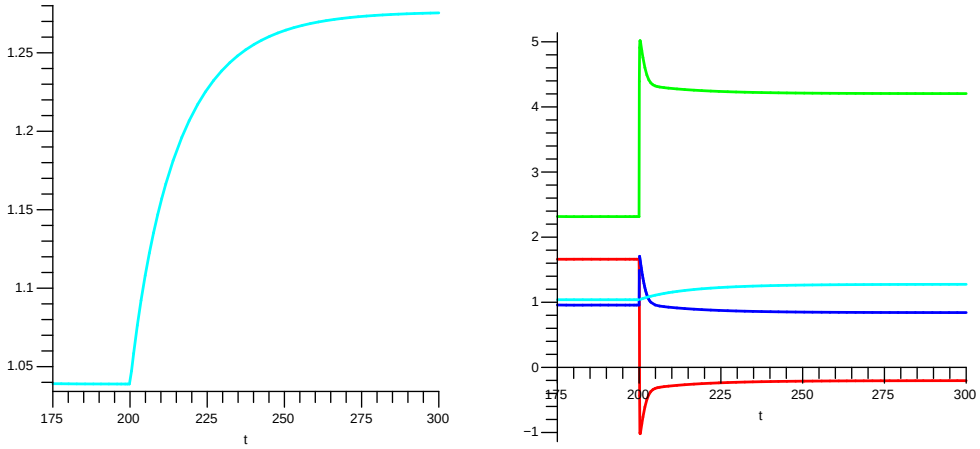

(a) C trajectory

(b) Return to pre-treatment equilibrium state, $(0.63, 6.93, 18.89, 16003.28)$

Figure 4.12: Expanded time (days) series plot immediately following treatment interruption

progression as determined by $\overline{U}$ and $\overline{V}$. We can examine all possible long-term behaviours of the system as we vary the removal rate parameter b_1 using bifurcation analysis.

Figure 4.13 shows that the fixed points are stable for a large range of b_1 values. When $0 < b_1 < 115.3$, the fixed points are stable and positive. The value of b_1 is directly related to the value of $\overline{U}$ and indirectly related to the values of $\overline{I}$, $\overline{C}$ and $\overline{V}$: larger b_1 values correspond to larger values of $\overline{U}$ and smaller values of $\overline{I}$, $\overline{C}$ and $\overline{V}$. A transcritical bifurcation occurs at $b_1 = 115.3$ where the fixed point $(\overline{U}, \overline{I}, \overline{C}, \overline{V}) = (500, 0, 10, 0)$ becomes stable. This implies

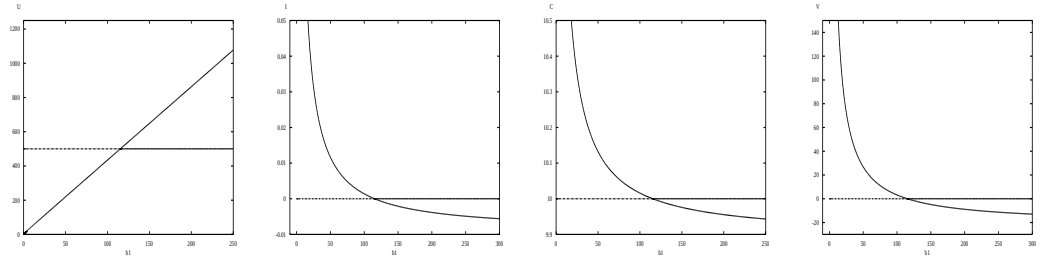

(a) b_1 varied with respect to $\overline{U}$

(b) b_1 varied with respect to $\overline{I}$

(c) b_1 varied with respect to $\overline{C}$

(d) b_1 varied with respect to $\overline{V}$

Figure 4.13: Bifurcation diagrams describing how $\overline{U}$, $\overline{I}$, $\overline{C}$ and $\overline{V}$ change as b_1 is varied ($r = 0$).

that when $b_1 = 115.3$, the infected cell and virus populations are extinct. The exchange of stability occurs where the fixed point at $\overline{V} = 0$ becomes stable where V coordinate of the original fixed point solution becomes unstable and negative. When $b_1 > 115.3$, the fixed points that have positive values are unstable. Thus, the model predicts a virus-free equilibrium state when b_1 is very high. It is unlikely based on parameter estimates from the literature that the removal rate parameter would ever have a value this high. Nonetheless, the model predicts that increasing efficacy of removal of infected cells from the system by the HIV-specific $CD8^+$ T cells is associated with equilibrium states whereby the values of $\overline{I}$, $\overline{C}$ and $\overline{V}$ become successively lower and the value of $\overline{U}$ becomes successively higher. This result is in accordance with the known effects of these cells and also the impact of the virus on these cells throughout immunopathogenesis.

Every value of b_1 in the range $0 < b_1 < 115.3$ elicits stability in the system

whereby the stable fixed points have positive-valued coordinates. Thus, for successively higher values of b_1, the host is living with the virus and controlling the virus with increasing efficiency. For example, an individual with a removal rate of $b_1 = 0.05$ yields a viral setpoint of 4.2, whereby an individual with a removal rate of $b_1 = 0.0005$ yields a viral setpoint value of 4.66.

We must also examine how the system changes as b_1 is varied on-treatment. Since treatment lowers $\overline{V}$ substantially, it is likely that the system will be more sensitive to small changes in b_1 on-treatment. Figure 4.14 shows the how the system changes when b_1 is varied on-treatment ($r = 100$) and demonstrates an amplified response from the system to changes in b_1.

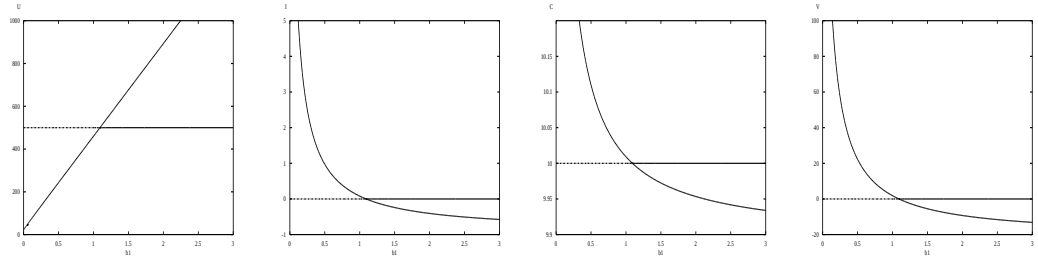

(a) b_1 varied with respect to $\overline{U}$

(b) b_1 varied with respect to $\overline{I}$

(c) b_1 varied with respect to $\overline{C}$

(d) b_1 varied with respect to $\overline{V}$

Figure 4.14: Bifurcation diagrams describing how $\overline{U}$, $\overline{I}$, $\overline{C}$ and $\overline{V}$ change as b_1 is varied ($r = 100$)

As anticipated, a bifurcation occurs at a much smaller value of b_1 on-treatment. When $b_1 = 1.092$, a transcritical bifurcation occurs whereby the infected cell and virus populations are extinct. This value is much closer to the given value for b_1 in Table 3.3 and confirms that the fixed points are more

sensitive to small changes in b_1 on-treatment. Clinically, this would imply that differences in removal rates will be more important when the individual is on treatment (functional deficiencies imply lower b_1 values). Figure 4.15 shows the comparison between the bifurcation diagrams when b_1 is varied, on and off-treatment. For both on and off-treatment scenarios, lower b_1 values yield lower $\overline{U}$ values and higher $\overline{I}$, $\overline{C}$ and $\overline{V}$ values.

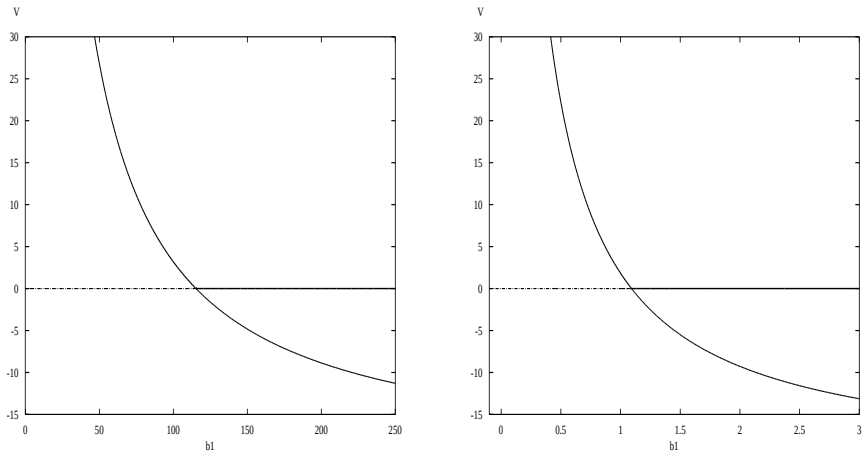

(a) $r = 0$ (b) $r = 100$

Figure 4.15: Bifurcation diagrams describing how $\overline{V}$ changes as b_1 is varied on and off-treatment.

Thus, bifurcation diagrams show us that fixed points are stable for a wide range of b_1 values ($0 < b_1 < 115.3$) off-treatment. However, on-treatment the fixed points are much more sensitive to small changes in b_1 whereby the fixed points are stable for a small range of b_1 values ($0 < b_1 < 1.092$). At this point, it would be interesting to find out how the system variables respond immediately following a treatment interruption for different values of b_1. We

established that lower values of b_1 yield higher values of $\overline{V}$. The value of b_1 in the given parameter set (Table 3.4) is $b_1 = 0.05$. Thus, we select another value for b_1 that is lower than this ($b_1 = 0.0005$) to examine the differences in disease progression patterns as portrayed in time series plots. We impose a single treatment phase (100 days) followed by a treatment interruption to determine how the variable trajectories behave immediately following the interruption. Figure 4.16 shows the time series plots following a single 100 day treatment phase when $b_1 = 0.05$ and $b_1 = 0.0005$.

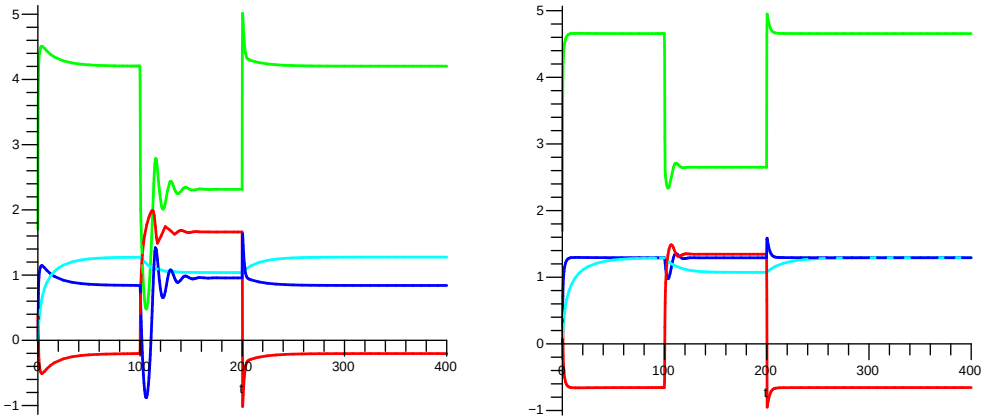

(a) $(0.63, 6.93, 18.89, 16003.28) \rightarrow ()$, $b_1 = 0.05$

(b) $(0.22, 19.63, 19.58, 45296.56) \rightarrow ()$, $b_1 = 0.0005$

Figure 4.16: Time (days) series plots showing the effect of a treatment interruption: two different removal rate parameter values (linear and log scales)

The time series plots (Figure 4.16(a),(b)) confirm that when $b_1 = 0.05$ and

when $b_1 = 0.0005$ treatment and treatment interruption affect the system in the much the same way. That is, treatment causes the infected cell, HIV-specific $CD8^+$ T cell and virus populations to decay and the uninfected cell population to grow. A major difference, as was previously established, is that the fixed point solutions are different. That is, $b_1 = 0.05$ yields the stable fixed

$$(\overline{U}, \overline{I}, \overline{C}, \overline{V}) = (0.63, 6.93, 18.89, 16003.28),$$

and $b_1 = 0.0005$ yields the stable fixed point

$$(\overline{U}, \overline{I}, \overline{C}, \overline{V}) = (0.22, 19.63, 19.58, 45296.56).$$

When $b_1 < 0.05$, the fixed point values $\overline{U}$ and $\overline{C}$ decrease and $\overline{I}$ and $\overline{V}$ increase.

Interestingly, the rates at which the variable populations change are also different as depicted by the slopes of the variable trajectories. In particular, when treatment is interrupted at day 200, the rate of change of V when $b_1 = 0.0005$ is slightly faster than the rate of change of V when $b_1 = 0.05$ as seen in Figure 4.17(a) and (b). The differences in the ways that the variable trajectories behave is partly due to the differences between their on-treatment numbers. The higher b_1 value yields higher values for U and lower values for V at the moment when treatment is withdrawn, so this changes the way in which they approach equilibrium. Ultimately, immediately following a treatment interruption, the V population grows at a faster rate because the removal rate parameter b_1 has a lower value. In addition, the U population decays earlier (and its slope is steeper) because b_1 has a lower value.

Thus, even though there are no qualitative differences in the system when $b_1 = 0.05$ and $b_1 = 0.0005$, quantitatively there are notable differences. These results confirm that the removal rate b_1 is indirectly related to $\overline{V}$. The model

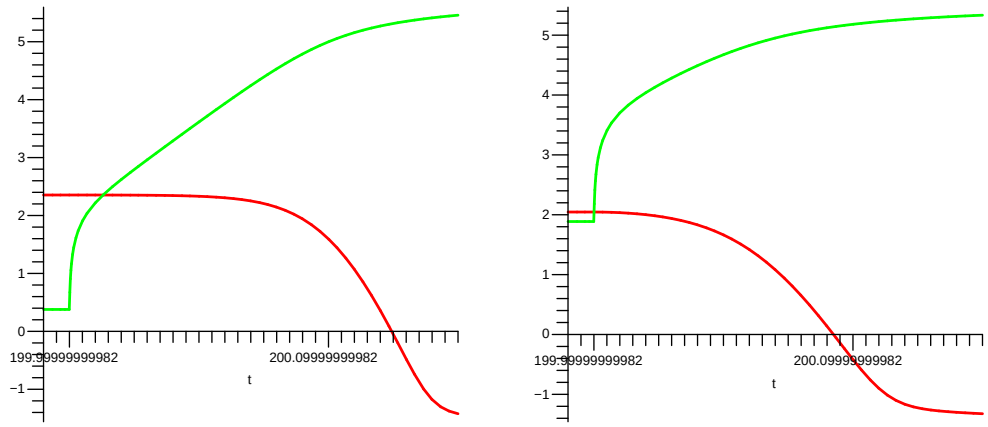

(a) $(0.63, 6.93, 18.89, 16003.28) \rightarrow ()$, $b_1 = 0.05$

(b) $(0.22, 19.63, 19.58, 45296.56) \rightarrow ()$, $b_1 = 0.0005$

Figure 4.17: Time (days) series plots showing the effect of a treatment interruption: two different removal rate parameter values

predicts that immediately following treatment interruption, the virus rebounds at a rate that is indirectly related to b_1: the rate of change of V is faster when b_1 is smaller. It also predicts that the uninfected $CD4^+$ T cell population decays faster under these same circumstances.

If we define disease progression by how quickly U falls and V rebounds immediately following a treatment interruption, the model predicts that disease progression rates are inversely related to infected cell removal rates. Subsequently, individuals with lower infected cell removal rates will progress through infection faster.

This leads to a very important part of this thesis: the clinical and experimental data. In this part of the study, I assess the role of HIV-specific $CD8^+$ T cells in controlling the virus load and maintaining stable $CD4^+$ T cell counts. In the following Chapter, I outline the experimental assay methodologies used in this study.

Chapter 5

Immunological Assays - Methodologies

5.1 Subjects

HIV-1-infected individuals were recruited through the Infectious Disease Clinic of the St. John's General Hospital, St. John's, Canada. Clinic visits were scheduled at approximately 3-month intervals or as necessary for appropriate clinical care. In conjunction with each visit, clinical evaluation was performed, plasma HIV RNA was measured using Amplicor HIV-1 Monitor kits (Roche Diagnostic Systems, Mississauga, Ontario, Canada) and peripheral blood lymphocyte subsets were assessed by flow cytometry. Ethical approval was obtained from the Memorial University Faculty of Medicine Human Investigation Committee and all participants provided informed consent for blood collection and access to clinical and laboratory records.

5.2 Lymphocyte Isolation

Human peripheral blood mononuclear cells (PBMC) were utilized for all tests, and all work with HIV-infected blood products was performed in a Level-3 Biohazard Facility. Blood was collected by venipuncture in vacutainers containing acid-citrate dextrose (ACD) and centrifuged for 10 minutes at 400 g (1300 rpm in Beckman T-J6 centrifuge). Plasma was removed and replaced by an equal amount of phosphate-buffered solution (PBS - PH 7.2). The PBS/cell mixture was transferred to a sterile 50 ml tube, layered over 15 ml of Ficoll-paque gradient separation medium (Pharmacia Chemicals, Dorval, Quebec, Canada) and centrifuged at 400 g for 30 minutes. Interface cells were collected, washed in 30 ml PBS, and centrifuged for 5 minutes. The cells were washed again in PBS + 1% fetal calf serum (FCS), centrifuged for 5 minutes at 300 g and resuspended in lymphocyte medium (RPMI 1640 with 10% FCS, 10 mM Hepes, 2 mM l-glutamine, 1% penicillin/streptomycin, and 2×10^{-5} M 2-mercaptoethanol (Gibco, Invitrogen Corporation, Carlsbad, California)). Cells were counted and cryopreserved in approximately 1 ml of sterile freezing medium and stored in sterile cryovials at $-70°$C for one week before transfer to liquid nitrogen for longer term storage.

5.3 Cell counting

Fifty ul of cell suspension was pipetted into a single well of a 96-well microtiter plate (Flow Laboratories, Virginia, USA) in conjunction with 50 ul of Trypan Blue (Sigma Chemical Co., St. Louis, Mo.). Trypan blue is an exclusion dye that stains dead cellular matter. Cells were counted using a cytometer

to obtain a viable cell count. Cell count was represented by total number of viable cells per ml of medium.

5.4 Reanimation of Frozen PBMC

Lymphocyte medium (10 ml) was pipetted into a sterile 15 ml tube. Cryopreserved cells were obtained from liquid nitrogen storage, immediately immersed into a 37°C waterbath and gently agitated until contents were almost completely thawed. Cells were then immediately transferred to the 15 ml tube containing 10 ml lymphocyte medium and centrifuged for 5 minutes at 300 g. The cells were then resuspended in 10 ml of fresh medium, counted and cultured at approximately 1 $\times 10^6$/ml in a sterile 10 ml tube overnight for direct use in experimental assays the following day.

5.5 Infection of PBMC

PBMC to be infected were counted and centrifuged at 300 g for 5 minutes. Pelleted cells were resuspended at 1.0×10^6/ml and dispensed into 1 ml aliquots into labelled sterile 15 ml tubes. Again PBMC were pelleted by centrifugation at 300 g for 5 minutes. The supernatant was discarded and cell pellets were directly infected with recombinant Vaccinia Viruses (rVVs) at a 2:1 multiplicity of infection (MOI) (2.0×10^6 plaque-forming units (PFU) per 1.0×10^6 cells) and incubated at 37°C, 5% CO_2 for 1 hour. Cells were resuspended at 2.0×10^6 PBMC per ml for direct use in ELIspot assay as described in section 5.6.

5.5.1 Recombinant Vaccinia Viruses

PBMC were infected with the following recombinant vaccinia viruses: vVK1 (gag/pol), vCF21 (pol), vPE16 (gp160), vNef (nef), and vSC8 (Escherichia coli-galactosidase, control) all from the NIH AIDS Research and Reference Reagent Program, Rockville, Maryland, USA.

5.6 ELISpot assay

Microtiter assay plates (Multiscreen; Millipore Corporation, Billerica, MA) were coated with 100 ul of 7.5 ug per ml anti-IFN-γ mAb 1-D1K (Mabtech, Stockholm, Sweden) overnight at 4°C. The plates were then washed six times with PBS, and 100 ul of recombinant vaccinia-infected PBMC (0.2×10^6) were added in duplicate and incubated at 37°C, 5% CO_2 for 16 hours. Negative control wells contained unstimulated PBMC and PBMC infected with vsc8 - a vaccinia virus vector expressing β-galactosidase. Positive control wells contained 4 ug per ml of phytohemagglutinin (PHA). Following incubation, the cells were removed and the wells were washed as described above followed by the addition of 100 ul of 1 ug per ml biotinylated anti-IFN-γ mAb 7-B6-1 (Mabtech) to each well. The plate was incubated for 2 additional hours at room temperature followed by washing six times, after which 100 ul of streptavidin alkaline phosphatase conjugate (Mabtech) diluted 1/1000 was added to each well. The plate was incubated for 1 hour at room temperature, followed by another six washes. 100 ul of chromogenic alkaline phosphatase substrate (Bio-Rad, Hercules, CA) diluted 1/10 in Tris buffer was then added to each well. After 30-45 minutes, plates were washed with tap water to stop color

reactions and then air-dried. Spots corresponding to the footprints of the IFN-γ-secreting cells were counted with an automated Elispot counter (Zellnet Consulting, New Jersey). Responses were considered positive if the number of spots was more than twice the negative control and greater than 50 per million PBMC. Results are expressed as spot forming cells per million PBMC (SFC per 10^6 PBMC) following subtraction of negative controls whereby a spot-forming cell is an IFN-γ-producing cell.

Chapter 6

Clinical and experimental results

The study cohort included 22 HIV-1-infected individuals and represents infected individuals with a variety of disease progression patterns in the chronic phase of infection. Table 6.1 summarizes the complete set of sample dates for each study participant and includes T cell counts, virus loads and treatment status at the time that each sample was taken. Sample dates are arranged chronologically. These particular samples were used in experimental assays to assess HIV-specific $CD8^+$ T cell activity in the contexts of high and low virus loads. Virus loads (VL) that are <1.7 or <2.6 (depending on the sensitivity of the RNA detection assay used) are considered undetectable.

Table 6.1: Summary data for study participants

subject	$CD4^+$ T cells	$CD8^+$ T cells[a]	VL[b]	sample date	treatment status
1	280	1360	3.75	1/12/2004	on
3	51	1122	4.87	9/30/1999	off
	270	954	<1.7	10/9/2003	on
	255	765	<1.7	12/23/2004	on
17	507	624	3.66	12/9/2004	off
20	285	1045	<2.6	4/19/1999	on
	374	1342	<1.7	4/17/2000	on
	378	1008	<1.7	8/17/2000	on
35	621	1173	3.25	8/26/1999	on
44	630	864	2.35	11/6/2003	on
51	186	1782	5.17	9/9/1998	on
	104	897	4.44	1/30/2003	on
	403	2201	<1.7	9/25/2003	on
55	305	1780	<1.7	1/27/1997	on
60	<1	476	4.93	12/12/2001	on
	<1	318	>5.88	11/6/2003	off

[a] - T cell counts are expressed as the number of T cells/ul of peripheral blood (linear scale)

[b] - VL are expressed as the number of HIV RNA copies/ml of plasma

ND - not done

Table 6.1: Summary data for study participants, cont'd

subject	$CD4^+$ T cells	$CD8^+$ T cells[a]	VL[b]	sample date	treatment status
64	608	688	2.46	8/30/1999	on
	629	799	3.05	3/14/2002	on
	570	1121	<1.7	3/9/2004	on
71	1624	870	<1.7	12/21/2001	on
	1479	957	<1.7	5/16/2002	on
	1161	1188	3	10/10/2002	off
	1102	1392	3.96	3/1/2004	off
	962	1300	4.37	9/13/2004	off
76	490	817	4.51	3/6/1997	off
	570	480	<1.7	2/8/2001	on
	507	481	2.13	8/29/2002	on
83	165	649	5.04	6/26/2003	off
	72	240	3.29	11/27/2003	on
92	663	731	<1.7	6/3/1999	on
	644	1764	4.8	1/15/2004	off

Table 6.1: Summary data for study participants, cont'd

subject	$CD4^+$ T cells	$CD8^+$ T cells[a]	VL[b]	sample date	treatment status
98	209	385	3.84	11/17/1999	on
	448	798	<2.6	2/14/2002	on
117	64	1040	3.32	12/16/1999	on
	144	1752	3.54	4/27/2000	on
136	400	416	4.2	1/24/2000	off
	162	261	3.15	7/5/2001	on
	187	296	4.42	5/27/2002	off
	253	319	4.91	12/15/2003	off
	200	320	4.88	5/27/2004	off
140	540	2772	4.31	7/10/2003	off
157	400	1320	5.12	11/7/2002	off
	ND	ND	<2.6	8/12/2004	on
166	276	696	<1.7	5/13/2004	on
174	513	1782	4.51	11/13/2003	off
	442	1716	3.26	5/3/2004	on
176	418	1210	<1.7	1/8/2004	on

6.1 Clinical laboratory data

Each HIV-infected individual in the cohort fits into one of two groups based on differences in disease progression patterns (rates) as indicated by clinical laboratory data. The groups are fast progressors and slow progressors. HIV-infected individuals who experienced rapidly falling CD4 counts and rapid viral rebound following treatment interruption (off-treatment), as indicated by clinical laboratory parameters, were classified as fast progressors. HIV-infected individuals who maintained stable CD4 counts and virus loads at controllable levels following treatment interruption (off-treatment), also indicated by clinical laboratory parameters, were classified as slow progressors. A clear distinction between fast and slow progressors can be illustrated with this example. Subject 136 had an on-treatment undetectable virus load (<2.6) on 11/20/2001 (not shown in Table 6.1 since this sample was not tested by Elispot) which rapidly rebounded to 4.42 by 5/27/2002 when treatment was withdrawn and peaked at 4.91 on 12/15/2003. The mean virus load during the off-treatment timeframe was 4.53. Concomitantly, CD4 counts rapidly fell from 220 on 11/20/2001 to 187 on 5/27/2002 and troughed at 176 on 05/05/2003. The mean CD4 count during the off-treatment timeframe was 216. Thus, subject 136 is a fast progressor. Subject 71 had an undetectable virus load (<1.7) on 5/16/2002 that slowly rose to 4.37 by 9/13/2004 when treatment was withdrawn and subsequently fell again to 3.98 while treatment remained off (not shown in Table 6.1). The mean virus load during the off-treatment timeframe was 3.61. CD4 counts remained high, troughing at 720 in the off-treatment timeframe. The mean CD4 count during the off-treatment timeframe was 937. Thus, subject 71 is a slow progressor.

The mean off-treatment trough CD4 counts (nadir) and peak virus loads for each of the 22 study subjects were used as indicators of disease progression rates and grouped according to a cluster analysis: a multivariate technique designed to create groups within multivariate data.

Table 6.2: Summary off-treatment data for fast progressors

subject	peak VL	trough CD4 count
1	5.49	200
3	4.87	28
20	5.5	76
35	4.77	245
51	5.01	117
55	5.54	311
60	>5.88	0
76	4.83	409
83	>5.88	40
92	4.93	340
98	5.73	69
117	5.84	27
136	4.91	176
157	5.81	40
166	>5.88	221
174	5.16	380

Table 6.3: Summary off-treatment data for slow progressors

subject	peak VL	trough CD4 count
17	4.32	296
44	4.37	480
64	3.72	594
71	3.76	925
140	4.32	462
176	1.7	245

The cluster analysis revealed two distinct groups ($p<0.05$) that adhered to the above principles, yielding 16 fast progressors and 6 slow progressors summarized in Tables 6.2 and 6.3. See Appendix for statistical reference.

The fast and slow progressor grouping reveals notable differences in trough CD4 counts and peak virus loads between the two groups. In the fast progressor group, virus loads are greater than 4.7 HIV RNA copies/ml blood and trough CD4 counts range from 0 to 409. In the slow progressor group, virus loads are less than 4.4 and CD4 counts range from 245 to 925. As discussed in the introduction, a controlled virus load is considered to be below 4.5 and an uncontrolled virus load is considered to be above 4.5 HIV RNA copies/ml blood. Thus, the fast progressors do not appear capable of inherently suppressing the virus load to controllable levels during the chronic phase of infection, but the slow progressors do.

For further comparison of the groups, the means and medians of the trough CD4 counts and peak virus loads were calculated and are shown in Table 6.4.

Table 6.4: Comparison of off-treatment trough CD4 counts and peak virus loads for fast and slow progressors

		fast progressor	slow progressor
mean	VL	**5.38** ± 0.44	**3.7** ± 1.02
	CD4	**167** ± 138	**500** ± 244
median	VL	**5.5**	**4.04**
	CD4	**147**	**471**

Fast and slow progressor groups differ significantly in mean off-treatment trough CD4 counts and peak virus loads (Kruskal-Wallis rank-sum test; $p<0.05$) revealing striking differences between the groups. The mean trough CD4 count in the fast progressor group is 3-fold lower than in the slow progressor group and the peak virus load is 1.5-fold higher. Subject 176 had an undetectable off-treatment virus load which skews the slow progressor virus load data resulting in a high standard deviation. This most likely arises due to residual drugs in the host system. This individual resumed treatment following a brief (one month) treatment holiday and subsequent measures of virus load remain undetectable (<1.7).

Thus statistical analysis of clinical lab data shows that among the 22-member cohort, 16 are fast progressors and 6 are slow progressors as determined by a cluster analysis of nadir and peak virus load data and the principles outlined at the beginning of this section. Having classified each member of the cohort as a fast or slow progressor, the role of HIV-specific $CD8^+$ T cells in contouring these classifications can be assessed.

6.2 Experimental observations

> If your experiment needs statistics, you ought to have done a better experiment. - Ernest Rutherford (1871-1937)

6.2.1 Quantity of responses

To assess the role of HIV-specific $CD8^+$ T cells in contouring the fast and slow progressor groups, measurements of IFN-γ production from HIV-specific $CD8^+$ T cells were taken for each of the 22 members of the cohort. The number of measurements taken for each individual was based on sample availability and ranged from 1 to 5. (See Table 6.1.) When possible, measurements were taken in pairs when virus loads were either low or high to enable a comparison between the HIV-specific $CD8^+$ T cell activities in both contexts. One HIV-specific $CD8^+$ T cell is represented by a spot on an Elispot plate. A minimum of 50 spot-forming cells (SFC) (background number) per million PBMC was considered a positive response.

The goal of these experiments was to assess each subject's ability to mount HIV-specific memory T cell responses against stimulating agents (HIV/vaccinia constructs) in the contexts of high and low virus loads and to evaluate the importance of both the quantity and quality of these cells in maintaining a controllable virus load. We hypothesized that the magnitudes of all positive responses, as defined above, would correlate with virus load. We also hypothesized that the magnitudes of responses in the fast progressor group would be lower than in the slow progressor group in the contexts of low and high virus loads, since the mean virus load of a fast progressor is higher than the

mean virus load of a slow progressor. The Elispot results for fast and slow progressors are shown in Tables 6.5 and 6.6.

Table 6.5: Compiled Elispot results - fast progressors

subject	sample date	vnef	vvk1	vpe16	combined	vnef + vvk1	VL	on/off
1	1/12/2004	1770	1625	405	**3800**	*3395*	3.75	on
3	9/30/1999	60	448	388	**896**	*508*	4.02	off
	10/9/2003	78	258	465	**801**	*336*	<1.7	on
	12/23/2004	25	83	45	**153**	*108*	<1.7	on
20	4/19/1999	470	413	ND	**883**	*883*	<2.6	on
	4/17/2000	405	383	ND	**788**	*788*	<1.7	on
	8/17/2000	403	388	208	**999**	*791*	<1.7	on
35	8/26/1999	245	1835	ND	**2080**	*2080*	3.25	on
51	9/9/1998	3	68	38	**109**	*71*	5.17	on
	1/30/2003	70	528	68	**666**	*598*	4.44	on
	9/25/2003	33	235	78	**346**	*268*	<1.7	on
55	1/20/1997	0	148	ND	**148**	*148*	4.66	on
60	12/12/2001	0	3	5	**8**	*3*	4.93	on
	11/6/2003	0	25	28	**53**	*25*	>5.88	off
76	3/6/1997	50	460	ND	**510**	*510*	4.51	off
	3/6/1997	80	425	33	**538**	*505*	4.51	off
	2/8/2001	35	83	ND	**118**	*118*	<1.7	on
	8/29/2002	285	465	ND	**750**	*750*	2.31	on
83	6/26/2003	1258	1538	ND	**2796**	*2796*	5.04	off
	11/27/2003	268	673	ND	**941**	*941*	>5.88	on

Table 6.5: Compiled Elispot results - fast progressors, cont'd

subject	sample date	vnef	vvk1	vpe16	combined	vnef+vvk1	VL	on/off
92	6/3/1999	530	755	288	**1573**	*1285*	<1.7	on
	1/15/2004	4208	3230	843	**8281**	**7438**	4.8	off
98	11/17/1999	95	90	8	**193**	*185*	3.84	on
	2/14/2002	160	203	48	**411**	*363*	<2.6	on
117	12/16/1999	198	118	133	**449**	*316*	5.15	on
	4/27/2000	225	175	228	**628**	*400*	3.54	on
136	1/24/2000	1070	1550	ND	**2620**	*2620*	4.2	off
	7/5/2001	80	145	100	**325**	*225*	3.15	on
	5/27/2002	405	510	573	**1488**	*915*	4.42	off
	12/15/2003	1240	408	533	**2181**	*1648*	4.91	off
	5/27/2004	120	83	40	**243**	*203*	4.88	off
157	11/7/2002	80	543	128	**751**	*623*	5.12	off
	8/12/2004	23	55	20	**98**	*78*	<2.6	on
166	5/13/2004	33	1523	350	**1906**	*1556*	<1.7	on
174	11/13/2003	1120	1778	780	**3678**	*2898*	4.51	off
	5/3/2004	733	775	433	**1941**	*1508*	3.26	on

Table 6.6: Compiled Elispot results - slow progressors

subject	sample date	vnef	vvk1	vpe16	combined	vnef+vvk1	VL	on/off
17	12/9/2004	338	3390	295	**4023**	*3728*	3.66	off
44	11/6/2003	5	300	468	**773**	*305*	2.35	on
64	8/30/1999	30	3600	823	**4453**	*3630*	2.46	on
	3/14/2002	88	2278	2113	**4479**	*2366*	3.05	on
	3/9/2004	40	1310	1025	**2375**	*1350*	<1.7	on
71	12/21/2001	1280	1240	293	**2813**	*2520*	<1.7	on
	5/16/2002	855	863	218	**1936**	*1718*	<1.7	on
	10/10/2002	260	990	350	**1600**	*1250*	3	off
	3/1/2004	1003	635	215	**1853**	*1638*	3.96	off
	9/13/2004	700	395	228	**1323**	*1095*	4.37	off
140	7/10/2003	1668	1555	1458	**4681**	*3223*	4.31	off
176	1/8/2004	43	620	45	**708**	*663*	<1.7	on

vnef - vaccinia virus vector expressing HIV nef

vvk1 - vaccinia virus vector expressing HIV gag/pol

vpe16 - vaccinia virus vector expressing HIV env

ND - not done

Tables 6.5 and 6.6 show a broad range of combined responses both in on and off-treatment contexts, as seen in bold text. The number of SFC produced by the 16 fast progressors varies from 8 SFC (subject 60) to 8281 SFC (subject 136) per million PBMC, whereas the number of SFC produced by the 6 slow progressors varies from 708 SFC (subject 176) to 4681 SFC (subject 140) per million PBMC. The range in the number of SFC is broader in the fast

progressor group indicating more variability in the numbers of SFC in this group. There are statistical outliers in the fast progressor data set, but the variability does not simply arise due to the presence of these statistical outliers. When the statistical outliers in the fast progressor group (53 SFC - subject 60; 8281 SFC - subject 92) are omitted, the range in the number of SFC produced by the fast progressors changes to 98 SFC (subject 157) to 3800 (subject 1), which, in spite of its similarity to the range of responses produced by the slow progressor group, is still more variable. This becomes apparent when the means and standard deviations are compared in Table 6.7. The on-treatment number of SFC on the sample date 12/12/2001 for subject 60 is not positive (<50 SFC/10^6 PBMC) thus are considered to be zero.

The data in the fast progressor group is not normally distributed ($p<0.05$) as confirmed by a continuous fitting distribution Shapiro-Wilk test statistic for normalcy, whereas the data in the slow progressor group is normally distributed ($p>0.05$). The non-normal distribution of the fast progressor data lends to the variability of the data as it produces a higher standard deviation.

Some samples in the fast progressor group were not tested for responses against vpe16 indicated by the ND (not done) label. For statistical purposes, the column showing responses against vpe16 is omitted in order to suitably compare the fast and slow progressor groups. We chose not to simply omit the individual sample dates (rows) that included vpe16 as a test antigen in order to maximize the number of fast progressor samples. The range of responses in the fast progressor group becomes 71 SFC (subject 51) to 7438 SFC (subject 92) and the range of responses in the slow progressor group becomes 305 SFC to 3728 SFC when the vpe16 column is omitted. As was the case in the combined

data set, the fast progressor vnef+vvk1 data set is not normally distributed ($p<0.05$) whereas the slow progressor data set is ($p>0.05$). In addition, the higher variability within the fast progressor data set remains. The numbers of SFC on sample dates 12/12/2001 and 11/6/2003 for subject 60 (highlighted) are not positive (<50 SFC/10^6 PBMC) thus are considered to be zero.

To further assess any quantitative differences in the numbers of SFC between the fast and slow progressor groups, the means and medians were calculated for on and off-treatment data, shown in Table 6.7.

Table 6.7: Comparison of mean and median HIV-specific $CD8^+$ T cell responses to vnef + vvk1 in fast and slow progressors for different VL

			on	off
mean	fp	VL	**3.04** ± 1.33	**4.63** ± 0.35
		SFC	**747** ± 795	**1879** ± 2106
	sp	VL	**2.09** ± 0.54	**3.86** ± 0.56
		SFC	**1793** ± 1149	**2187** ± 1206
median	fp	VL	**2.6**	**4.51**
		SFC	**400**	**915**
	sp	VL	**<1.7**	**3.96**
		SFC	**1718**	**1638**

On-treatment mean numbers of SFC in the slow progressor group are significantly higher than in the fast progressor group ($p<0.05$). This suggests that fast and slow progressors make different amounts of SFC on-treatment

when the virus load is reduced. Conversely, there is no significant difference between off-treatment numbers of SFC ($p>0.05$) between the two groups suggesting that both groups have similarly high numbers of off-treatment SFC.

There is a significant difference between the on and off-treatment numbers of SFC ($p<0.05$) in the fast progressor group, but not in the slow progressor group ($p>0.05$). In fact, in the slow progressor group the number of SFC does not change considerably despite an approximate 2-log change in virus load. Thus, refering to the hypothesis in subsection 6.2.1, the magnitude of positive SFC responses in the fast progressor group are indeed lower than in the slow progressor group. In addition, in the fast progressor group, the magnitude of positive SFC responses positively correlates with the virus load: higher mean virus loads are associated with higher numbers of SFC. However, in the slow progressor group, the magnitude of positive SFC responses negatively correlates, if anything, with the virus load: higher mean numbers are associated with lower virus loads. Thus, the data show that there are significant quantitative differences in the numbers of SFC between the fast and slow progressor groups in the contexts of high and low virus loads.

Notably, off-treatment, the virus load was maintained at controllable levels (3.86) in the slow progressor group in the presence of high frequencies of SFC (2187) which implies that these cells are able to control the virus to suppress the virus load. In the fast progressor group, this is not the case. Although the mean off-treatment numbers of SFC (1879) are high, the mean off-treatment virus load is also high (4.63). Therefore, even in the presence of high quantities of HIV-specific $CD8^+$ T cells, viral control is not achieved in the fast progressor group. This implies that the quantity of HIV-specific $CD8^+$ T cells, although

important in controlling the virus, is not the only factor. This, in turn, implies that the HIV-specific $CD8^+$ T cells in the two groups are qualitatively different. Subject 92 is a good example of this observation. Even though the magnitude of SFC is extremely high off-treatment (7438), the virus is not under control, as indicated by the high off-treatment virus load (4.8).

6.2.2 Quality of HIV-specific $CD8^+$ T cells

The data imply that the HIV-specific $CD8^+$ T cells in the fast and slow progressor groups differ qualitatively. The fact that the range of SFC responses in the fast progressor group (78-7438) is broader than the slow progressor group (305-3728) is one point that implies qualitative differences. That is, the level of positive responses fluctuates more in the fast progressor group implying lack of stability in these responses. In addition, the small change in the mean numbers of on and off-treatment SFC in the slow progressor group indicates that the responses are more stable than the responses in the fast progressor group.

Fast progressors may have impaired HIV-specific $CD8^+$ T cell responses in terms of proliferative ability and in general, maturation. If the HIV-specific $CD8^+$ T cell responses were functionally impaired, virus loads would potentially be consistently high due to a lack of control of viral replication by these cells [Appay *et al.*, 2000; Hess *et al.*, 2004; Shankar *et al.*, 2000]. Simply put, these cells may not be able to do what they are meant to do. In short, higher virus loads are associated with functionally impaired cells and lower virus loads are associated with functionally intact cells that impose "negative pressure" on the virus [Betts *et al.*, 2005].

To illustrate the potential impact of qualitative differences of the HIV-specific $CD8^+$ T cells in the fast and slow progressor groups and to assess the stabilities of these responses, subjects 136 and 71 were selected from the fast and slow progressor groups as representatives of each group. These subjects were selected based on the relatively high number of samples (5) available for each. The high number of samples taken over a period of approximately 3 years allows us to clearly represent how the SFC and virus loads change with respect to time over an extended period of time and to examine the stability of these responses in different treatment contexts.

To illustrate potential differences in qualities of responses, the number of SFC per million PBMC and the virus loads for these subjects (y-axis on linear and $\log_{10}$ scales, respectively) were graphed against sample dates (x-axis) as seen in Figure 6.1. The number of SFC are represented by bars (off-treatment samples are black; on-treatment samples are grey) and virus loads are represented by lines. Undetectable virus loads (< 1.7) were assumed to be the minimum cut-off value for the virus load and are therefore portrayed as "zero" values on the graphs as seen on the secondary y-axis on the right. All SFC responses are positive (> 50 SFC above background).

Subject 136 is initially off treatment. The virus load is detectable (4.2) on this sample date (1/24/2000). The number of SFC is highest (2620) on this date. The virus load subsequently falls (3.15) upon initiation of treatment by 7/5/2001. This is associated with an 11-fold reduction in the number of SFC (225). Subsequent to treatment withdrawal, over the following three years, the virus load steadily climbs (4.42), peaks (4.91) until it reaches a setpoint level (4.88). Concomitantly, the number of SFC also steadily climbs (915), peaks

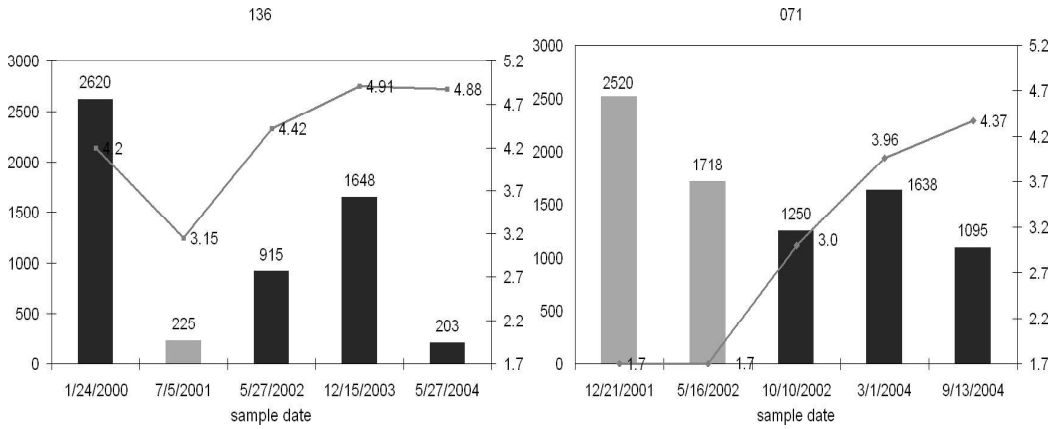

(a) Representative fast progressor, 136 (b) Representative slow progressor, 71

Figure 6.1: Comparison of SFC/10^6 PBMC and virus loads for the fast and slow progressor representatives

(1648), but then drops 8-fold (203) by 5/27/2004. The number of SFC drops while the virus load remains high and therefore these responses are unstable.

The fact that the virus load remains high despite potent anti-HIV responses (high numbers of SFC) implies that these cells may be ineffective and the responses unstable. If these cells were functioning normally and efficiently to remove infected cells and to impose anti-viral pressure on the virus, the viral loads would most likely be reduced and perhaps the responses would be more stable. When the virus load rebounds following treatment interruption, the HIV-specific $CD8^+$ T cells respond rapidly by proliferating due to increased antigen load, but do not maintain these proliferative responses over time, as indicated by the drop in number of SFC. Concomitantly, they do not clear the virus effectively to reduce the virus load or maintain it at controllable levels. The inability of the HIV-specific $CD8^+$ T cells in the fast progressor

representative to control the virus off-treatment demonstrates that these cells are ineffective *in vivo*. This ineffectiveness may be due to stunted maturation. If these cells were preterminally differentiated, they would not serve their roles as fully-functional effector cells. This may manifest in the reduced ability to clear infected cells from the system. This supports the theory that the HIV-specific $CD8^+$ T cell responses are functionally impaired in all fast progressors.

Subject 71 is initially on treatment. The virus load is undetectable (<1.7) on the first two sample dates. The numbers of SFC are highest (2520 and 1718) on these dates. When treatment is withdrawn, the virus load subsequently increases (3.0) by 10/10/2002 and steadily climbs (3.96) over the following two years to a setpoint level (4.37) by 9/13/2004. Concomitantly, the number of SFC decreases (1250), rises slightly (1638) and then decreases again (1095) by the fifth sample date 9/13/2004. The virus load continues to drop (3.98) to lower levels by 3/10/2005 (not shown). The fact that the virus load is maintained at controllable levels in the presence of lower stable frequencies of HIV-specific $CD8^+$T cells implies that these cells are functionally intact; or at least more effective than those of the fast progressor representative. Prior to treatment interruption, the HIV-specific $CD8^+$ T cells demonstrate unimpaired proliferative abilities as indicated by high numbers of on-treatment SFC. When the virus load rebounds following treatment interruption, the HIV-specific $CD8^+$ T cells maintain these good proliferative responses over time, as indicated by the relatively constant number of SFC. Concomitantly, they clear the virus effectively to keep the virus load down and to maintain it at controllable levels. The fact that the slow progressor representative demonstrates the ability to control the virus via HIV-specific $CD8^+$ T cell responses supports

the theory that the HIV-specific $CD8^+$ T cell responses are more functionally intact in slow progressors than they are in fast progressors.

Therefore, these data indicate that there are qualitative differences between the HIV-specific $CD8^+$ T cells in the fast and slow progressor groups.

6.2.3 Comparison of theoretical and experimental data

When comparing quantitative results obtained mathematically and experimentally, we see that the model accurately predicts on and off-treatment disease equilibrium states with respect to HIV-specific $CD8^+$ T cell frequencies and virus loads.

Table 6.8: Comparison of theoretical and experimental $CD8^+$ T cell responses and virus loads

			on	off	ratio
exp	fp	VL	**3.04**	**4.63**	1.52
		SFC	**747**	**1879**	**2.52**
math	fp	$\overline{V}$	**2.65**	**4.66**	1.76
		$\overline{C}^*$	**1183**	**1958**	**1.66**
exp	sp	VL	**2.09**	**3.86**	1.85
		SFC	**1793**	**2187**	**1.22**
math	sp	$\overline{V}$	**2.32**	**4.20**	1.81
		$\overline{C}^*$	**1094**	**1889**	**1.73**

* - SFC $\rightarrow$ SFC/10^6 PBMC; $\overline{C} \rightarrow$ cells/100ul

Table 6.8 shows that the experimental and theoretical trends are the same with respect to HIV-specific $CD8^+$ T cell responses and virus loads on and

off treatment. Since we assume that the fast progressors have impaired HIV-specific $CD8^+$ T cell responses, we assign a lower value to b_1 (infected cell removal rate) for the fast progressors. This qualitative difference, represented by differences in this parameter between the two groups, yields different equilibrium values as seen in Table 6.8. In the fast progressor group, the virus load is 1.52 times higher off-treatment (than on-treatment) according to experimental results and is 1.76 times higher according to the model (infected cell removal rate $b_1 = 0.0005$). There are 2.52 times as many SFC off-treatment (than on-treatment) and 1.66 times as many HIV-specific cells according to the model. In the slow progressor group, the virus load is 1.85 times higher off-treatment (than on-treatment) according to experimental results and is 1.81 times higher according to the model (infected cell removal rate $b_1 = 0.05$). There are 1.22 times as many SFC off-treatment and 1.73 times as many HIV-specific $CD8^+$ T cells according to the model. The only considerable discrepancies between experimental results and the model are the on-treatment numbers of SFC in the fast and slow progressor groups. The model predicts smaller differences in on and off-treatment numbers of SFC in the fast progressor group and larger differences in on and off-treatment numbers of SFC in the slow progressor group. These differences arise from the differences in the theoretically-determined $\overline{C}$ values whereby this value is predicted to be higher in the fast progressor group, and lower in the slow progressor group on-treatment than the experimentally-obtained values. It is important to bear in mind that the value $r = 100$ was the "selected" treatment parameter value. See Chapter 4. Therefore, in the case of the fast progressors, if treatment is more efficacious, that is, if the treatment parameter value was higher, then

the theoretically-determined value would be lower. A higher r value would also reduce the viral setpoint to a lower level. However, in the slow progressor group, a lower value for r would need to be selected to allow for a higher theoretically-determined value. A lower r value would subsequently result in a higher viral setpoint. Thus, we can narrow the gap between the theoretical and experimental results by selecting a different value for r.

What is most important in comparing the theoretical and the experimental results is the relative proportion of the number of SFC to virus load on and off-treatment. For example, despite the difference between the absolute numbers of SFC in the theoretical and experimental settings, the number of SFC is higher off-treatment in both. Likewise, in the slow progressor group, the number of theoretically and experimentally-determined SFC are greater off-treatment. The fact that the theoretically-determined numbers of SFC are more disparate than the experimentally-determined numbers in the slow progressor group, and less disparate in the fast progressor group, does not take away from the predictive potential of the model due to the fact that we can modify the theoretically-determined numbers by simply modifying the treatment parameter value to more appropriately describe the efficacy of treatment.

In summary, I report quantitative and qualitative differences in the HIV-specific $CD8^+$ T cell responses between two clinically-determined subgroups of HIV-1-infected indidviduals. One group, the fast progressors, showed impaired responses which matched consistently high virus loads, as determined by high off-treatment peak virus loads and high mean on and off-treatment virus loads. Another group, the slow progressors, showed stable effective responses which matched virus loads that were at controllable levels as determined by

low off-treatment peak virus loads and low mean on and off-treatment virus loads. In the following section, we further examine the reasons for these differences and the impact that qualitative differences in HIV-specific $CD8^+$ T cells has on mathematical modeling of HIV-immunopathogenesis and the effects of treatment interruption.

Chapter 7

Discussion and conclusions

The novel mathematical model of HIV immunopathogenesis I constructed predicts the existence of a single stable fixed point. Although global stability of the stable fixed point had not been demonstrated, numerical simulations have not demonstrated the existence of limit cycles chaos or any other phenomena. With a single stable fixed point, the initial conditions do not affect the eventual arrival at this single equilibrium point. These initial conditions represent the initial numbers of T cells and the virus load. Therefore, the model predicts that regardless of the initial number of T cells or the amount of virus that enters the system or where/how it enters the system at the point of infection, the outcome of infection, as defined by the numbers of T cells at equilibrium and the viral setpoint, does not change. This is not to say that all infected individuals will have the same setpoint. The setpoint is determined by the parameter values used in the model.

Naturally, as previously predicted, the existence of a single stable fixed point means that treatment cannot be used to reset the viral setpoint. When

treatment is imposed on the system, the system behaves according to known effects of treatment on the HIV-infected immune system. The virus load falls and the uninfected $CD4^+$ T cell population rises. Bifurcation analysis confirmed an indirect relationship between the treatment parameter r, or the efficacy of treatment, and the viral setpoint $\overline{V}$ and a direct relationship between r and the number of infected cells at equilibrium, $\overline{U}$. Thus, treatment functions to transiently lower the viral load but not to permanently reduce it to a lower setpoint level.

Another implication of a single stable fixed point is that death is never predicted as a stable state. All biological systems are finite. Thus, future work will involve modifying the model to predict at least two stable biologically relevant equilibrium states: one to represent the host living with virus and one to represent the death of the host. A way to do this may involve including an additional term in the model that represents interactions between HIV-specific $CD4^+$ T cells and HIV-specific $CD8^+$ T cells.

The model also predicted a virus-free equilibrium state at very high treatment values. That is, the model is sensitive to small changes in drug efficacies that result in very low on-treatment virus loads. This result implies that, according to the model, it is theoretically possible to clear the virus from the system if treatment is virtually 100% effective and maintained *ad infinitum*. However, treatment is never this effective in reality or maintained *ad infinitum*. This result simply reflects the fact that if treatment reduces the viral production rate beyond some threshold, the virus population decays faster than it grows. However, even if the virus population does decay, which it does in some individuals, this decay is not fast enough for eradication to occur during

a normal lifespan.

It is important to reiterate that the single stable fixed point is the product of a particular parameter set. If the parameter set was different, it is possible that the model would predict more than a single stable equilibrium point. The existence of at least two stable fixed points would allow for alternate states of being resulting in more than a single potential outcome in terms of equilibrium states. For example, an infected individual may tend to an equilibrium state whereby they are controlling the virus reasonably well if their $CD4^+$ T cell count is above some threshold. In addition, the model solutions for the chosen parameter set approach the single stable fixed point according to numerical simulations and bifurcation diagrams. However, it should be noted that for a different parameter set, the model may in fact predict the existence of more complicated behaviour such as limit cycles. In this thesis, more complicated behaviours were not observed: all solutions for the chosen parameter set approached the single stable fixed point.

An analysis of the model without the explicit inclusion of a population of cells representative of an HIV-specific $CD8^+$ T cell population showed two important things. One, the predicted single stable fixed point value obtained from analysis of the three-dimensional system comprised equilibrium values representative of an HIV-infected individual not controlling the virus. The same parameter set was used in both the three and four-dimensional models. Two, the treatment parameter had to be higher to induce analogous effects on the three-dimensional system. These observations reflect the important role of HIV-specific $CD8^+$ T cells in controlling the virus, at least in the theoretical setting, and provide support for the importance of including this

variable explicitly in the model. Therefore, the model reflects the dual role of HIV-specific $CD8^+$ T cells and antiretroviral treatment to suppress the virus load to lower levels. This makes the model strong and reasonable with respect to accurately describing immunopathogenesis and the effects of treatment.

The C equation in the four-dimensional model imposes a term on the infected cell equation that removes infected cells from the system at a particular rate. Clinical data showed that the HIV-infected individuals can be categorized as fast or slow progressors. We hypothesized that the rate of removal of infected cells partially dictates status as one or the other. That is, fast and slow progressors have different removal rate parameter values. Bifurcation diagrams supported this hypothesis. An inverse relationship was observed between the removal rate and the infected cell and virus populations at equilibrium. Lower values of b_1, or the removal rate parameter, were associated with higher fixed point values for infected cells $\overline{I}$ and viral loads $\overline{V}$, and lower fixed point values for uninfected cells $\overline{U}$. Higher fixed point values for $\overline{V}$ and lower fixed point values for $\overline{U}$ are typical of a fast progressor. Disease progression was defined by both the rate of viral rebound and the loss of HIV-specific $CD4^+$ T cells immediately following a treatment interruption and by the values of the fixed point coordinates $\overline{U}$ and $\overline{V}$ in the model. Therefore, an inverse relationship was observed between disease progression and the removal rate. Disease progression was found to be slower when the removal rate was higher and thus fast progressors are assumed to have a lower removal rate parameter value than slow progressors.

The model predicts that differences in removal rates of infected cells (differences in fast and slow progressors), are more significant when treatment is on.

When treatment was off, a bifurcation occured at a considerably higher value of b_1 than when treatment was on. Knowing this, we investigated whether treatment interruptions could be used to boost HIV-specific $CD8^+$ T cell activity (as determined by the trajectories in the time series plots) during the off-treatment phases to lower the viral setpoint, even when the removal rates are different. The model predicted that this could not happen, regardless of the value of b_1, unless the value of the rate actually changed *during* infection. Therefore, since the rates are constant, the model predicts that treatment interruptions can transiently boost HIV-specific $CD8^+$ T cell frequencies but cannot be used to reset the viral setpoint. It seems as though the removal rate should increase with increased HIV-specific $CD8^+$ T cell frequency, but it does not. This rate remains constant and the changes in the HIV-specific $CD8^+$ T cell population are the result of the value of the parameter, and not by the number of cells at any given point.

Due to factors such as CTL exhaustion, the removal rate parameter very likely becomes smaller as the disease progresses. Theoretically, the removal rate parameter could be written as a function of the virus, which inevitably, would cause the system to elicit different behaviours. Future work will involve replacing one or more constant parameters by functions of either variables or time.

Experimental observations showed distinct differences between the clinically-determined fast and slow progressor groups. The number of SFC (number of HIV-specific cells producing IFN-γ) varied quantitatively both within the fast and slow progressor groups, and within on and off-treatment settings. Experimental evidence supports the theory that there are also qualitative differences

between the SFC in the fast and slow progressor groups. Future work will involve determining why this is and incorporating this into the model.

There are at least several causes for diminished functional ability of HIV-specific $CD8^+$ T cells but all are spurred by the presence of HIV. Whether it is a result of the loss of help from HIV-specific $CD4^+$ T cells [Lichterfeld *et al.*, 2004; Yue *et al.*, 2004], or high turnover of HIV-specific $CD8^+$ T cells leading to exhaustion, it is evident that disease progression is linked to the inability of HIV-specific $CD8^+$ T cells to do what they are meant to do. It is therefore likely that infected individuals who progress quickly through disease (fast progressors) have decreased IL-2 production and a larger fraction of preterminally differentiated cells resulting in overall loss of control of viral replication which translates into low CD4 T cell counts and high virus loads. On the other hand, infected individuals who do not progress quickly through disease (slow progressors) have normal IL-2 production and a larger fraction of terminally differentiated cells [Betts *et al.*, 2005].

We can further speculate as to how the HIV-specific $CD8^+$ T cells examined in the HIV-1-infected individuals in this study are qualitatively different. Functionally intact HIV-specific $CD8^+$ T cells produce cytokines such as IFN-γ and IL-2 and can differentiate into terminally-differentiated effector CTL as part of normal immune responses against the virus. Functionally impaired cells are characterized by a loss of ability to produce and respond to these cytokines and to fulfill functional effector CTL duties [Wherry & Ahmed, 2004; Kristensen *et al.*, 2002; Appay *et al.*, 2000]. Studies relate progressive HIV infection to decreased IL-2 production by HIV-specific T cells [Zimmerli *et al.*, 2005; Kinter & Fauci, 1996; Ghezzi *et al.*, 1997]. IL-2 is a T cell growth factor

and controls the functions of T cells. HIV-specific $CD8^+$ T cells that become activated to impose effector functions require IL-2 to drive clonal expansion (proliferation) and differention into effector and memory T cells. Therefore, a lack of sufficient IL-2 to drive clonal expansion of T cells translates into progressive infection associated with low $CD4^+$ T cell counts and high virus loads. We saw this trend in the fast progressor group.

Decreased IL-2 production may play a role in improper maturation of HIV-specific $CD8^+$ T cells into fully functional immune effector cells [Kristensen *et al.*, 2002; Wherry & Ahmed, 2004]. Memory differentiation has been linked to the appearance of cells with the capacity to produce IL-2 [Kristensen *et al.*, 2002; Saparov *et al.*, 1999]. Studies show that progressive HIV disease is associated with expansion of HIV-specific $CD8^+$ T cells with a preterminally differentiated phenotype [Appay *et al.*, 2000; Champagne *et al.*, 2001; Yue *et al.*, 2004]. Preterminal differentiation of HIV-specific $CD8^+$ T cells would create a pool of cells unable to fulfill effector duties as expected for inapparent slow disease progression.

Studies have also linked progressive HIV infection to loss of functional CTL [Chia *et al.*, 1994]. HIV-specific $CD8^+$ T cells (CTL) can become functionally impaired over time by becoming perforin-deficient [Migueles *et al.*, 2002; Appay *et al.*, 2000]. A perforin-deficient HIV-specific $CD8^+$ T cell will have diminished capacity to kill virally-infected cells, which would likely translate into higher virus loads [S.A. Migueles *et al.*, 2002; Borrow *et al.*, 1994; V. Appay *et al.*, 2000]. The loss of functional CTL is likely linked to the perpetual generation of these cells in response to the presence of the virus. The precursor cells for these CTL may also have limited regenerative capacity and eventu-

ally become deleted or clonally exhausted and disappear completely [Wolthers *et al.*, 1996; Mackall *et al.*, 1997]. Studies have indeed suggested that HIV-specific $CD8^+$ T cells have a high turnover rate based on progressively reduced chromosome telomere length of these cells in HIV-infected individuals and may result in the rapid consumption of terminally differentiated HIV-specific $CD8^+$ T cells. (Each time a cell divides, its telomere length shortens [Allsopp *et al.*, 1995].)

Future work may involve assessing the proliferative abilities of HIV-specific $CD8^+$ T cells by measuring IL-2 responses from clinically-defined fast and slow progressors from a larger cohort of infected individuals and thus allow a determination of the functional ability of these cells to proliferate in response to restimulation. The ratio between the amount of IFN-γ and IL-2 produced by the HIV-specific $CD8^+$ T cells could be determined for each of the fast and slow progressor groups to further define the qualitative differences between these cells.

In addition, assessments of the phenotypic markers for the HIV-specific $CD8^+$ T cells in the fast and slow progressor groups could be done to determine potential differences in differentiation stages of the HIV-specific $CD8^+$ T cells. As previously discussed, progressive disease is associated with skewed maturation of memory HIV-specific T cells. Studies designed to delineate the phenotypes of the HIV-specific $CD8^+$ T cells in fast and slow progressors may help to elucidate the reasons why the differentiation pathways are different.

Maintenance of effective immune responses and stimulation of cellular immune response mechanisms are essential to the health of an HIV-infected individual. Both mathematical and experimental assessments of the quantita-

tive and qualitative differences between clinically-defined subgroups of a small HIV-infected cohort show that slow progressors have lower off-treatment viral setpoints which are determined by both the quantity of HIV-specific $CD8^+$ T cells and by their quality. The rate at which these cells remove infected cells appears to be linked to the ability of the immune system to suppress the virus to controllable levels in the absence of treatment. The HIV-specific $CD8^+$ T cells are thus more functionally efficient in slow progressors.

Ultimately, the model indicates that, despite differences in removal rates among HIV-infected individuals, treatment interruption can be used to transiently boost HIV-specific $CD8^+$ T cell responses but cannot be used to reset the viral setpoint. The model predicted that treatment interruption can only be used to transiently delay disease progression implying no constructive immune enhancement during the treatment interruption phases. Our results thus corroborate that treatment interruption is in fact useful, but limited as a means to perturb the system toward a more desirable state.

The results of this work can be used to promote the potential usefulness of interrupting treatment. Ultimately, it is the choice of the individual as to whether or not the benefits of interrupting treatment outweigh the risks. A month break from the toxic drugs would be a great relief for most and if carefully monitored, an individual should, in theory, be able to take these breaks.

Chapter 8

Appendix

Cluster 1 of 2 contains 16 cases

Members			Statistics				
Case	Distance		Variable	Min.	Mean	Max.	St.Dev.
Case 7	0.17		VL	4.77	5.38	5.88	0.44
Case 8	0.58		CD4	1.43	2.09	2.61	0.42
Case 9	0.17						
Case 10	0.48						
Case 11	0.26						
Case 12	0.31						
Case 13	0.50						
Case 14	0.53						
Case 15	0.50						
Case 16	0.44						
Case 17	0.31						
Case 18	0.57						

```
Case  19    0.35   |
Case  20    0.46   |
Case  21    0.40   |
Case  22    0.38   |
------------------------------------------------------------
Cluster 2 of 2 contains 6 cases
         Members                        Statistics
  Case    Distance |  Variable Min.  Mean  Max. St.Dev.
Case   1    0.46   |  VL       1.70  3.70  4.37 1.02
Case   2    0.48   |  CD4      2.39  2.66  2.97 0.21
Case   3    0.08   |
Case   4    0.22   |
Case   5    0.44   |
Case   6    1.43   |
```

Chapter 9

Bibliography

Adams, B.M., H.T. Banks, H.D. Kwon, H.T. Tran (2004). Dynamic multidrug therapies for HIV: optimal and STI control approaches. *Mathematical Biosciences* **1**, 223-241.

Agrawal, N.G.B. and J.J. Linderman (1996). Mathematical modeling of helper T lymphocyte/antigen-presenting cell interactions: analysis of method for modifying antigen processing and presentation. *J. Theor. Biol.* **182** 487-504.

Allsopp, R.C., E. Chang, M. Kashefi-Aazam, E.I. Rogaev, M.A. Piatyszek, J.W. Shay, C.B. Harley (1995). Telomere shortening is associated with cell division *in vitro* and *in vivo*. *Exp. Cell. Res.* **220** 194-200.

Altes, H.K., R.M. Ribeiro, R.J. de Boer (2003). The race between initial T-helper expansion and virus growth upon HIV infection influences polyclonality

of the response and viral set-point. *Proc. R. Soc. Lond.* **270** 1349-1358.

Altfeld, M., E.S. Rosenberg, R. Shankarappa, J.S. Mukherjee, F.M. Hecht, R.L. Eldridge, M.M. Addo, S.H. Poon, M.N. Phillips, G.K. Robbins, P.E. Sax, S. Boswell, J.O. Kahn, C. Brander, P.J. Goulder, J.A. Levy, J.I. Mullins, B.D. Walker (2001). Cellular immune responses and viral diversity in individuals treated during acute and early HIV-1 infection. *J. Exp. Med.* **193** 169-180.

Altfeld, M. and B. Walker (2005) *HIV Medicine: Acute HIV-1 Infection*, Steinhauser Verlag, Flying Publisher, Druckhaus Sud GmgH and Co.

Appay, V., D.F. Nixon, S.M. Donahoe, G.M. Gillespie, T. Dong, A. King, G.S. Ogg, H.M. Spiegel, C. Conlon, C.A. Spina, D.V. Havlir, D.D. Richman, A. Waters, P. Easterbrook, A.J. McMichael, S.L. Rowland-JonesL (2000). HIV-specific $CD8^+$ T cells produce antiviral cytokines but are impaired in cytolytic function. *J. Exp. Med.* **192** 63-75.

Appay, V., P. Dunbar, M. Callan, P. Klenerman, G.M.A. Gillespie, L. Papagno, G.S. Ogg, A. King, F. Lechner, C.A. Spina, S. Little, D.V. Havlir, D.D. Richman, N. Gruener, G. Pape, A. Waters, P. Easterbrook, M. Salio, V. Cerundolo, A.J. McMichael, S.L. Rowland-Jones (2002). Memory $CD8^+$ T cells vary in differentiation phenotype in different persistent virus infections. *Nature Medicine* **8** 379-385.

Appay, V., P. Hansasuta, J. Sutton, R.D. Schrier, J.K. Wong, M. Furtado,

D.V. Havlir, S.M. Wolinsky, A.J. McMichael, D.D. Richman, S.L. Rowland-Jones, C.A. Spina (2002). Persistent HIV-1-specific cellular responses despite prolonged therapeutic viral suppression. *AIDS* **16** 161-170.

Bajaria, S.H., G. Webb, M. Cloyd, D. Kirschner (2002). Dynamics of Naive and Memory CD4+ T Lymphocytes in HIV-1 Disease Progression. *JAIDS* **30** 41-58.

Benito, J.M., M. Lopez, S. Lozano, P. Martinez, M. Kuroda, J. Gonzalez-Lahoz, V. Soriano (2003). Phenotype and functional characteristics of HIV-specific cytotoxic CD8+ T cells in chronically infected patients: dual effects of highly active antiretroviral therapy. *J. Acquir. Immune Defic. Syndr.* **34** 255-266.

Betts, M.R., M.C. Nason, S.M. West, S.C. De Rosa, S.A. Migueles, J. Abraham, M.M. Lederman, J.M. Benito, P.A. Goepfert, M. Connors, M. Roederer, R.A. Koup (2005). HIV nonprogressors preferentially maintain highly functional HIV-specific $CD8^+$ T-cells. *Blood* **107** 4781-4789.

Blower, S.M., and P. Volberding (2002). What can modeling tell us about the threat of antiviral drug resistance? *Curr. Opin. Infectious Diseases* **15** 609-614.

Bonhoeffer, S., M. Rembiszewski, G.M. Ortiz, D.F. Nixon (2000). Risks and benefits of structured antiretroviral drug therapy interruptions in HIV-1 infec-

tion. *AIDS* **14** 2313-2322.

Borghans, J.A., L.S. Taams, M.H.M. Wauben, R.J. De Boer (1999). Competition for antigenic sites during T cell proliferation: a mathematical interpretation of *in vitro* data. *Proc. Natl. Acad. Sci.* **96** 10782-10787.

Borghans, J.A., M.D. Hazenberg, F. Miedema (2005). Limited role for the thymus in SIV pathogenesis. *Eur. J. Immunol.* **35** 42-45.

Borrow, P., H. Lewicki, B.H. Hahn, G.M. Shaw, M.B. Oldstone (1994). Virus-specific CD8+ cytotoxic T-lymphocyte activity associated with control of viremia in primary human immunodeficiency virus type 1 infection. *J. Virol.* **68** 6103-6110.

Boyce, W.E. and R.C. DiPrima, WIE Elementary Differential Equations and Boundary Value Problems, 8th Edition, John Wiley and Sons, Inc., 2006.

Brandt, M.E. and G. Chen (2001). Feedback control of a biodynamical model of HIV-1. *IEEE Transactions on Biomedical Engineering* **48** 754-757.

Callaway, D.S. and A.S. Perelson (2002). HIV-1 infection and low steady state viral loads. *Bulletin of Mathematical Biology* **64** 29-64.

Casazza, J.P., M.R. Betts, B.J. Hill, J.M. Brenchley, D.A. Price, D.C. Douek, R.A. Koup (2005). Immunologic pressure within class I-restricted cognate hu-

man immunodeficiency virus epitopes during highly active antiretroviral therapy. *J. Virol.* **79** 3653-3663.

Centers for Disease Control, Mortality patterns - United States, 1989, MMWR 41: 121-125.

Champagne, P., G.S. Ogg, A.S. King, C. Knabenhans, K. Ellefsen, M. Nobile, V. Appay, G.P. Rizzardi, S. Fleury, M. Lipp, R. Forster, S.L. Rowland-Jones, R.P. Sekaly, A.J. McMichael, G. Pantaleo (2001). Skewed maturation of memory HIV-specific CD8 T lymphocytes. *Nature* **410** 106-111.

Chouquet, C., B. Autran, E. Gomard, J.M. Bouley, V. Calvez, C. Katlama, D. Costagliola, Y. Riviere (2002). Correlation between breadth of memory HIV-specific cytotoxic T cells, viral load and disease progression in HIV infection. *AIDS* **16** 2399-2407.

Chun, T.W. and A.S. Fauci (1999), Latent reservoirs of HIV: Obstacles to the eradication of virus. *Proc. Nat. Acad. Sci. U.S.A.* **96** 10958-10961.

Cooper, L.N. (1986) Theory of an immune system retrovirus. *Proc. Natl Acad. Sci. U.S.A.* **83** 9159-9163.

Dalgleish, A.D., P.C.L. Beverley, P.R. Clapham, D.H. Crawford, M.F. Greaves, R.A. Weiss (1984), The CD4 (T4) antigen is an essential component of the receptor for the AIDS retrovirus. *Nature* **312** 763-767.

Dalod, M., M. Dupuis, J.C. Deschemin, D. Sicard, D. Salmon, J.F. Delfraissy, A. Venet, M. Sinet, J.G. Guillet (1999). Broad, intense anti-human immunodeficiency virus (HIV) *ex vivo* $CD8^+$ responses in HIV type 1-infected patients: comparison with anti-Epstein-Barr virus responses and changes during antiretroviral therapy. *J. Virol.* **73** 7108-7116.

DeBoer, R.J., and C.A.B. Boucher (1996). Anti-CD4 therapy for AIDS suggested by mathematical models. *Proc. R. Soc. Lond. B.* **263** 889-905.

DeJong, M.D., R.J. de Boer, F. de Wolf, N.A. Foudraine, C.A.B. Boucher, J. Goudsmit, J.M.A. Lange (1997). Overshoot of HIV-1 viraemia after early discontinuation of antiretroviral treatment. *AIDS* **11** F79-F84.

Coffin, J.M. (1995) HIV population dynamics *in vivo*: implications for genetic variation, pathogenesis, and therapy. *Science* **267** 483-489.

Douek, D.C., J.M. Brenchley, M.R. Betts, D.R. Ambrozak, B.J. Hill, Y. Okamoto, J.P. Casazza, J. Kuruppu, K. Kunstman, S. Wolinsky, Z. Grossman, M. Dybul, A. Oxenius, D.A. Price, M. Connors, R.A. Koup (2002). HIV preferentially infects HIV-specific $CD4^+$ T cells. *Nature* **417** 95-98.

Douek, D.C., L.J. Picker, R.A. Koup (2003). T Cell Dynamics in HIV-1 Infection. *Annu. Rev. Immunol.* **21** 265-304.

Ermentrout, B., *Simulating, Analyzing, and Animating Dynamical Systems: A Guide To XPPAUT for Researchers and Students*

Essunger, P. and A.S. Perelson (1994). Modeling HIV infection of $CD4^+$ T-cell populations. *J. Theor. Biol.* **170** 367-391.

Fagard, C., A. Oxenius, H. Gunthard, F. Garcia, M. Le Braz, G. Mestre, M. Battegay, H. Furrer, P. Vernazza, E. Bernasconi, A. Telenti, R. Weber, D. Leduc, S. Yerly, D. Price, S.J. Dawson, T. Klimkait, T.V. Perneger, A. McLean, B. Clotet, J.M. Gatell, L. Perrin, M. Plana, R. Phillips, B. Hirschel (2003). A prospective trial of structured treatment interruptions in human immunodeficiency virus infection. *Arch. Intern. Med.* **163** 1220-1226.

Frost, S.D.W. (2002). Structured Antiretroviral Therapy Interruption as a form of Immune-based Therapy in HIV-1 Infection. *J. Virol.* **76** 968-979.

Garcia F., J.M. Mir, J.M. Gatell (2000). Structured Antiretroviral Therapy Interruption as a form of Immune-based Therapy in HIV-1 Infection. *AIDS* **2** 3-8.

Ghezzi. S., E. Vicenzi, L. Soldini, G. Tambussi, M. Murone, A. Lazzarin, G. Poli (1997). Experiences in immune reconstitution. The rationale for interleukin-2 administration to HIV-infected individuals. *J. Biol. Regul. Homeost. Agents.* **11** 74-78.

Griffiths, D.F., *Learning LaTeX,* Society for Industrial and Applied Mathematics, Philadelphia (1997).

Guidelines for the Use of Antiretroviral Agents in HIV-1-Infected Adults and Adolescents, Developed by the DHHS Panel on Antiretroviral Guidelines for Adults and Adolescents, A Working Group of the Office of AIDS Research Advisory Council, updated May 4, 2006.

Gulzar, N. and K.F. Copeland (2004). $CD8^+$ T cells: function and response to HIV infection. *Current HIV Res.* **2** 23-37.

Hale and Koçak, *Dynamics and Bifurcations*, Springer-Verlag (1991).

Hess, C., M. Altfeld, S.Y. Thomas, M.M. Addo, E.S. Rosenberg, T.M. Allen, R. Draenert, R.L. Eldrige, J. van Lunzen, H.J. Stellbrink, B.D. Walker, A.D. Luster (2004). HIV-1 specific $CD8^+$ T-cells with an effector phenotype and control of viral replication. *Lancet* **362** 863-866.

Ho, D.D., A.U. Neumann, A.S. Perelson, W. Chen, J.M. Leonard, M. Markowitz (1995). Rapid turnover of plasma virions and CD4 lymphocytes in HIV-1 infection. *Nature* **373** 123-26.

Hraba, T. and J. Dolezal (1996). A mathematical model and $CD4^+$ lymphocyte dynamics in HIV infection. *Emerging Infectious Diseases* **2** 299-306.

Isaaz, S., K. Baetz, K. Olsen, E. Podack, G.M. Griffiths (1995). Serial killing by cytotoxic T lymphocytes: T cell receptor triggers degranulation, re-filling of the lytic granules and secretion of lytic proteins via a non-granule pathway. *Eur. J. Immunol.* **25** 1071-1079.

Janeway, C.A., P. Travers, M. Walport, M. Schlomchik, (2001). *Immunobiology, fifth ed*, Garland Publishing, Taylor and Francis Group.

Jansen, C.A., E. Piriou, C. Bronke, J. Vingerhoed, S. Kostense, D. van Baarle, F. Miedema (2004). Characterization of virus-specific $CD8^+$ effector T cells in the course of HIV-1 infection: longitudinal analyses in slow and rapid progressors. *Clin. Immunol.* **113** 299-309.

Kalams, S.A., S.P. Buchbinder, E.S. Rosenberg, J.M. Billingsley, D.S. Colbert, N.G. Jones, A.K. Shea, A.K. Trocha, B.D. Walker. (1999). Association between virus-specific cytotoxic T-lymphocyte and helper responses in human immunodeficiency virus type 1 infection. *J. Virol.* **73** 6715-6720.

Kawamura, D., H. Gatanaga, D.L. Borris, M. Connors, H. Mitsuya, A. Blauvelt (2003). Decreased Stimulation of $CD4^+$ T Cell Proliferation and IL-2 Production by Highly Enriched Populations of HIV-Infected Dendritic Cells. *The Journal of Immunology* **170** 4260-4266.

Kinter, S. and A.S. Fauci (1996). Interleukin-2 and human immunodeficiency virus infection: pathogenic mechanisms and potential for immunologic en-

hancement. *Immunol. Res.* **15** 1-15.

Kirschner, D.E. and A.S. Perelson (1995). A model for the immune system response to HIV: AZT treatment studies. *Mathematical Population Dynamics: Analysis of Hetergeneity and Theory of Epidemics* Wuerz Publishing, Winnipeg, 295-310.

Kirschner, D.E., Using mathematics to understand HIV immune dynamics. *Notices of the AMS* **43** 191-202.

Kirschner, D.E. and G.F. Webb (1998). Immunotherapy of HIV-1 infection. *J. Biol. Systems* **6** 71-83.

Kirschner, D.E., G.F. Webb, M. Cloyd (2000). Model of HIV-1 disease progession based on virus-induced lymph node homing-induced apoptosis of $CD4^+$ lymphocytes. *JAIDS* **24** 352-362.

Klatzmann, D., E. Champagne, S. Chamaret, J. Gruest, D. Guetard, T. Hercend, J.C. Gluckman, L. Montagnier (1984). T-lymphocyte T4 molecule behaves as the receptor for human retrovirus LAV. *Nature* **312** 767-768.

Komarova, N.L., E. Barnes, P. Klenerman, D. Wodarz (2003). Boosting immunity by antiviral drug therapy: a simple relationship among timing, efficacy, and success. *PNAS* **100** 1855-1860.

Kristensen, N.N., J.P. Christensen, A.R. Thomsen (2002). High numbers of IL-2-producing $CD8^+$ T cells during viral infection: correlation with stable memory development. *J. Gen. Virol.* **83** 2123-2133.

Lacabaratz-Porret, C., A. Urrutia, J.M. Doisne, C. Goujard, C. Deveau, M. Dalod, L. Meyer, C. Rouzioux, J.F. Delfraissy, A. Venet, M. Sinet (2003). Impact of antiretroviral therapy and changes in virus load on human immunodeficiency virus (HIV)-specific T cell responses in primary HIV infection. *J. Infect. Dis.* **187** 748-757.

Landay, A.L., C.E. Mackewicz, J.A. Levy (1993). An activated CD8+ T cell phenotype correlates with anti-HIV activity and asymptomatic clinical status. *Clin. Immunol. Immunopathol.* **69** 106-116.

Levy, J.A. (1996). Infection by human immunodeficiency virus - CD4 is not enough. *New England J. Med.* **335** 1528-1530.

Lichterfeld, M., D.E. Kaufmann, X.G. Yu, S.K. Mui, M.M. Addo, M.N. Johnston, D. Cohen, G.K. Robbins, E. Pae, G. Alter, A. Wurcel, D. Stone, E.S. Rosenberg, B.D. Walker, M. Altfeld (2004). Loss of HIV-1-specific $CD8^+$ T cell proliferation after acute HIV-1 infection and restoration by vaccine-induced HIV-1-specific $CD4^+$ T cells. *J. Exp. Med.* **200** 701-712.

Lori, F. and J. Lisziewicz (2001). Structured treatment interruptions for the management of HIV infection. *J. American. Med. Assoc.* **23** 2981-2987.

Macatonia, S.E. (1991). Primary proliferative and cytotoxic T-cell responses to HIV induced *in vitro* by human dendritic cells. *Immunology* **74** 399-406.

Mackall, C.L., T.A. Fleisher, M.R. Brown, M.P. Andrich, C.C. Chen, I.M. Feuerstein, I.T. Magrath, L.H. Wexler, D.S. Dimitrov, R.E. Gress (1997). Distinctions between $CD8^+$ and $CD4^+$ T-Cell regenerative pathways result in prolonged T-cell subset imbalance after intensive chemotherapy. *Blood* **89** 3700-3707.

McClean, A.R. and M.A. Nowak (1992). Models of interactions between HIV and other pathogens. *J. Theor. Biol.* **155** 6986.

McCune, J.M. (2001). The dynamics of $CD4^+$ T cell depletion in HIV disease. *Nature* **410** 974-978.

McMichael, A.J. and S.L. Rowland-Jones (2001). Cellular immune responses to HIV. *Nature* **410** 980-987.

McNeil, A.C., W.L. Shupert, C.A. Iyasere, C.W. Hallahan, J. Mican, R.T. Davey Jr., M. Connors (2001). High level HIV-1 viremia suppresses viral antigen-specific $CD4^+$ T cell proliferation. *Proc. Nat. Acad. Sci. U.S.A.* **98** 13878-13883.

Mehandru, S., M.A. Poles, K. Tenner-Racz, A. Horowitz, A. Hurley, C. Hogan,

D. Boden, P. Racz, M. Markowitz (2004). Primary HIV-1 Infection Is Associated with Preferential Depletion of $CD4^+$ T Lymphocytes from Effector Sites in the Gastrointestinal Tract. *J. Exp. Med.* **200** 761-770.

Mellors, J.W., L.A. Kingsley, C.R. Rinaldo, J.A. Todd, B.S. Hoo, R.P. Kokka, P. Gupta (1995). Quantitation of HIV-1 RNA in plasma predicts outcome after seroconversion. *Annals of Internal Medicine* **122** 573-579.

Migueles, S.A., A.C. Laborico, W.L. Shupert, M.S. Sabbaghian, R. Rabin, C.W. Hallahan, D. van Baarle, S. Kostense, F. Miedema, M. McLaughlin, L. Ehler, J. Metcalf, S. Liu, M. Connors (2002). HIV-specific $CD8^+$ T cell proliferation is coupled to perforin expression and is maintained in nonprogressors. *Nature Immunology* **3** 1061-1068.

Montaner, L.J. (2001). Structured treatment interruptions to control HIV-1 and limit drug exposure. *Trends in Immunology* **22** 92-96.

Musey, L., J. Hughes, T. Schacker, T. Shea, L. Corey, M.J. McElrath (1997). Cytotoxic-T-Cell Responses, Viral Load, and Disease Progression in Early Human Immunodeficiency Virus Type 1 Infection. *The New England Journal of Medicine* **337** 1267-1274.

Nikolova, M.H., M.N. Muhtarova, H.B. Taskov, K. Kostov, L. Vezenkov, A. Mihova, L. Boumsell, A. Bensussan (2005). The CD160+ CD8 high cytotoxic T cell subset correlates with response to HAART in HIV-1^+ patients. *Cell*

Immunology **237** 96-105.

Notermans, D.W., J. Goudsmit, S.A. Danner, A.S. Perelson, J. Mittler (1998). Rate of HIV-1 decline following antiretroviral therapy is related to viral load at baseline and drug regimen. *AIDS* **12** 1483-1490.

Nowak, M.A. and C.R. Bangham (1996). Population dynamics of immune responses to persistent viruses. *Science* **272** 74-79.

Ortiz, G.M., J. Hu, J.A. Goldwitz, R. Chandwani, M. Larsson, N. Bhardwaj, S. Bonhoeffer, B. Ramratnam, L. Zhang, M.M. Markowitz, D.F. Nixon (2002). Residual viral replication during antiretroviral therapy boosts human immunodeficiency virus type 1-specific $CD8^+$ T cell responses in subjects treated early after infection. *Journal of Virology* **76** 411-415.

Oxenius, A., D.A. Price, P.J. Easterbrook, C.A. O'Callaghan, A.D. Kelleher, J.A. Whelan, G. Sontag, A.K. Sewell, R.E. Phillips (2000). Early highly active antiretroviral therapy for acute HIV-1 infection preserves immune function of $CD8^+$ and $CD4^+$ T lymphocytes. *Proc. Nat. Acad. Sci. U.S.A.* **97** 3382-3387.

Oxenius, A., D.A. Price, H.F. Gnthard, S.J. Dawson, C. Fagard, L. Perrin, M. Fischer, R. Weber, M. Plana, F. Garca, B. Hirschel, A. McLean, R.E. Phillips (1993). Stimulation of HIV-specific cellular immunity by structured treatment interruption fails to enhance viral control in chronic HIV infection. *Proc. Nat. Acad. Sci. U.S.A.* **21** 13377-13378.

Perelson, A.S., D.E. Kirschner, R. deBoer (1993). Dynamics of HIV infection of CD4$^+$ T cells. *Mathematical Biosciences* **114** 81-125.

Perelson, A.S., A.U. Neumann, M. Markowitz, J.M. Leonard, D.D. Ho (1995). HIV-1 dynamics in vivo: virion clearance rate, infected cell life-span, and viral generation time. *Science* **271** 1582-1586.

Perelson, A.S. and P.W. Nelson (1999). Mathematical analysis of HIV-1 dynamics in vivo. *Siam Review* **41** 3-44.

Perelson, A.S. (2002). Modeling viral and immune system dynamics. *Nat. Rev. Immunol.* **2** 28-36.

Piatak, M., M.S. Saag, L.C. Yang, S.J. Clark, J.C. Kappes, K.C. Luk, B.H. Hahn, G.M. Shaw, J.D. Lifson (1993). High levels of HIV-1 in plasma during all stages of infection determined by competitive PCR. *Science* **259** 1749-1754.

Picker, L.J. and V.C. Maino (2000). The CD4$^+$ T cell response to HIV-1. *Curr. Opin. Immunol.* **12** 381-386.

Qingsheng, L., L. Duan, J.D. Estes, Z.M. Ma, T. Rourke, Y. Wang, C. Reilly, J. Carlis, C.J. Miller, A.T. Haase (2005). Peak SIV replication in resting memory CD4$^+$ T cells depletes gut lamina propria CD4$^+$ T cells. *Nature* **434** 1148-1152.

Ribeiro, R.M., H. Mohri, D.D. Ho, A.S. Perelson (2002). In vivo dynamics of T cell activation, proliferation, and death in HIV-1 infection: Why are $CD4^+$ but not $CD8^+$ T cells depleted?. *Proc. Natl Acad. Sci. U.S.A.* **99** 15572-15577.

Rosenberg, E.S., M. Altfeld, S.H. Poon, M.N. Phillips, B.M. Wilkes, R.L. Eldridge, G.K. Robbins, R.T. D'Aquila, P.J. Goulder, B.D. Walker (2000). Immune control of HIV-1 after early treatment of acute infection. *Nature* **407** 523-526.

Ruiz, L., J. Martinez-Picado, J. Romeu, R. Paredes, M. K. Zayat, S. Marfil, E. Negredo, G. Sirera, C. Tural, B. Clotet (2000). Structured treatment interruption in chronically HIV-1 infected patients after long-term viral suppression. *AIDS* **14** 397-403.

Sallusto, F., J. Geginat, A. Lanzavecchia (2002). Central memory and effector memory T cell subsets: function, generation, and maintenance. *Annu. Rev. Immunol.* **22** 745-763.

Saparov, A., F.H. Wagner, R. Zheng, J.R. Oliver, H. Maeda, R.D. Hockett, C.T. Weaver (1999). Interleukin-2 expression by a subpopulation of primary T cells is linked to enhanced memory/effector function. *Immunity* **11** 271-280.

Shankar, P., M. Russo, B. Harnisch, M. Patterson, P. Skolnik, J. Lieberman

(2000). Impaired function of circulating HIV-specific $CD8^+$ T cells in chronic human immunodeficiency virus infection. *Blood* **96** 3094-3101.

Stafford, M.A., L. Corey, Y. Cao, E.S. Daar, D.D. Ho, A.S. Perelson (1999). Modeling plasma virus concentration and $CD4^+$ T cell kinetics during primary HIV infection. J. Theor. Biol. **203** 1-38.

Tepic, S. (2004). Could a simple surgical intervention eliminate HIV infection? *Theoretical Biology and Medical Modeling* **1** 1-8.

UNAIDS/WHO 2005 Report on the global AIDS epidemic, website.

Van Baarle, D. (2002). Failing immune control as a result of impaired $CD8^+$ T cell maturation: CD27 might provide a clue. *Trends Immunol.* **23** 586-591.

Wherry, E.J. and R. Ahmed (2004). Memory CD8 T-Cell Differentiation during Viral Infection. *J. Virol.* **11** 5535-5545.

Wick, W.D., O.O. Yang, L. Corey, S.G. Self (2005). How many human immunodeficiency virus type 1-infected target cells can a cytotoxic T-lymphocyte kill? *J. Virol.* **79** 13579-13586.

Witten, G.Q. and A.S. Perelson (2004). Modelling the cellular-level interaction between the immune system and HIV. *South African Journal of Science* **100** 1-5.

Wodarz, D. and M.A. Nowak (2002). Mathematical models of HIV pathogenesis and treatment. *Bioessays* **24** 1178-1187.

Wolthers, K.C., G. Bea, A. Wisman, S.A. Otto, A.M. de Roda Husman, N. Schaft, F. de Wolf, J. Goudsmit, R.A. Coutinho, A.G.J. van der Zee, L. Meyaard, F. Miedema (1996). T Cell Telomere Length in HIV-1 Infection: No Evidence for Increased $CD4^+$ T Cell Turnover. *Science* **274** 1543-1547.

Wu, H. and A.A. Ding (1999). Population HIV-1 Dynamics In Vivo: Applicable Models and Inferential Tools for Virological Data from AIDS Clinical Trials. *Biometrics* **55** 410.

Yue, F.Y., C.M. Kovacs, R.C. Dimayuga, P. Parks, M.A. Ostrowski (2004). HIV-1-specific memory $CD4^+$ T cells are phenotypically less mature than cytomegalovirus-specific memory $CD4^+$ T cells. *J. Immunol.* **172** 2476-2486.

Zimmerli, S.C., A. Harari, C. Cellerai, F. Vallelian, P.A. Bart, G. Pantaleo (2005). HIV-1-specific IFN-γ/IL-2-secreting CD8 T cells support CD4-independent proliferation of HIV-1-specific CD8 T cells. *Proc. Nat. Acad. Sci. U.S.A.* **102** 7239-7244.